



LUND UNIVERSITY

Assessment of "Zero Point" radiation around the ESS facility

Bernhardsson, Christian; Stenström, Kristina; Jönsson, Mattias; Mattsson, Sören; Pedehontaa-Hiaa, Guillaume; Rääf, Christopher; Sundin, Kurt; Waldner, Lovisa

2019

Document Version:

Publisher's PDF, also known as Version of record

[Link to publication](#)

Citation for published version (APA):

Bernhardsson, C., Stenström, K., Jönsson, M., Mattsson, S., Pedehontaa-Hiaa, G., Rääf, C., Sundin, K., & Waldner, L. (2019). *Assessment of "Zero Point" radiation around the ESS facility*. (MA RADFYS 2018:01), (BAR-2018/04). Lund University.

Total number of authors:

8

Creative Commons License:

Unspecified

General rights

Unless other specific re-use rights are stated the following general rights apply:

Copyright and moral rights for the publications made accessible in the public portal are retained by the authors and/or other copyright owners and it is a condition of accessing publications that users recognise and abide by the legal requirements associated with these rights.

- Users may download and print one copy of any publication from the public portal for the purpose of private study or research.
- You may not further distribute the material or use it for any profit-making activity or commercial gain
- You may freely distribute the URL identifying the publication in the public portal

Read more about Creative commons licenses: <https://creativecommons.org/licenses/>

Take down policy

If you believe that this document breaches copyright please contact us providing details, and we will remove access to the work immediately and investigate your claim.

LUND UNIVERSITY

PO Box 117
221 00 Lund
+46 46-222 00 00



Faculty of Medicine

Department of Translational Medicine
Medical Radiation Physics
*Environmental Radiology and Emergency
Preparedness Group*

Faculty of Science

Department of Physics
Division of Nuclear Physics
*Biospheric and Anthropogenic Radioactivity
(BAR) Group*

Assessment of “Zero Point” radiation around the ESS facility

List of authors

Christian Bernhardsson	christian.bernhardsson@med.lu.se
Kristina Eriksson Stenström	kristina.stenstrom@nuclear.lu.se
Mattias Jönsson	mattias.jonsson@med.lu.se
Sören Mattsson	soren.mattsson@med.lu.se
Guillaume Pedehontaa-Hiaa	guillaume.pedehontaa-hiaa@med.lu.se
Christopher Rääf	christopher.raaf@med.lu.se
Kurt Sundin	kurt.sundin@med.lu.se
Lovisa Waldner	lovisa.waldner@med.lu.se

This document is the public version of the report “Assessment of “Zero Point” radiation around the ESS facility”.

In this public version Annex C has been excluded. Annex C contains raw data of assessed dose rates and concentrations of various radionuclides of all samples measured within the study. The data is available upon request (please contact the authors).

**Faculty of Medicine**

Department of Translational Medicine
Medical Radiation Physics
*Environmental Radiology and Emergency
Preparedness Group*

Faculty of Science

Department of Physics
Division of Nuclear Physics
*Biospheric and Anthropogenic Radioactivity
(BAR) Group*

Assessment of “Zero Point” radiation around the ESS facility

List of authors

Christian Bernhardsson	christian.bernhardsson@med.lu.se
Kristina Eriksson Stenström	kristina.stenstrom@nuclear.lu.se
Mattias Jönsson	mattias.jonsson@med.lu.se
Sören Mattsson	soren.mattsson@med.lu.se
Guillaume Pedehontaa-Hiaa	guillaume.pedehontaa-hiaa@med.lu.se
Christopher Rääf	christopher.raaf@med.lu.se
Kurt Sundin	kurt.sundin@med.lu.se
Lovisa Waldner	lovisa.waldner@med.lu.se

Reviewed by: Daniela Ene, ESS, daniela.ene@esss.se

Approved by: Peter Jacobsson, ESS, peter.jacobsson@esss.se

Approved by: Lars E. Olsson, LU, lars_e.olsson@med.lu.se

Department of Translational Medicine
Medical Radiation Physics
Carl-Bertil Laurells gata 9
SE-205 02 Malmö

Report MA RADFYS 2018:01
Malmö 2018

Department of Physics
Division of Nuclear Physics
Professorsgatan 1
SE-223 63 Lund

Report BAR-2018/04
Lund 2018

TABLE OF CONTENT

PAGE

1.	INTRODUCTION	9
1.1.	Summary of the report	9
2.	SELECTION OF LOCATIONS FOR MEASUREMENTS AND SAMPLING.....	11
2.1.	Locations for gamma spectrometry and soil samples.....	11
2.2.	Locations for ground- and surface water samples.....	15
2.3.	Locations for bioindicators, grass, crops, milk and sewage sludge	17
2.4.	Sampling locations for ^{14}C analysis	18
3.	METHODS FOR SAMPLE COLLECTION AND ANALYSIS.....	23
3.1.	Field gamma spectrometry and measurement of ambient dose equivalent rate.....	23
3.2.	Sampling and measurement of soil, bioindicators, grass, crops, milk and sewage sludge	23
3.2.1.	Sampling of soil	23
3.2.2.	Sampling of bioindicators	23
3.2.3.	Sampling of grass.....	24
3.2.4.	Sampling of crops	24
3.2.5.	Sampling of milk	24
3.2.6.	Sampling of sewage sludge	24
3.2.7.	Laboratory high-resolution gamma spectrometry.....	24
3.3.	Sampling and measurements of ^3H in water, milk and sewage sludge	24
3.4.	Sampling and measurements of ^{14}C in trees, milk and fullerene soot.....	24
3.4.1.	Collection and pretreatment of annual tree rings.....	24
3.4.2.	Collection and pretreatment of vegetation and fodder samples	25
3.4.3.	Collection and pretreatment of milk.....	25
3.4.4.	Sampling using soot monitors.....	25
3.4.5.	Graphitization and ^{14}C measurement	25
3.4.6.	Storage of samples.....	25
4.	RESULTS	27
4.1.	Assessment of the radiation background.....	27
4.1.1.	Field gamma spectrometry.....	27
4.1.2.	Ambient dose equivalent rate	27
4.2.	Analysis of the activity concentration of gamma-emitting radionuclides in soil, grass, milk, crops, sewage sludge and bioindicators.....	29
4.2.1.	Soil samples	29
4.2.2.	Grass samples	33
4.2.3.	Milk samples	33
4.2.4.	Samples of crops.....	33
4.2.5.	Samples of sewage sludge.....	34
4.2.6.	Samples of bioindicators.....	34
4.2.7.	Quality assessment of the gamma spectrometry measurements	34
4.3.	Analysis of ^3H in water and some bioindicators.....	36

4.3.1.	^3H in ground water and surface water.....	36
4.3.2.	^3H in sewage sludge.....	36
4.3.3.	^3H in bioindicators.....	36
4.3.4.	Quality assurance of the ^3H assessments	36
4.4.	^{14}C analysis	36
4.4.1.	Quality assessment.....	36
4.4.2.	Organic material.....	37
4.4.3.	Fullerene soot monitors	42
5.	SUMMARY AND CONCLUSIONS.....	47
6.	ACKNOWLEDGMENT	47
7.	REFERENCES	49
ANNEX A	RADIATION IN THE ENVIRONMENT	51
	Gamma emitters in the environment	51
	Tritium in the environment.....	54
	^{14}C in the environment and previous measurements in the Lund area	58
	Long-lived spallation and activation products in accelerator driven systems	59
ANNEX B	MATERIALS AND METHODS	65
ANNEX B1	ASSESSMENT OF <i>IN SITU</i> AND MOBILE GAMMA SPECTROMETRY AND AMBIENT DOSE EQUIVALENT.....	67
ANNEX B2	SAMPLING, SAMPLE PREPARATION AND LABORATORY MEASUREMENTS USING HIGH-RESOLUTION GAMMA SPECTROMETRY	71
ANNEX B3	SAMPLING, SAMPLE PREPARATION AND MEASUREMENTS OF ^3H ACTIVITY CONCENTRATION USING LIQUID SCINTILLATOR COUNTING	79
ANNEX B4	SAMPLING, SAMPLE PREPARATION AND MEASUREMENTS OF ^{14}C	85
ANNEX C	RESULTS	97

LIST OF TABLES

Table 1.	List of the selected sites in Figure 1 and the measurements and/or samplings carried out. The sites marked with "k:a" refer to cemeteries around the churches.	13
Table 2.	List of sampling sites for ^{14}C measurements, some of which are the same as in Table 1 (Table 1 site name within parenthesis).	19
Table 3.	Ambient dose equivalent rate ($\text{H} \cdot 10$) at the various sites.....	28
Table 4.	Average activity concentration in the 20 cm deep STS cores for the natural occurring radionuclides investigated. The uncertainties are given as the standard deviation divided by the mean activity for each radionuclide distributed homogeneously within the core.....	32
Table 5	Estimated activity concentration of $^{14}\text{CO}_2$ in southern Sweden for years 2012-2016.....	38

Table 6	Estimated activity concentration of ^{14}C various sample types in southern Sweden in 2017. Values of proportion carbon are taken from Ref [35].	41
---------	---	----

LIST OF FIGURES

Figure 1.	Map of the north-eastern part of Lund where the red circles indicate sites for measurements of ambient dose rate, <i>in situ</i> gamma spectrometry and soil sampling.	12
Figure 2.	Map of Lund (ESS area is marked) and the sites (marked in blue) where water was sampled.	16
Figure 3.	Positions for sampling of groundwater (A) and surface water (B) at the ESS site (Site 31).	16
Figure 4.	Map of Lund with sampling sites for various bioindicators (marked in green).	17
Figure 5.	Map of the surrounding farmlands (Site 36) around the ESS area (marked) where crops (A: rapeseed; B: barley; C: wheat) were sampled (marked in green).	18
Figure 6.	Sampling sites for ^{14}C measurements. 🌲 : Tree rings (2012-2016), grass, moss, crops, and fullerene monitors (the latter not on C5); 📌 : grass, moss and/or crops; 🧺 : grass, moss, fodder, milk. See Table 2 for more information about the sampling sites.	21
Figure 7.	Gamma dose rate variability around the ESS facility, as measured by NaI(Tl) detectors in a car.	29
Figure 8.	Activity concentration of ^{226}Ra in 7 cm surface soil at the sites indicated. The uncertainty bars represent 1 standard uncertainty of the mean.	30
Figure 9.	Activity concentration of ^{137}Cs in 7 cm surface soil at the sites indicated. The uncertainty bars represent 1 standard uncertainty of the mean.	30
Figure 10.	Activity concentration of ^{228}Ac in 7 cm surface soil at the sites indicated. The uncertainty bars represent 1 standard uncertainty of the mean.	31
Figure 11.	Activity concentration of ^{40}K in 7 cm surface soil at the sites indicated. The uncertainty bars represent 1 standard uncertainty of the mean.	31
Figure 12.	Examples of the ^{137}Cs activity concentration down in soil at Site 24 (homogenous distribution) and Site 40 (exponential distribution).	32
Figure 13.	Average activity concentration (Bq kg^{-1}) of ^{40}K in grass samples for each sampling month (2017).	33
Figure 14	Top left frame: constancy control over time for various radionuclides (^{137}Cs , ^{60}Co , ^{241}Am) for a 55% HPGe detector (MCB4); Top right frame: constancy control over time for various radionuclides (^{137}Cs , ^{60}Co , ^{241}Am) for a 92.5% HPGe detector (MCB5); Lower frame: constancy control over time for various radionuclides (^{137}Cs , ^{60}Co , ^{241}Am) for a 100% HPGe detector (MCB7).	35

Figure 15.	Results of the ^{14}C measurements of standard samples IAEA C7, SRM 4990B (also known as OxI) and SRM 4990C (also known as OxII). Uncertainty bars refer to 1σ .	37
Figure 16.	Results of the ^{14}C measurements of annual tree rings. The uncertainty of the Schauinsland data is the standard deviation of monthly $F^{14}\text{C}$ data from May to August ($N=4$) [32, 33], while the uncertainties of sites C1-C5 is the analytical uncertainty.	38
Figure 17.	a) Results of the ^{14}C measurements of grass and crops/fruits from 2017. b) Box plot showing that the mean $F^{14}\text{C}$ value of grass was not significantly different from the crops/fruit data of 2017 ($p>0.05$, one-way ANOVA).	39
Figure 18.	Results of the ^{14}C measurements at the dairy farm at site C13, compared to vegetation samples at the rural and urban background sites C1 and C2. The grass sample from August 2017 is an outlier according to Grubb's test.	40
Figure 19.	Results from ^{14}C measurements of moss samples, compared to grass samples collected at the various sites.	41
Figure 20.	Number of counts registered in the ^{14}C window of the detector during 120 s as a function of measured ion beam current of $^{12}\text{C}^-$ for all fullerene soot samples.	42
Figure 21.	Measured $^{14}\text{C}/^{12}\text{C}$ ratios of soot monitors at the sites C1-C4, unexposed soot (blank soot) as well as graphitized fossil carbon (Abs1 and W6C).	43
Figure 22.	Measured $^{14}\text{C}/^{12}\text{C}$ ratios of soot monitors at the sites C1-C4, unexposed soot (blank soot) as well as graphitized fossil carbon (Abs1 and W6C), in more detail compared to Figure 21.	44
Figure 23.	Current of negative ^{12}C ions measured at the high-energy side of the SSAMS system.	44

List of abbreviations

$\delta^{13}\text{C}$	Delta- ^{13}C (isotope fractionation)
d.w.	Dry weight
EPS	Emergency Preparedness Sampler
ESS	European Spallation Source
F ^{14}C	Fraction Modern Carbon
HPGe	High Purity Germanium
LSC	Liquid Scintillation Counting
LU	Lund University
MDA	Minimum Detectable Activity concentration
SSAMS	Single Stage Accelerator Mass Spectrometry
SSM	Swedish Radiation Safety Authority
STS	Split Tube Sampler
SUM	Standard Uncertainty of the Mean

1. INTRODUCTION

Within a few years, one of the most powerful spallation sources in the world, the European Spallation Source (ESS), will be in operation in Lund. During operation, the ESS facility will produce a large number of different radionuclides which have a potential to be released to the environment [1]. According to the requirements of the Swedish Radiation Safety Authority (SSM), the annual effective dose to members of the public, resulting from release of radioactive substances and by direct radiation from the ESS facility, must not exceed 0.1 mSv per year [2].

This report presents the results of a collaboration project between Lund University (Medical Radiation Physics Malmö and Division of Nuclear Physics) and ESS entitled “Monitoring of environmental radioactivity and radiation levels for “Zero Point” assessment and contributions to ESS environmental monitoring plan” [3]. The aim was to establish the current levels of ionizing radiation and concentration of various radionuclides, natural as well as artificial, in the surroundings of ESS prior to start of operation of the facility. The data generated in this “Zero Point” assessment, performed during 2017-2018, may be used to determine future potentially unobserved and diffuse discharges from ESS to the environment. Such comparisons can also provide information of possible long-term changes in the radionuclide concentrations in the environment as well as assessments of the exposure to the public before and after operation of ESS.

The radionuclides selected for the “Zero Point” assessment represent natural as well as man-made radionuclides and include gamma-emitters as well as the pure beta-emitters ^3H (tritium) and ^{14}C . The latter two are frequently used as tracers in research and industry. The measurements and specific radionuclides here reported included:

- Ambient dose equivalent rate
- *In situ* gamma spectrometry (^7Be , ^{137}Cs , ^{40}K , ^{226}Ra (^{238}U daughter) and ^{228}Ac (^{232}Th daughter))
- Gamma spectrometry of soil profiles, bioindicators, grass, crops and forage, milk and sewage sludge (with activity determinations of ^{137}Cs , ^{40}K , ^{226}Ra , ^{228}Ac and ^{131}I)
- ^3H measurements of ground- and surface water, sewage sludge, bioindicators, crops and milk
- ^{14}C measurements of annual tree rings, grass, bioindicators, milk and in fullerene soot monitors

An introduction to environmental radiation and radioactivity, focussing on the radionuclides assessed in this report, is provided in Annex A.

1.1. Summary of the report

At the 46 sites surveyed for gamma-emitting radionuclides, the following assessments were carried out:

- Activity concentration of gamma-emitting radionuclides in soil, by “split tube” samples (STS, vertical radionuclide concentration/distribution down to a depth of 20 cm) and by “emergency preparedness” samples (EPS, horizontal radionuclide concentration/distribution down to a depth of 7 cm) collected at 22 and 29 sites, respectively;

- activity concentration of gamma-emitting radionuclides in grass, crops and forage, sewage sludge and bioindicators collected at 20, 12, 1, and 13 sites, respectively;
- *in situ* high resolution gamma spectrometry was carried out at 21 sites;
- ambient dose equivalent rate, and its variability, was carried out at 29 sites plus one assessment by car covering the ESS nearby areas (about 2 km in radius).

The activity concentration of ^3H in samples of water, sewage sludge and bioindicators were collected and analysed from 9, 1 and 2 sites, respectively. ^3H was also analysed in milk at one dairy farm in the vicinity of ESS.

The ^{14}C content of annual tree rings, representing the ^{14}C specific activity in atmospheric CO_2 during each growing season of years 2012-2016 was measured at 4 sites (2 around ESS, 1 urban background and 1 rural background site). Fullerene soot monitors – absorbing gases from the atmosphere, then analysed for ^{14}C content - were placed at these sites for four 4-week periods. Furthermore, the ^{14}C concentration was measured in samples of grass, moss and/or crops/fodder at 23 sites, including samples from the urban and rural background sites. A special study was undertaken at a dairy farm, analysing ^{14}C in milk, silage, fodder and vegetation.

The main outcomes of these assessments were:

- The concentrations of natural occurring radionuclides in the ground were similar, with only small variations observed between the sites. Expected differences between the sites were observed for ^{137}Cs , in terms of depth distribution and total inventory in the soil.
- No unexpected gamma emitters were observed in the various samples collected:
 - ^{131}I was observed in the majority of the samples of sewage sludge. Other medically used radionuclides might have been found if the time between sampling and measurements had been shortened.
- Only small variations were observed for the radionuclides investigated with *in situ* gamma spectrometry at the various sites, except for ^{137}Cs that was observed to vary between some sites.
- An average value of the ambient dose equivalent rate 1 meter above the ground was determined as well as the variability within and between the sites.
- The tritium levels were below the minimum detectable activity concentration (MDA) in all samples analysed, except two samples of sewage sludge, where the activity concentration was slightly above the MDA.
- The sampling sites in the Lund area showed no signs of local anthropogenic contamination of ^{14}C .

2. SELECTION OF LOCATIONS FOR MEASUREMENTS AND SAMPLING

Initially, the “Zero Point assessment” aimed to include 36 sites located within approximately 1.5 km of the planned target location of the ESS facility (see [4]). However, to find suitable sites and samples for the different radionuclides assessed - and to include supplementary material - additional and more distant sites were also included.

In general, the sites were selected according to the following criteria: The sites should

- cover all directions from the ESS site,
- be preserved over time and available in the future,
- be representative and reflect the current population density in the area.

The selection of a large number of sites aimed to guarantee that enough number of sites (in various directions from ESS) will be accessible for future measurements.

The sites selected were located outside the fence of the ESS facility area, except for a limited number of ground- and surface water samples that were taken from drilled holes and ponds inside the ESS area.

2.1. Locations for gamma spectrometry and soil samples

The background gamma radiation was assessed at specific sites around the ESS facility by means of *in situ* spectrometry, measurement of the ambient dose equivalent and gamma analysis the activity concentration of soil.

The assessments were carried out within areas of approximately 30 m in radius, defined as a ground surface where the ground was even and smooth and where no, or a minimum of, obscuring trees or constructions could influence the radiation fields. These sites are presented in Table 1, which also provides the sites where samples of water, grass and various types of bioindicators were sampled. The sites used for the background gamma radiation mapping are graphically shown in Figure 1, which includes the ESS site (marked in orange) and MAX IV (marked in yellow).

The *in situ* gamma spectrometry (HPGe) measurements were carried out at 21 sites at the centre of each surface. Assessment of the ambient dose equivalent rate ($\dot{H}^*(10)$) was carried out at 29 sites. Soil sampling was performed at 29 sites. Two different types of soil samples were collected: STS (down to ~20 cm, analysed by different depth layers) and EPS (down to 7 cm, analysed as one core).

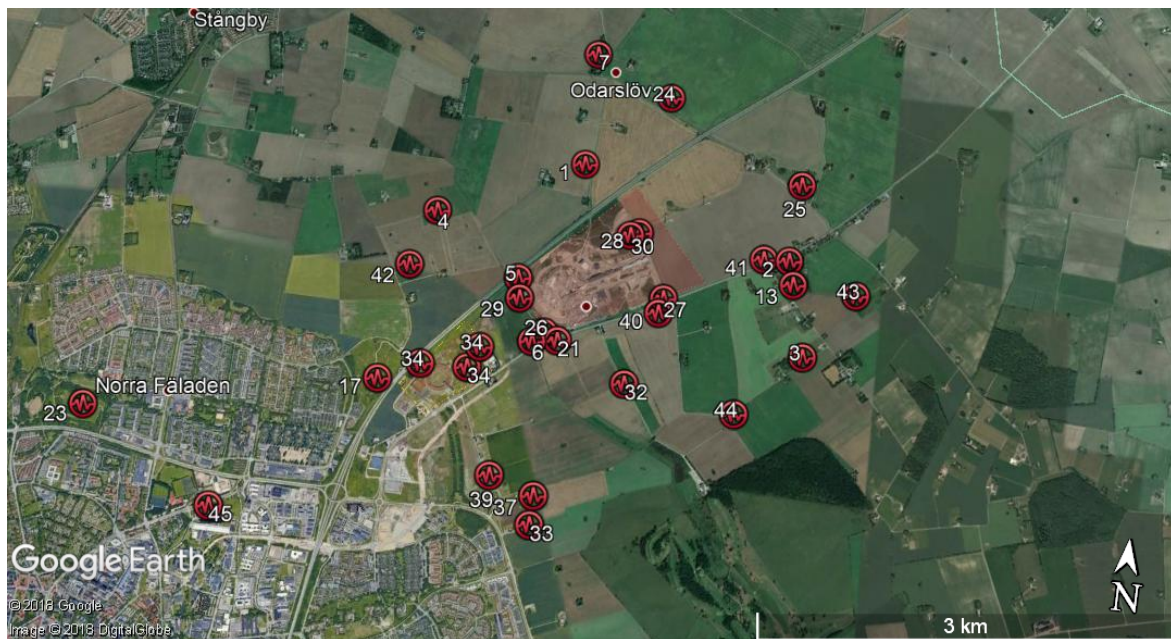


Figure 1. Map of the north-eastern part of Lund where the red circles indicate sites for measurements of ambient dose rate, *in situ* gamma spectrometry and soil sampling.

Table 1. List of the selected sites in Figure 1 and the measurements and/or samplings carried out. The sites marked with "k:a" refer to cemeteries around the churches.

Site	Description	GPS coordinates	Soil down to 20 cm	Soil down to 7 cm	Water	Grass	Bio-indicators*	HPGe	Dose rate
1.	Västra Odarslöv 341	N55.74310 E13.24773	x	x		x	x ^{1,2}	x	x
2.	Östra Odarslöv 651	N55.73805 E13.27359	x	x				x	x
3.	Östra Odarslöv 164	N55.73195 E13.27548		x					x
4.	Ladugårds- marken 461	N55.73863 E13.23066	x	x	x	x	x ^{1,3}	x	x
5.	Switchgear (SW of ESS)	N55.73466 E13.24149	x	x		x		x	x
6.	Möllegården	N55.73049 E13.24411	x	x			x ^{1,2,3}	x	x
7.	Odarslövs k:a	N55.75110 E13.24760	x	x		x	x ^{1,3}	x	x
8.	Igelösa k:a	N55.763084 E13.274332					x ^{1,3}		
9.	Håstad k:a	N55.774173 E13.226917					x ^{1,3}		
10.	Västra Hoby k:a	N55.786015 E13.167867					x ^{1,3}		
11.	Stångby k:a	N55.764912 E13.171910					x ^{1,3}		
12.	Vallkärra k:a	N55.741028 E13.171630					x ^{1,3}		
13.	Östra Odarslöv 264	N55.73644 E13.27433	x	x		x	x ^{1,2,3}	x	x
14.	Gårdstånga k:a	N55.759156 E13.327494					x ^{1,3}		
15.	Holmby k:a	N55.747017 E13.400596					x ^{1,3}		
16.	Svenstorps gods	N55.741108 E13.258403					x ¹		
17.	Klosterängs- höjden	N55.72678 E13.22656	x	x		x	x ¹	x	x
18.	Knästorps k:a	N55.675834 E13.199446					x ³		
19.	Hardeberga k:a	N55.697974 E13.293402					x ^{1,3}		
20.	Stora Råby k:a	N55.685918 E13.225191					x ^{1,3}		

Table 1 cont. List of the selected sites in Figure 1 and the measurements and/or samplings carried out. The sites marked with "k:a" refer to cemeteries around the churches.

Site	Description	GPS coordinates	Soil down to 20 cm	Soil down to 7 cm	Water	Grass	Bio-indicators*	HPGe	Dose rate
21.	Östra Torn 121	N55.73074 E13.24710	x	x			x ^{1,3}	x	x
22.	Sandby 5:91	N55.728939 E13.340461			x	x	x ^{1,4,8,9,11}		
23.	S:t Hans backar	N55.72267 E13.19258	x	x		x		x	x
24.	Västra Odarslöv 421	N55.74856 E13.25723	x	x	x	x		x	x
25.	Västra Odarslövs skola	N55.74342 E13.27426	x	x		x		x	x
26.	ESS SW corner	N55.73119 E13.24539		x		x			x
27.	ESS SE corner	N55.73445 E13.25906		x		x			x
28.	ESS NE corner	N55.73876 E13.25526		x		x			x
29.	ESS NW corner	N55.73331 E13.24197		x		x			x
30.	Koppar-staden (windmill)	N55.73852 E13.25427	x	x		x		x	x
31.	ESS-area (target site)	N55.734557 E13.248714			x				
32.	Damms-torpsvägen 16	N55.72840 E13.25561	x	x		x			x
33.	Utmarks-vägen 55	N55.71848 E13.24665	x	x	x	x		x	x
34.	MAX IV-area	N55.727459 E13.233718	x	x	x		x ⁵	x	x
35.	Källby (sewage treatment plant) VA SYD	N55.695209 E13.163787			x				
36.	Svenstorp's gods	N55.766913 E13.253258					x ^{4,6,7}		
37.	Utmarks-vägen 39	N55.72037 E13.24667	x	x	x	x		x	x
38.	Västra Odarslöv 362	N55.75016 E13.24731			x				
39.	Utmarks-vägen 23	N55.72134 E13.24126	x	x		x		x	x

Table 1 cont. List of the selected sites in Figure 1 and the measurements and/or samplings carried out. The sites marked with "k:a" refer to cemeteries around the churches.

Site	Description	GPS coordinates	Soil down to 20 cm	Soil down to 7 cm	Water	Grass	Bio-indicators*	HPGe	Dose rate
40.	Östra Odarslöv 301	N55.73343 E13.25866	x	x		x		x	x
41.	Östra Odarslöv 291	N55.73796 E13.27053	x	x				x	x
42.	Ladugårds- marken (cell tower)	N55.73470 E13.22829		x					x
43.	Östra Odarslöv 541 (slate quarry)	N55.73621 E13.28190		x					x
44.	Kärrpäng- vägen 6 (Hobykrok)	N55.72729 E13.26884	x	x		x		x	x
45.	Kemicentrum	N55.71713 E13.20938	x	x		x		x	x
46.	Lunnarp 231 (Dalby)	N55.645322 E13.315064					x ¹⁰		

*Bioindicators: 1-moss; 2-spruce needles; 3-lichen; 4-barley; 5-clover; 6-rapeseed; 7-wheat; 8-forage; 9-silage; 10-sugar beet; 11-milk.

2.2. Locations for ground- and surface water samples

For the assessment of ³H in surface water and ground water, 21 sites were used for collecting 42 samples (Figure 2 and Figure 3). Surface water was sampled from ponds located within and around the ESS site perimeter, as well as from the five water outlet ponds at Källby sewage treatment plant in the south-west of Lund (Figure 2). Water was also sampled from four privately owned drinking-water wells (not all of them currently in use). Ground water was sampled from existing drill holes on the ESS site or in the close vicinity of the ESS site (see Figure 3). In addition, and to serve as a future reference, water was also collected from a water reservoir outside Malmö (Grevie PV5, VA SYD Bulltofta VV) with a well-documented and low ³H content.

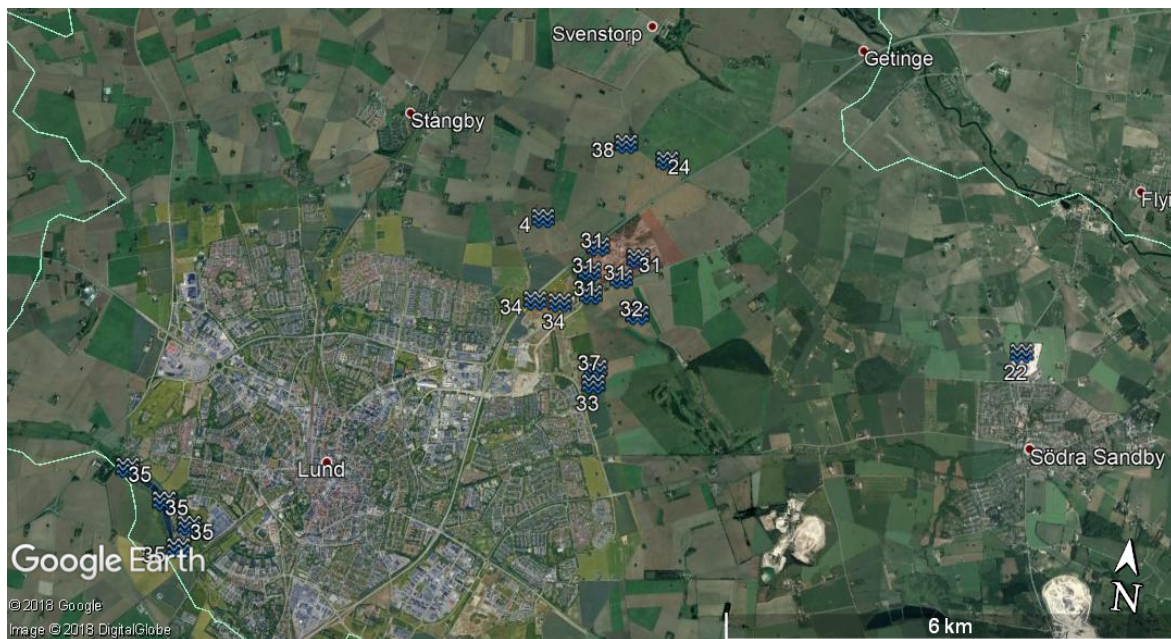


Figure 2. Map of Lund (ESS area is marked) and the sites (marked in blue) where water was sampled.

Figure 3 shows the positions of the water sampling spots inside the ESS area (including some points outside the area). These sampling spots were the same as used by Skanska during the construction of the ESS facility for monitoring environmental impact.



Figure 3. Positions for sampling of groundwater (A) and surface water (B) at the ESS site (Site 31).

2.3. Locations for bioindicators, grass, crops, milk and sewage sludge

Bioindicators (moss, spruce needles, lichen), sewage sludge, grass, and agricultural products such as barley, clover, rapeseed, wheat, forage, silage, sugar beets and milk were sampled around the ESS site. However, to be able to sample all these matrices, some samples were collected at larger distances than 1.5 km from the ESS site (see Figure 4).

Lichens, moss and spruce needles have since long been used as bioindicators and bioaccumulators of air and rainwater pollution in the terrestrial environment [5-7]. These are however not frequently growing in the ESS surroundings and if found, the localities can quickly be destroyed. Therefore, bioindicator sampling was concentrated to cemeteries that often contain mosses and lichens and where they, in addition, are well protected from changes and reconstruction due to urban management.

Lichens in the form of *Xanthoria parietina* (in Swedish: gul vägglav) and moss *Pleurozium schreberi* (in Swedish: väggmossa), *Holycomium splendens* (in Swedish: husmossa) were collected where available.

Xanthoria was taken from standing gravestones or from cemetery walls and moss from tombstones laying on the ground or directly from the ground. Needles from spruce were collected where available.

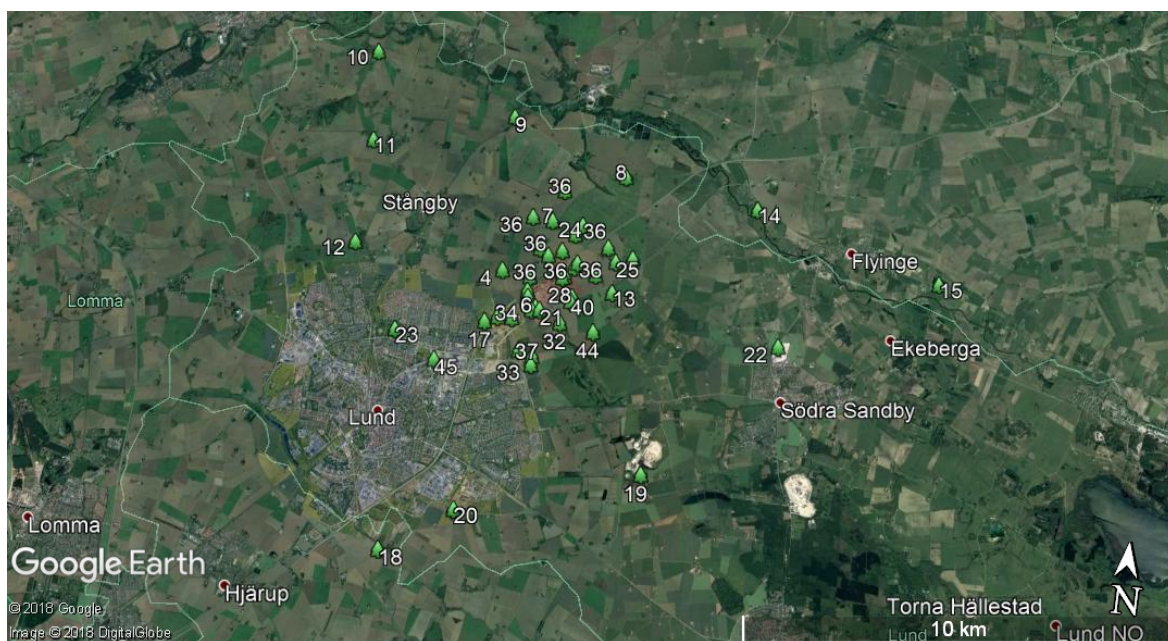


Figure 4. Map of Lund with sampling sites for various bioindicators (marked in green).

Grass is considered as a bioindicator of high relevance and importance for the future and can be found at the majority of the sites during a long period of the year. Grass samples were collected at sites, from a 1 m² surface, when available (Table 1). The grass samples were analysed for the concentration of gamma-emitting radionuclides.

Samples of crops were collected on 10 farmlands located in the western and northern directions from ESS, see Figure 5. The sampling was performed by the staff at Svenstorp's county estate (in Swedish: Svenstorps gods), by collecting a representative average sample for each farmland during harvest.



Figure 5. Map of the surrounding farmlands (Site 36) around the ESS area (marked) where crops (A: rapeseed; B: barley; C: wheat) were sampled (marked in green).

Only one farmer with dairy cows was identified in the vicinity (5.8 km) of the ESS area (Site 22 in Table 1 and Figure 4). At this farmer, milk was sampled from the cooled milk storage tank, that was emptied by a dairy every 48 hours. The milk was analysed for gamma-emitting radionuclides as well as ^3H and ^{14}C (see below). The various types of fodder (commercial fodder pellets, own silage, grass and clover) were analysed for gamma-emitting radionuclides and ^{14}C (see below).

On a monthly basis and during one year, sewage sludge was collected at the sewage treatment plant in Lund, VA Syd Källby (Site 35). The samples consisted of representative monthly samples, which in turn consisted of subsamples from each day the centrifuge was running during each month. Both gamma-emitting radionuclides and ^3H were analysed in the sludge samples to observe possible seasonal changes over the year.

In addition, although not possible to collect within 1.5 km during the year of this study, sugar beets were sampled to obtain background data also for this widespread type of crop (at Site 46). The bioindicators as well as the samples of grass, crops, cow fodder, milk and sewage sludge were analysed in a well-background-shielded high-resolution gamma spectrometer.

2.4. Sampling locations for ^{14}C analysis

All sampling sites for ^{14}C are shown in Table 2 and Figure 6. ^{14}C values of clean air CO_2 are commonly used as reference data for ^{14}C in vegetation and biota. To obtain clean air $^{14}\text{CO}_2$ data for southern Sweden, a rural background site Borrby (site C1), located 70 km ESE from the ESS site, was chosen. To assess the local Suess effect (the influence from combustion of fossil fuels, see ANNEX A), an urban sampling site was selected in northern Lund (site C2), located 4.6 km (WSW) from the ESS site. To establish the current levels of ^{14}C in Lund prior to operation of ESS, vegetation (grass, fruit, berries and crops), which had grown during 2017 close to the ESS site, was analysed. Annual tree rings for the years 2012-2016 (reflecting ^{14}C in CO_2 during the growing season of a particular year) were analysed at the rural and urban background sites (C1 and C2) as well as three sites located in various directions within 1.4 km of the centre of the ESS site (sites C3, C4 and C5).

In Lund, we have previously observed increased ^{14}C concentrations in vegetation (see ANNEX A). We have also detected contamination of ^{14}C in workers handling ^{14}C -labelled substances [8, 9]. Therefore, samples of fruit and berries were also collected at various places in Lund with potential ^{14}C sources (mainly in the north-eastern part of Lund, sites C18-C21, C23).

Trees, grass, crops, fruit and berries will mainly reflect the ^{14}C concentration of atmospheric CO_2 . We have previously found that samples of moss may indicate the presence of airborne ^{14}C particulates [10, 11]. Therefore, moss samples from selected site (C1-C13) were collected. Furthermore, as moss grows from the top, different layer of moss should reflect different time periods [11]. Moss samples from the rural and urban background sites (C1 and C2) were therefore divided into layers prior to analysis.

A special investigation was performed at the dairy farm (site 22 in Table 1, referred to as site C13 in Table 2 and Figure 6), located 5.7 km from the centre of the ESS site. Milk was collected in June (2017-06-14) and August (2017-08-30). Additionally, the food consumed by the cows was collected (in June: commercial fodder pellets, own silage from 2016 and grass and clover from a pasture; in August: autumn barley harvested in 2017, silage from 2016 and grass and clover from another pasture). Moss was also collected in June.

The sampling sites C1-C4 were also subjects to monitoring using fullerene soot. Fullerene soot is known to absorb gases from the air, and we have previously used this approach to monitor contamination of ^{14}C in Lund [12].

Table 2. List of sampling sites for ^{14}C measurements, some of which are the same as in Table 1 (Table 1 site name within parenthesis).

Site	Description	GPS co-ordinates	Annual tree rings	Grass	Moss	Crops/ fodder	Milk	Fullerene monitors
C1.	Borrby	N55.42556 E14.22361	x^1	x	x	x^4		x
C2.	Timjanvägen 5, Lund	N55.71861 E13.18278	x^1	x	x	x^4		x
C3. (6.)	Möllegården	N55.73056 E13.24389	x^2	x	x	x^4		x
C4. (13.)	Östra Odarslöv 264	N55.73667 E13.27444	x^3	x	x	x^4		x
C5. (1.)	Västra Odarslöv 341	N55.74278 E13.24833	x^2	x	x	x^4		
C6. (4.)	Ladugårdsmarken 461	N55.73833 E13.23139		x	x	x^4		
C7. (17.)	Klosterängshöjden	N55.72833 E13.22806		x	x			
C8.	Straw dump	N55.74111 E13.25833		x	x			
C9. (21.)	Östra Torn 121	N55.73056 E13.24722		x	x			
C10. (32.)	Dammtorps-vägen 16	N55.72806 E13.25611		x	x			

Table 2 cont. List of sampling sites for ^{14}C measurements, some of which are the same as in Table 1 (Table 1 site name within parenthesis).

Site	Description	GPS co-ordinates	Annual tree rings	Grass	Moss	Crops/fodder	Milk	Fullerene monitors
C11.	Dammtorps-vägen	N55.73000 E13.25389				x ⁵		
C12. (27.)	Kärrpängavägen bus stop	N55.73444 E13.26028		x	x	x ⁶		
C13. (22.)	Sandby 591	<i>Farm</i> N55.72889 E13.34056 <i>Pasture 1</i> N55.73556 E13.34528 <i>Pasture 2</i> N55.73472 E13.34417		x	x	x ^{7,8,9,10}	x	
C14.	Field Ladugårdmarken close to MaxIV	N55.72917 E13.22944				x ¹¹		
C15.	ESS 2d wind power tower	N55.74000 E13.25861				x ⁶		
C16.	Field NW of E22_2	N55.73694 E13.24361				x ¹¹		
C17.	Field NW of E22_3	N55.73722 E13.24389				x ⁴		
C18.	Professorsgatan 1	N55.70972 E13.20472				x ¹²		
C19.	Rättsmedicinal- verket	N55.71250 E13.20333				x ¹³		
C20. (45.)	Lophtet	N55.71750 E13.21056				x ⁴		
C21.	Active Biotech	N55.71694 E13.22056				x ¹²		
C22.	Stadsodlingen Brunnshög	N55.72083 E13.24111				x ⁹		
C23.	Scheelevägen at Medicon Village	N55.71111 E13.21667				x ⁴		

Tree rings (2012, 2013, 2014, 2015, 2016): 1: pine, 2: spruce, 3: fir.

Crops/fodder: 4: apple 2017, 5: rye 2017, 6: rapeseeds 2017, 7: commercial fodder pellets <2017; 8: silage 2016, 9: clover, 10: autumn barley 2017, 11: wheat 2017, 12: rowan berries 2017, 13: hawthorn berries 2017.

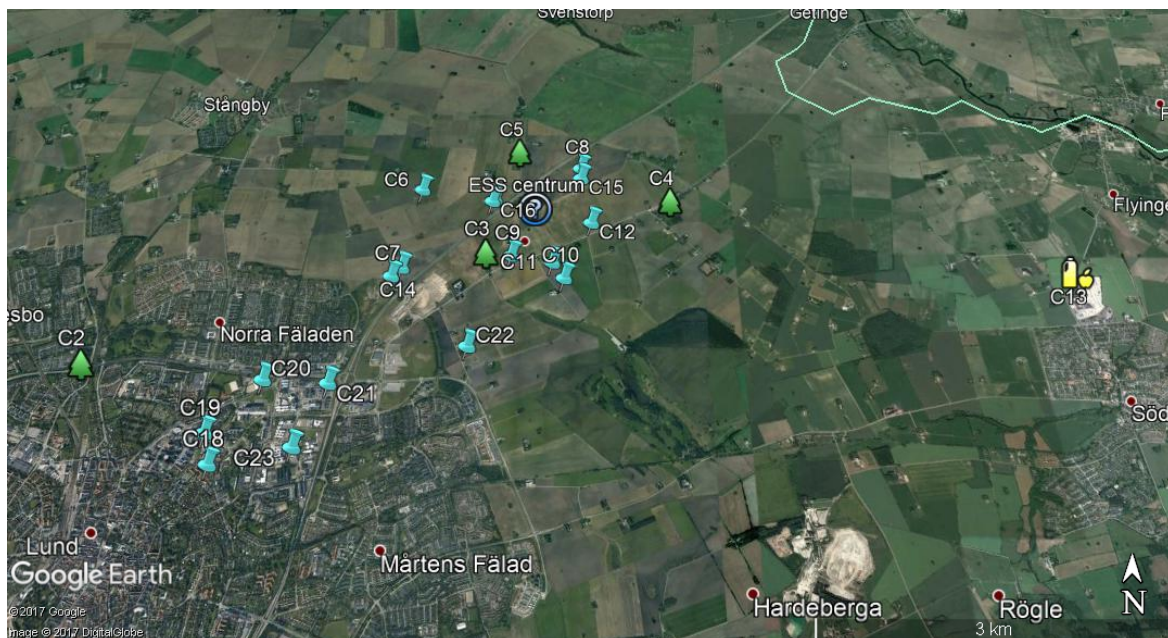
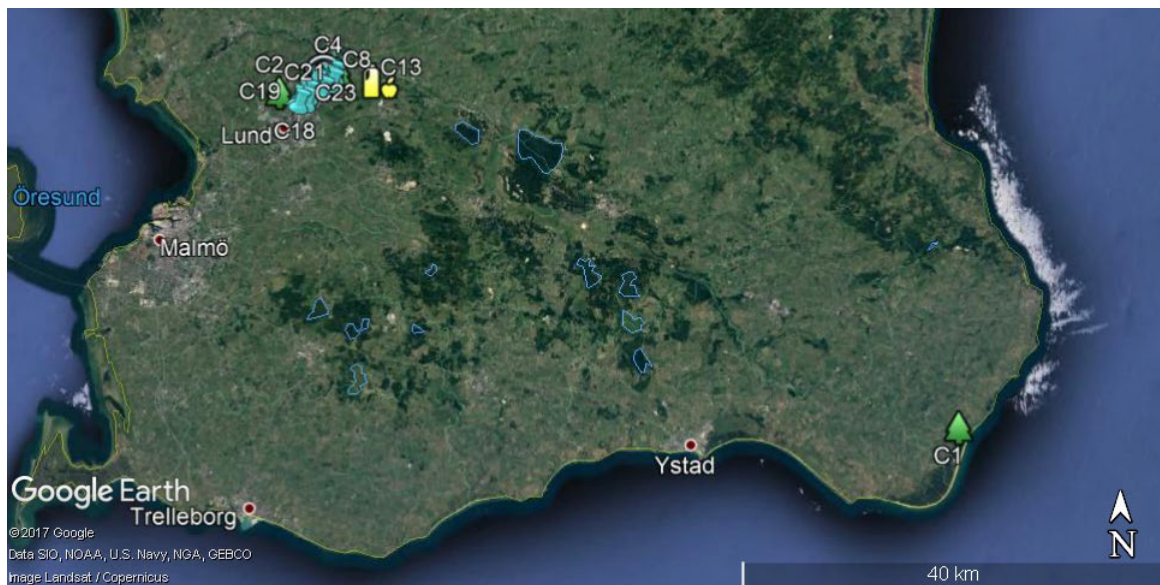


Figure 6. Sampling sites for ^{14}C measurements. 🌲 : Tree rings (2012-2016), grass, moss, crops, and fullerene monitors (the latter not on C5); 📌 : grass, moss and/or crops; 🍏 : grass, moss, fodder, milk. See Table 2 for more information about the sampling sites.

3. METHODS FOR SAMPLE COLLECTION AND ANALYSIS

3.1. Field gamma spectrometry and measurement of ambient dose equivalent rate

At the specific locations provided in Table 1 and Figure 1, *in situ* high-resolution gamma spectrometry was carried out based on the method provided in ANNEX B1 (Assessment of *in situ* and mobile gamma spectrometry and ambient dose equivalent). The spectral information from the HPGe *in situ* gamma radiation measurements, at specific sites (Table 1), was evaluated in terms of equivalent surface activity (surface deposition) or activity concentration (uniform distribution in the soil). The radionuclides evaluated using the surface deposition (Bq m⁻²) model were ⁷Be (477.6 keV) and ¹³⁷Cs (661.7 keV) and the radionuclides evaluated using the uniform depth distribution (Bq kg⁻¹) were ⁴⁰K (1460.8 keV), ²²⁶Ra (186.2 keV) and ²²⁸Ac (911.2 keV). For these measurements, two p-type HPGe detectors with relative efficiencies of 25% and 123% were used at the various sites (see footnote in Section 3.2.7).

The average ambient dose equivalent rate at each site was determined by a scintillator-based detector (AUTOMESS, Germany) positioned on a tripod 1 m above the ground. The variability in ambient dose equivalent rate over the surfaces (at least 30×30 m²) was determined using a back-pack LaBr₃:Ce detector system. ANNEX B1 provides the procedure for the assessment of the ambient dose equivalent rate using the mobile LaBr₃:Ce detector as well as the handheld scintillator-based detector.

An additional mapping of the dose rate variability between the sites (inter-site variability), was carried out by car-borne measurements using NaI(Tl) detectors (2×4 litre) on the roads within a few km around the ESS facility.

3.2. Sampling and measurement of soil, bioindicators, grass, crops, milk and sewage sludge

The procedures for sampling of soil, bioindicators, grass, crops, milk and sewage sludge are provided in ANNEX B2 (Sampling, sample preparation and laboratory measurements using high-resolution gamma spectrometry). All samples, except sewage sludge and water, were collected during the period from early to later summer in 2017.

3.2.1. Sampling of soil

At the sites where *in situ* gamma spectrometry was carried out (Table 1), two different kinds of soil samples were taken:

- STS for the depth distribution down to about 20 cm, divided and analysed in eight different layers;
- EPS as a surface layer, down to about 7 cm (analysed as one sample).

The average of five STS samples and four EPS samples was used to characterise the gamma activity concentration in the soil and the distribution down in the soil. At some sites, only EPS samples were collected, which are of special importance for a fresh deposition of radionuclides.

3.2.2. Sampling of bioindicators

Various bioindicators were collected depending on availability. Various types of cow fodder (commercial fodder pellets, silage, grass and clover) was collected at the one farmer with dairy cows. The bioindicators and the fodder were analysed for gamma-emitting radionuclides.

3.2.3. Sampling of grass

Grass was collected at various sites (where grass was available) over a surface corresponding to 1 m² and analysed for gamma-emitting radionuclides.

3.2.4. Sampling of crops

In connection with harvest (summer 2017), the available types of crops (rape, barley, wheat) were collected near the ESS facility and analysed for gamma-emitting radionuclides.

3.2.5. Sampling of milk

Samples of milk were collected at one single farmer with dairy cows. The milk samples were analysed for gamma-emitting radionuclides, as well as activity concentrations of ³H and ¹⁴C (see below).

3.2.6. Sampling of sewage sludge

Samples of sewage sludge were collected on a monthly basis (sub-samples taken and averaged over one month, from April 2017 to April 2018) from Källby sewage treatment facility (VA Syd) in Lund. The monthly samples were divided in two portions, one for gamma spectrometry analysis and one for analysis of ³H.

3.2.7. Laboratory high-resolution gamma spectrometry

For the assessment of the radionuclide concentration in the various samples, three different gamma spectrometers were used. All spectrometers are based on HPGe crystals (ORTEC, USA) in low background lead housings, but with varying relative efficiency¹:

- detector 4: 55%;
- detector 5: 92.5%;
- detector 7: 100%.

The methods, from collection of samples to storage of samples, are provided in ANNEX B2.

3.3. Sampling and measurements of ³H in water, milk and sewage sludge

Ground water and surface water collected at the sites given in Table 1, Figure 2 and Figure 3 were analysed for the activity concentration of ³H. In addition, the ³H activity concentration in sewage sludge and milk was analysed as well. The methods, from sample preparation to storage of the samples, are provided in ANNEX B3 (Sampling, sample preparation and measurements of ³H activity concentration using liquid scintillator counting).

3.4. Sampling and measurements of ¹⁴C in trees, milk and fullerene soot

3.4.1. Collection and pretreatment of annual tree rings

Carbon in the cellulose of each annual tree ring represents atmospheric CO₂ during the growing season of that year. A tree core drill was used to collect several drill cores from one well-grown tree at each site (spruce, fir or pine tree). At the Laboratory for Wood Anatomy and Dendrochronology at Lund University [13], the drill cores were divided into separate years (2012-

¹ Relative count rate to a NaI(Tl)-scintillator with the dimensions 76.2 mm × 76.2 mm (length × diameter) in the 1332 keV full energy peak from a ⁶⁰Co point source at a distance of 25 cm.

2016). At the Radiocarbon Dating Laboratory at Lund University [14] cellulose was extracted. For further information, see ANNEX B4 (^{14}C – Sampling, sample preparation and measurements of ^{14}C activity concentration using accelerator mass spectrometry).

3.4.2. Collection and pretreatment of vegetation and fodder samples

Details of collection and pretreatment (drying and cutting into small pieces) of vegetation and fodder samples are given in ANNEX B4. A few strands of one of the moss samples collected at the rural background site C1 were divided into two fractions: an upper part and a lower part. Another sample from the C1 site was divided into 3 parts.

3.4.3. Collection and pretreatment of milk

Milk was collected from the milk storage tank at the farm and freeze-dried (see ANNEX B4 for details).

3.4.4. Sampling using soot monitors

Monitors with fullerene soot of fossil origin were exposed in four 4-week periods to ambient air at the four sampling sites C1, C2, C3 and C4 (fullerene absorbs gases from the air, see ANNEX B4 for details).

3.4.5. Graphitization and ^{14}C measurement

Carbon was extracted from all organic samples and the ^{14}C content was measured at the Single Stage Accelerator Mass Spectrometry (SSAMS) facility at Lund University [15, 16]. The ^{14}C to ^{12}C ratios in the fullerene capsules were monitored in the SSAMS system, as well as a number of standard samples of known activity and graphitized background samples (referred to as Abs and W6). Levels were compared to ^{14}C absorbed into fullerene soot monitors in 2009, when a contamination of ^{14}C was observed in Lund [12]. See ANNEX B4 for details.

3.4.6. Storage of samples

Material from all organic samples were kept for the records of SSM. For all samples, Lund University store excess sample material (dried samples, not graphitized). See ANNEX B4 for details.

4. RESULTS

The results provided in ANNEX C (available upon request) are reported according to the SSM report “Granskningsrapport” SSM2014-127-1 [17]. The following principles have been applied in the reporting of the results:

- All detection limits (MDA) of the assessed radionuclides are provided.
- All results that are above half of the detection limit (MDA) are reported with the measured value.
- Measurement results that are less than half of the detection limit (MDA) are reported as one fourth of the MDA.

4.1. Assessment of the radiation background

4.1.1. Field gamma spectrometry

The results from the *in situ* gamma spectrometry measurements are provided in the ANNEX C (Table C 1, available upon request). The average activities found were, in terms of:

- equivalent surface activity: 249 Bq m⁻² (⁷Be), 121 Bq m⁻² (¹³⁷Cs);
- activity concentration: 407 Bq kg⁻¹ (⁴⁰K), 42 Bq kg⁻¹ (²²⁶Ra), 21 Bq kg⁻¹ (²²⁸Ac).

4.1.2. Ambient dose equivalent rate

The results from the assessments of the ambient dose equivalent rate at the various sites are presented in Table 3. On average in the surveyed area, within the sites (intra-site variability), the dose rate varied with 20%. Based on this, the average ambient dose equivalent rate at the studied sites was determined as 85±17 nSv h⁻¹.

The inter-site variability observed by the car-borne measurements was <3% for the entire area in Figure 7. The field-of-view of the detectors for the principal gamma-emitters is about 100 m on each side along the road path.

Table 3. Ambient dose equivalent rate ($\dot{H}^*(10)$) at the various sites.

Site	Description	$\dot{H}^*(10)$ (nSv h⁻¹)
1	Västra Odarslöv 341	88
2	Östra Odarslöv 651	88
3	Östra Odarslöv 164	88
4	Ladugårds-marken 461	98
5	Switchgear (SW of ESS)	94
6	Möllegården	76
7	Odarslövs k:a	84
13	Östra Odarslöv 264	81
17	Klosterängshöjden	85
21	Östra Torn 121	86
23	S:t Hans backar	84
24	Västra Odarslöv 421	84
25	Västra Odarslövs skola	84
26	ESS SW corner	84
27	ESS SE corner	91
28	ESS NE corner	100
29	ESS NW corner	103
30	Kopparstaden (windmill)	79
32	Dammstorpsvägen 16	84
33	Utmarksvägen 55	79
34	MAX IV area	82
37	Utmarksvägen 39	80
39	Utmarksvägen 23	80
40	Östra Odarslöv 301	81
41	Östra Odarslöv 291	82
42	Ladugårdsmarken (cell tower)	83
43	Östra Odarslöv 541 (slate quarry)	79
44	Kärrpängavägen 6	79
45	Kemicentrum	84

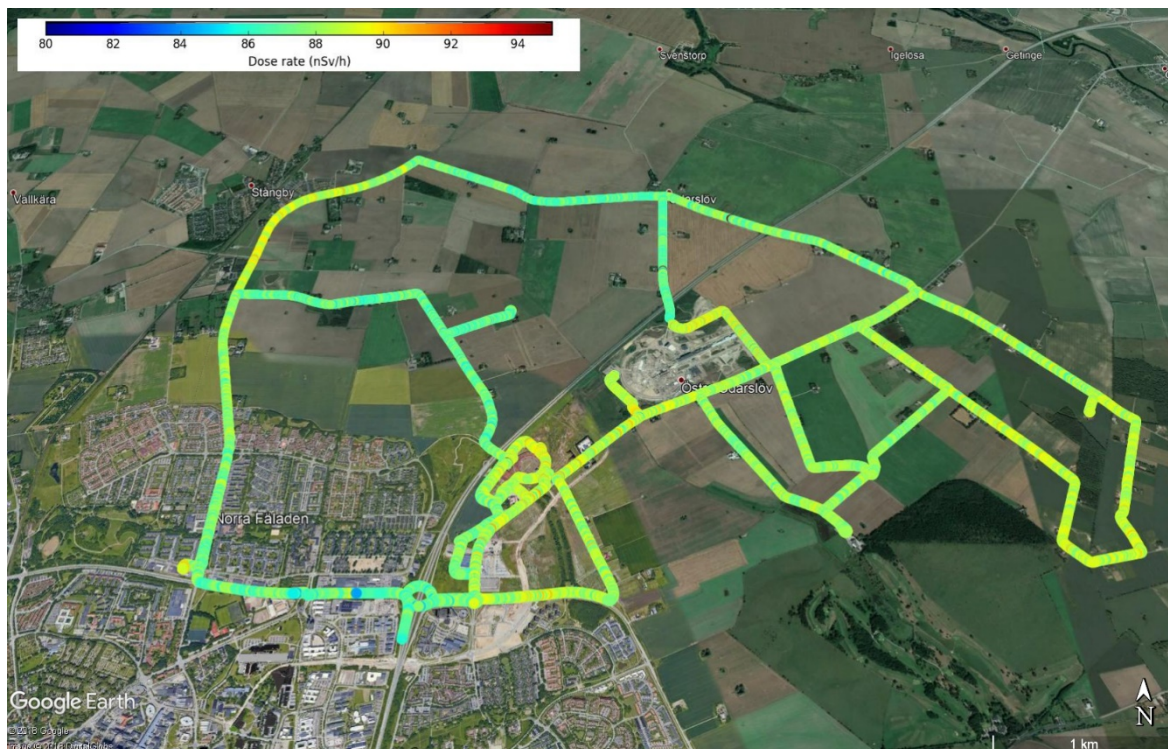


Figure 7. Gamma dose rate variability around the ESS facility, as measured by NaI(Tl) detectors in a car.

4.2. Analysis of the activity concentration of gamma-emitting radionuclides in soil, grass, milk, crops, sewage sludge and bioindicators

4.2.1. Soil samples

The activity concentration in soil per dry-weight (d.w.) of ^{226}Ra (^{238}U daughter), ^{137}Cs , ^{40}K and ^{228}Ac (^{232}Th daughter), and their respective MDA values (Bq kg^{-1}) as measured in various laboratory-configured HPGe detectors is provided in the ANNEX C (Table C 2, available upon request). Figures 8-11 graphically illustrate the activity concentration of the investigated radionuclides, as assessed from the EPS soil cores, and calculated as the average value of the 4 cores at each site.

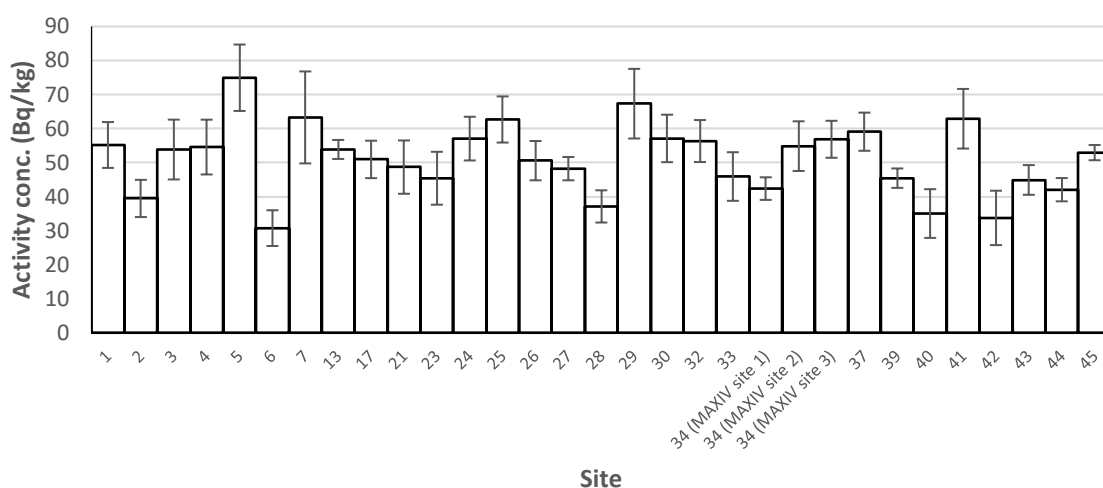


Figure 8. Activity concentration of ^{226}Ra in 7 cm surface soil at the sites indicated. The uncertainty bars represent 1 standard uncertainty of the mean.

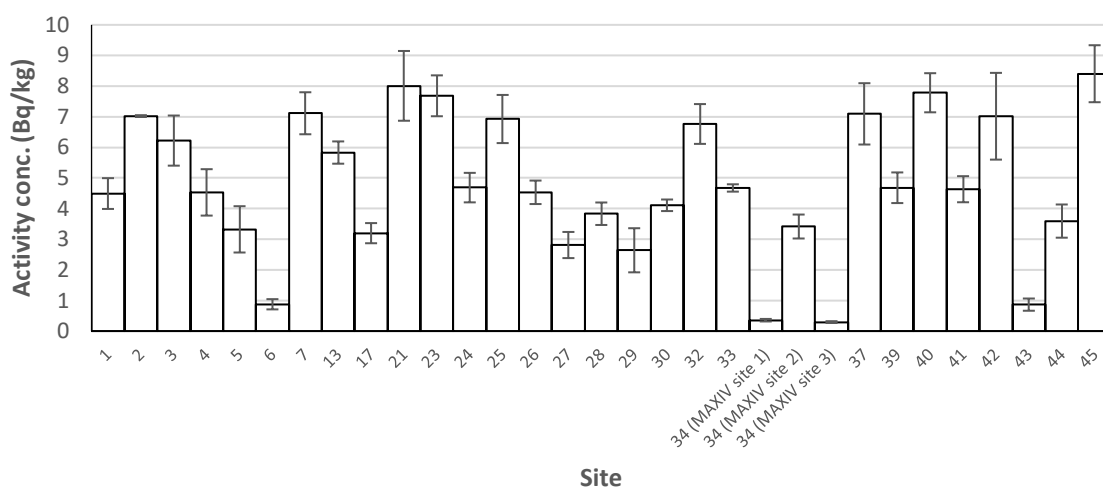


Figure 9. Activity concentration of ^{137}Cs in 7 cm surface soil at the sites indicated. The uncertainty bars represent 1 standard uncertainty of the mean.

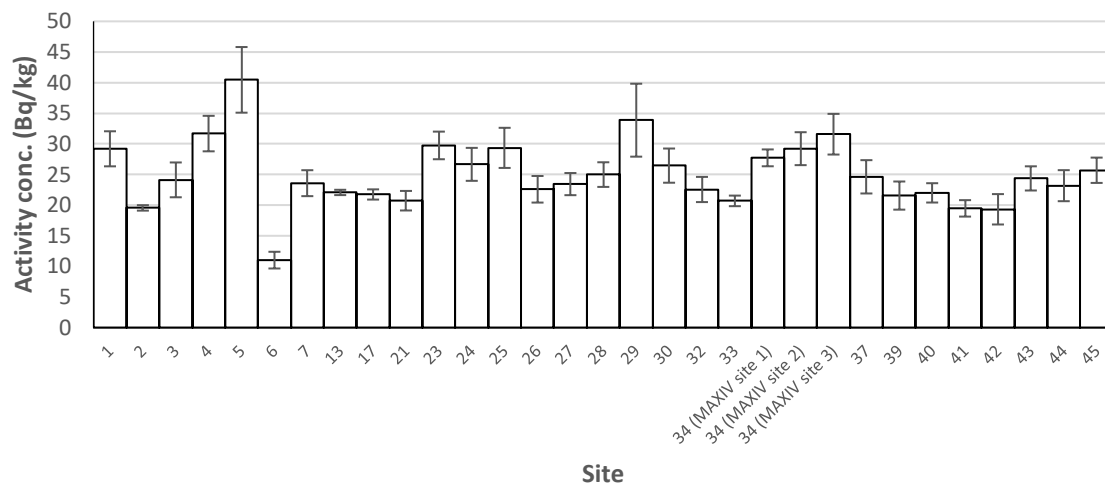


Figure 10. Activity concentration of ^{228}Ac in 7 cm surface soil at the sites indicated. The uncertainty bars represent 1 standard uncertainty of the mean.

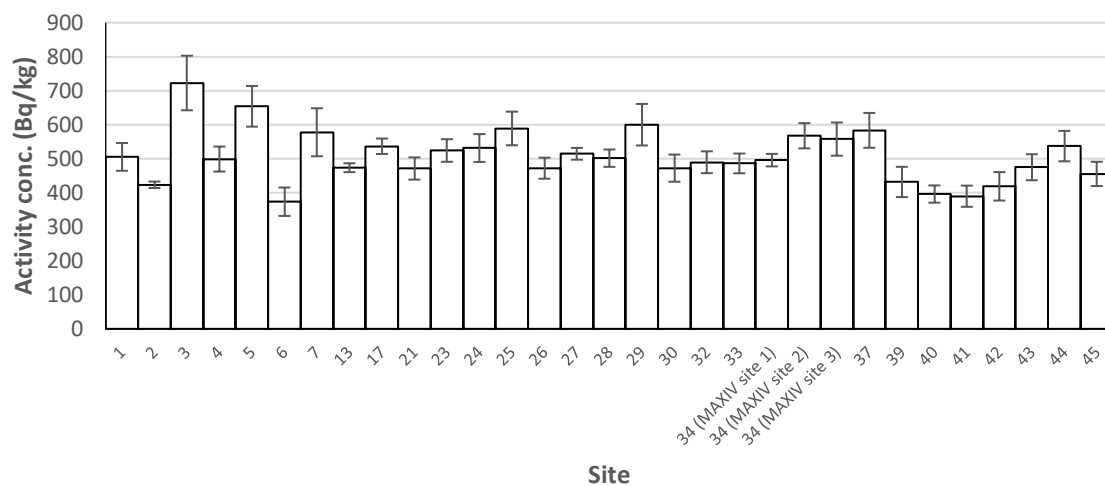


Figure 11. Activity concentration of ^{40}K in 7 cm surface soil at the sites indicated. The uncertainty bars represent 1 standard uncertainty of the mean.

The activity concentration (A_{conc}) in the 20 cm deep STS soil cores can be described as homogenously distributed for the natural radionuclides (^{226}Ra , ^{228}Ac , ^{40}K), with average activity concentrations as provided in Table 4.

Table 4. Average activity concentration in the 20 cm deep STS cores for the natural occurring radionuclides investigated. The uncertainties are given as the standard deviation divided by the mean activity for each radionuclide distributed homogenously within the core.

Nuclide	A_{conc} (Bq kg ⁻¹)
^{226}Ra	75±14
^{228}Ac	35±2
^{40}K	694±104

The vertical activity distribution of ^{137}Cs in the soil may be described by two typical distributions: i) homogenous and ii) exponential. The majority of the sites investigate have a homogenous distribution, with low activity concentration throughout the soil 0-20 cm. In Figure 12 are two examples illustrating the two typical ^{137}Cs activity distributions observed at the various sites.

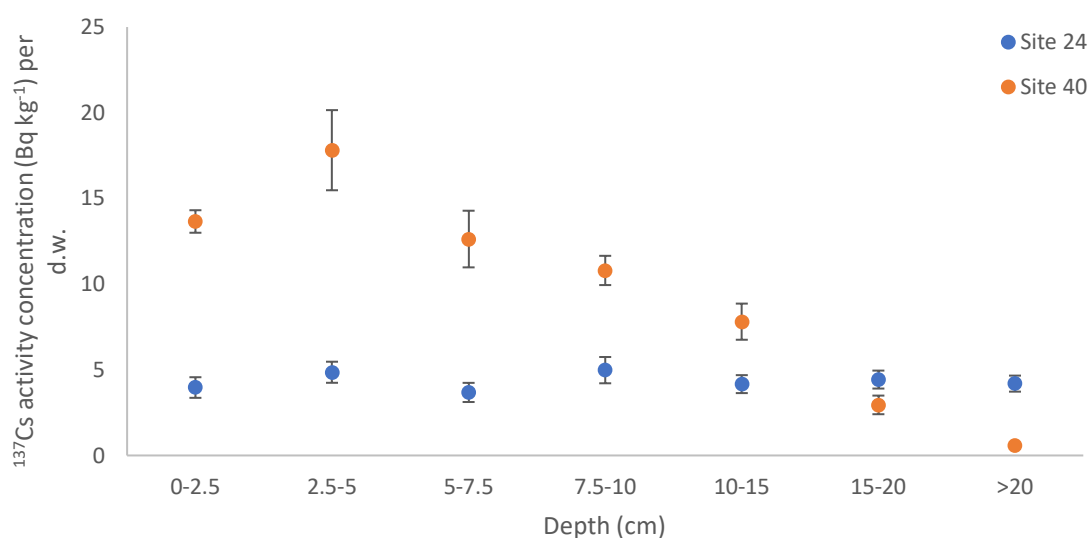


Figure 12. Examples of the ^{137}Cs activity concentration down in soil at Site 24 (homogenous distribution) and Site 40 (exponential distribution).

At some sites (2, 13, 21, 32, 40, 45), the main part of the ^{137}Cs activity concentration was in the top soil layers. A possible explanation to this, is that e.g. grass surfaces in private gardens and Site 45 have not been touched or cultivated since 1986 (^{137}Cs deposited after the Chernobyl accident). Another observation, in terms of ^{137}Cs activity distribution in the soil, is what is observed at the Site 34 (MAX IV). At this site the ^{137}Cs activity concentration in the soil is significantly lower than at the other sites, possibly due to the soil being put there from deep (>1 m) soil layers when constructing the site.

4.2.2. Grass samples

The results of the laboratory gamma spectrometry of grass samples collected at various sites are provided in ANNEX C (Table C 3). Depending on individual measuring time, the minimum detectable activity (MDA) may vary. The activity concentrations of the radionuclides ^{226}Ra , ^{137}Cs and ^{228}Ac are below the MDA (except for one grass sample with ^{228}Ac activity concentration slightly above the MDA). The ^{40}K activity concentration in the various grass samples range from $137\pm24\text{ Bq kg}^{-1}$ to $1583\pm244\text{ Bq kg}^{-1}$ (on average 774 Bq kg^{-1}) during the sampling period (July–November 2017), see Figure 13.

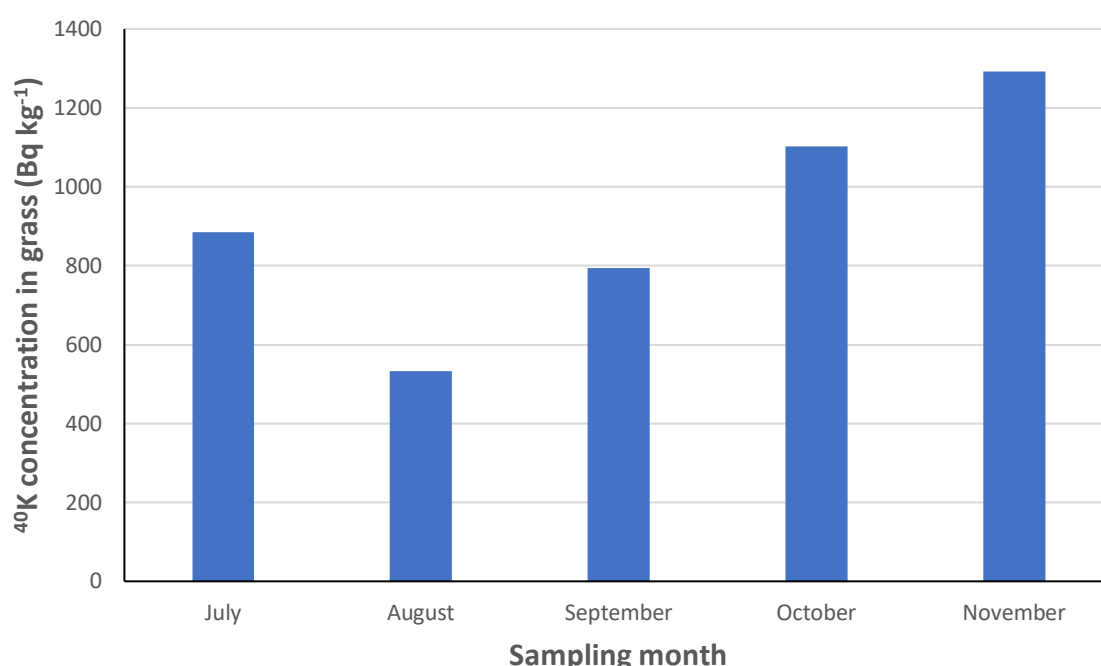


Figure 13. Average activity concentration (Bq kg^{-1}) of ^{40}K in grass samples for each sampling month (2017).

4.2.3. Milk samples

Two milk samples have been collected from one single farmer (Site 22) and analysed for gamma-emitting radionuclides. The activity concentration of ^{40}K was measured as $67\pm8\text{ Bq l}^{-1}$ (MDA at 24 Bq l^{-1}) and $54\pm8\text{ Bq l}^{-1}$ (MDA at 26 Bq l^{-1}). No other radionuclides were identified with significance in these samples (see ANNEX C (Table C 4, available upon request) for details).

4.2.4. Samples of crops

The results of the laboratory gamma spectrometry of the crop samples are provided in ANNEX C (Table C 4, available upon request). This table also includes activity concentration in forage samples collected at the farmer (Site 22) where milk was sampled.

The measured activity concentration for ^{226}Ra , ^{137}Cs and ^{228}Ac were below the MDA values for all of the measured samples. The activity concentration (mean ± 1 standard uncertainty of the mean) of ^{40}K was generally lower in crops samples (179 Bq kg^{-1}) as compared to grass and it was observed that the different parts of sugar beet had various ^{40}K activity concentrations: $1749\pm75\text{ Bq kg}^{-1}$ (haulm), $441\pm21\text{ Bq kg}^{-1}$ (root outer layer) and $258\pm14\text{ Bq kg}^{-1}$ (root).

4.2.5. Samples of sewage sludge

The concentrations of gamma emitting radionuclides in sewage sludge are provided in ANNEX C (Table C 5, available upon request).

All the radionuclides studied had an activity concentration (per d.w.) above the MDA, except for ^{137}Cs that was below the MDA in all but one sample (January 2018). The average activity concentrations, observed during the one-year period, were 112 Bq kg^{-1} (^{226}Ra), 50 Bq kg^{-1} (^{228}Ac) and 144 Bq kg^{-1} (^{40}K), respectively. Apart from the data in the Annex, ^{131}I was found in several of the sewage sludge samples analysed. If decay corrected, to the 15th of the month of the sample collection, the ^{131}I activity concentration was in the order of 500 to 5000 Bq kg^{-1} . In the samples where no ^{131}I was observed, it is likely that the time between sample collection and measurements was too long for ^{131}I to be detected. Furthermore, it is expected that other medically used radionuclides might be found if the time between sampling and measurements is shortened [18]. This means that we can expect measurable concentrations also of other radionuclides used for therapy (e.g., ^{177}Lu , ^{90}Y , ^{225}Ac) and diagnostics (e.g. ^{111}In , $^{99\text{m}}\text{Tc}$, ^{68}Ga).

4.2.6. Samples of bioindicators

The activity concentrations per d.w. (Bq kg^{-1}) for the radionuclides ^{226}Ra , ^{137}Cs , ^{228}Ac , and ^{40}K as well as the respective MDA values (Bq kg^{-1}) are provided in ANNEX C (Table C 6, available upon request) for various samples of bioindicators (lichen and moss).

As the amount of sample material from many of the sites was very small (about 10-20 g), it was expected to be difficult to determine the concentration of ^{226}Ra , ^{228}Ac , ^{40}K and ^{137}Cs by means of gamma spectrometry. However, the ^{40}K concentration in *Pleurozium schreberi* and *Xanthoria parietina*, $342 \pm 95 \text{ Bq kg}^{-1}$ and 224 Bq kg^{-1} , respectively, was significantly above the MDA. After the start of ESS these types of samples will also be of interest for analysis of alpha-emitters and heavy metals.

4.2.7. Quality assessment of the gamma spectrometry measurements

Efficiency calibrations using reference sources from AEA Technology were used for a number of geometries (e.g. 200 ml unity density, 200 ml density 1.5) [19, 20]. Standard samples from the International Atomic Energy Agency (IAEA) [21-25] and from an aliquot of a standard solution (QX48) have been used for constancy control of the detector calibrations over time for all the HPGe-detectors used in the current project.

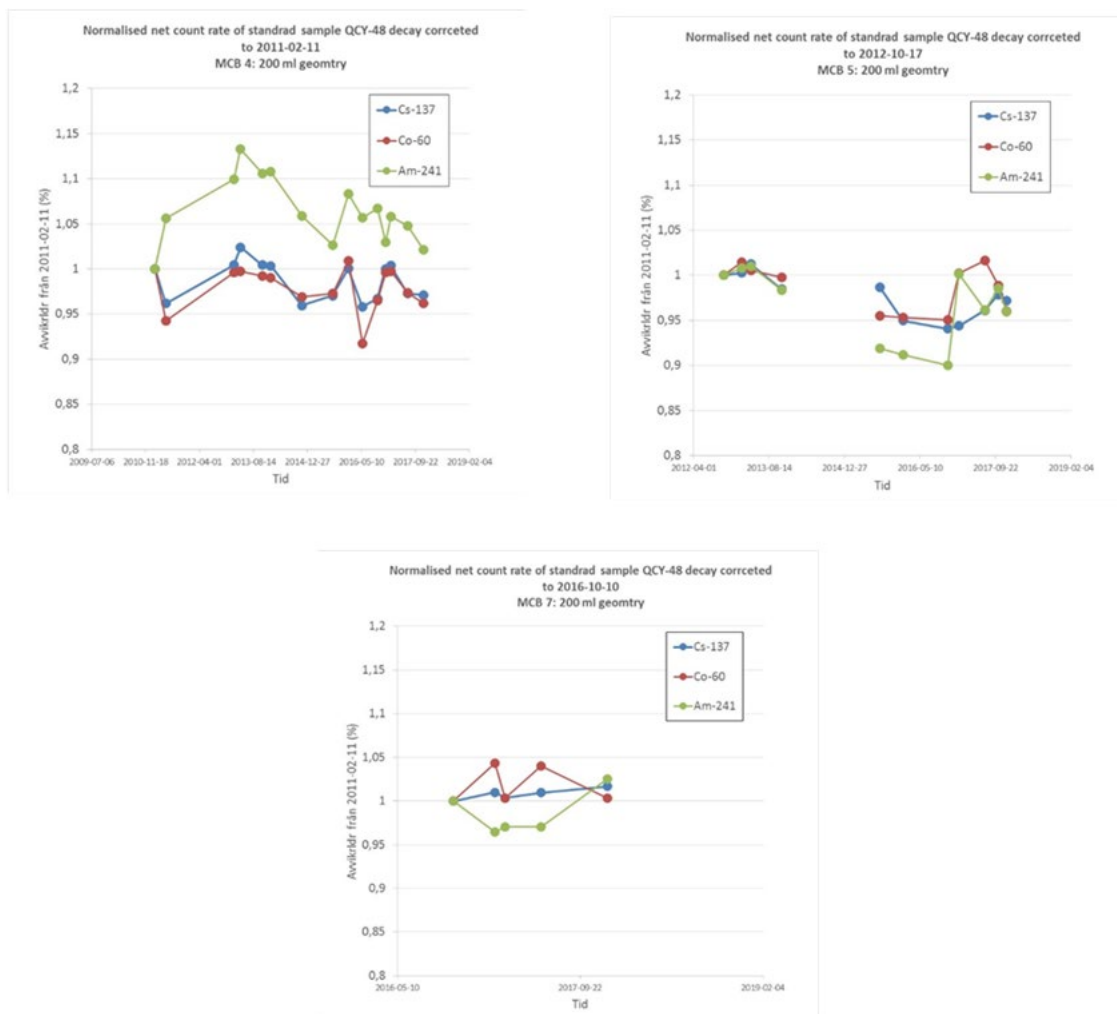


Figure 14 Top left frame: constancy control over time for various radionuclides (^{137}Cs , ^{60}Co , ^{241}Am) for a 55% HPGe detector (MCB4); Top right frame: constancy control over time for various radionuclides (^{137}Cs , ^{60}Co , ^{241}Am) for a 92.5% HPGe detector (MCB5); Lower frame: constancy control over time for various radionuclides (^{137}Cs , ^{60}Co , ^{241}Am) for a 100% HPGe detector (MCB7).

The activity concentration (Bq kg^{-1}) of the samples was calculated by:

$$A = \frac{n_{\text{net}}}{m_{\text{sample}} \times \varepsilon_{\text{abs}} \times n_{\gamma}} \times k_{\text{dec}} \times k_{\text{eff}} \quad \text{Eq. 1}$$

where k_{dec} is the decay correction factor to the time of sampling, m_{sample} is the mass of the sample used for gamma spectrometry, and ε_{abs} is the absolute efficiency (cps/dis) for the specific measuring geometry. The factor k_{eff} is a photon energy dependent correction factor that has been applied to adjust for any discrepancy from the original reference calibration detected by the QA-assurance. The mass of sample may either refer to dry mass or fresh mass, depending on the type of sample. In all cases, it will be specified which of the two is used in a given sample.

The stationary HPGe detectors used in this study were calibrated in 2012 by the aforementioned calibration samples [19, 20]. Ever since, the efficiency, resolution and other parameters have been checked every 2nd or 3rd month using the calibration source. To perform a thorough validation of the calibration, a new standard source containing several radionuclides with gamma energies ranging from 47 keV (^{210}Pb) to 1836 keV (^{88}Y) was obtained in the spring of 2018 [26]. New calibration sources, containing saw dust, water (0.01 M HCl) and soil were

prepared, for various geometries. For each geometry and sample density, measurements were carried out during the summer 2018 in the three stationary HPGe detectors. The results showed that the current calibration from 2012 was still valid.

4.3. Analysis of ^3H in water and some bioindicators

4.3.1. ^3H in ground water and surface water

The activity concentrations (Bq l^{-1}) of ^3H in various water bodies (ground water; surface water; tap water; drinking water), relative to a background water sample (deep-well water), are presented in ANNEX C (Table C 7, available upon request). All of the water samples analysed had ^3H levels below the MDA (14 Bq l^{-1} and 29 Bq l^{-1}), only three water samples were above half of the MDA.

4.3.2. ^3H in sewage sludge

The activity concentration (Bq l^{-1}) of ^3H in sewage sludge (monthly between April 2017 and April 2018) is provided in ANNEX C (Table C 8, available upon request). The ^3H activity concentration was below the MDA (varying from 2.6 Bq l^{-1} to 29 Bq l^{-1}) in all but two samples. The sludge sample collected in June 2017 was slightly above the MDA (14 Bq l^{-1}) with a ^3H activity concentration of $16 \pm 3 \text{ Bq l}^{-1}$, while the corresponding value in January 2018 was $2.9 \pm 0.7 \text{ Bq l}^{-1}$ (MDA 2.7 Bq l^{-1}).

4.3.3. ^3H in bioindicators

A limited amount of bioindicators were analysed for the ^3H concentration, including milk and sugar beet, these results are provided in ANNEX C (Table C 9, available upon request). The observed ^3H levels in these bioindicators were below half the MDA level (29 Bq l^{-1}).

4.3.4. Quality assurance of the ^3H assessments

The results of the liquid scintillator measurements were assured using a reference tritium solution (TRY44 number R8/12/123 by Eckert and Ziegler, Germany) with a reported uncertainty of 1.5%. A calibration curve was carried out where the ^3H measurement were found to be linear from 0 to 100 Bq l^{-1} . A quenching curve was also obtained using the method described by the cocktail provider Perkin Elmer [27].

4.4. ^{14}C analysis

All results of the ^{14}C analysis are reported in ANNEX C (Table C 10, Table C 11, Table C 12, Table C 13, Table C 14, Table C 15, available upon request). The results are expressed as $F^{14}\text{C}$ [28, 29], see ANNEX B4 for definition. Basically, $F^{14}\text{C}$ values corresponding to naturally produced ^{14}C are around 1, while the maximum $F^{14}\text{C}$ values observed in 1963 after the extensive testing of atmospheric nuclear weapons in the late 1950s and early 1960s was around 2. Today, $F^{14}\text{C}$ in atmospheric CO_2 is approaching the pre-bomb levels. Typical $F^{14}\text{C}$ values found in environmental samples in the vicinity of light water reactors display an excess of less than 10% compared to $F^{14}\text{C}$ values at sites remote from such facilities [30, 31].

4.4.1. Quality assessment

The results of the measurements of the standard samples IAEA C7, SRM 4990B and SRM 4990C are shown in Figure 15. All samples were within 3σ of the nominal values, and only 2 out of 44 samples lied outside the 1σ range.

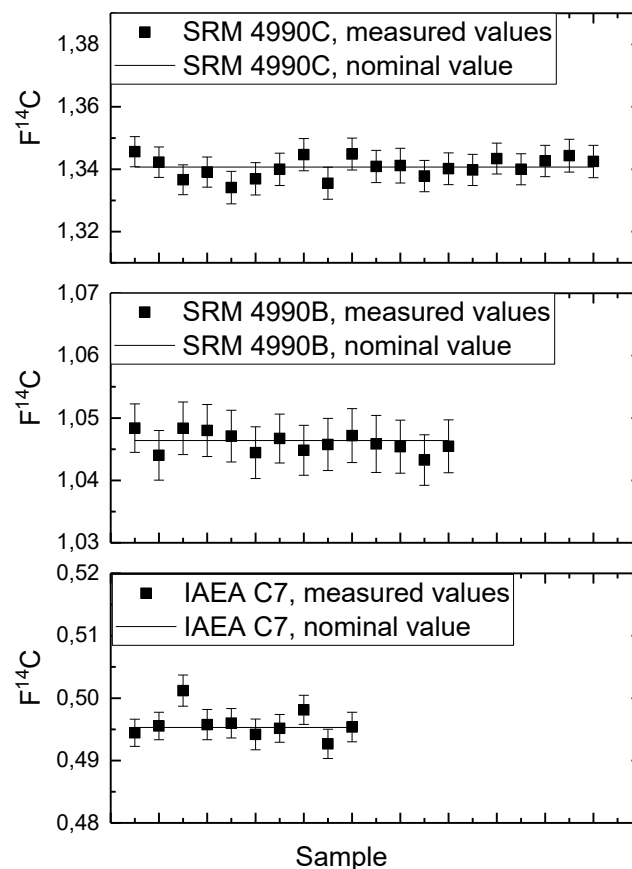


Figure 15. Results of the ^{14}C measurements of standard samples IAEA C7, SRM 4990B (also known as OxI) and SRM 4990C (also known as OxII). Uncertainty bars refer to 1σ .

4.4.2. Organic material

The results of the annual tree ring analysis are graphically presented in Figure 16. The average of monthly $F^{14}C$ values in CO_2 , collected during summer time (May-August) at the background station Schauinsland in Black Forest in Germany (1205 m above sea level; 47°55'N, 7°54'E), serve as additional reference values [32, 33]. Moderate air pollution from the densely populated and heavily industrialized Rhine valley is expected to reach the Schauinsland station, which is also influenced by boundary layer air [32]. Compared to the Schauinsland and the Borby data (C1), the sites in Lund (C2-C5) showed no significant contamination of ^{14}C .

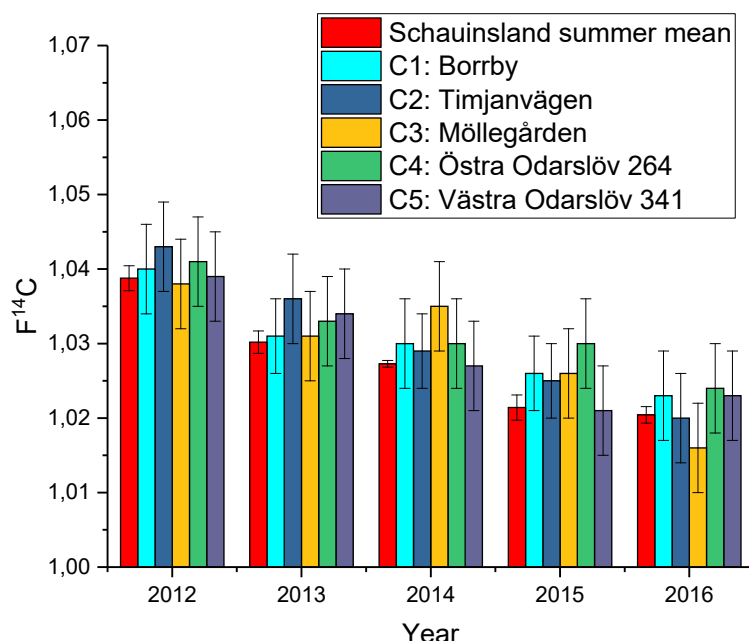


Figure 16. Results of the ^{14}C measurements of annual tree rings. The uncertainty of the Schauinsland data is the standard deviation of monthly F^{14}C data from May to August ($N=4$) [32, 33], while the uncertainties of sites C1-C5 is the analytical uncertainty.

The tree ring data were used to estimate the ^{14}C activity concentration in atmospheric CO_2 for years 2012 to 2016, see Table 5 (temperature $T=293\text{ K}$ and $\delta^{13}\text{C} = -9\text{‰}$ have been used in the calculations, performed according to ANNEX B4).

Table 5 Estimated activity concentration of $^{14}\text{CO}_2$ in southern Sweden for years 2012-2016.

Year	Average F^{14}C ($\pm \text{SUM}$)	Average CO_2 molar parts per million [34]	Activity concentration of $^{14}\text{CO}_2$ in air (Bq/m^3)
2012 ($N = 5$)	1.040 ± 0.001	394	0.047
2013 ($N = 5$)	1.033 ± 0.001	397	0.047
2014 ($N = 5$)	1.030 ± 0.001	399	0.048
2015 ($N = 5$)	1.026 ± 0.001	401	0.048
2016 ($N = 5$)	1.021 ± 0.001	404	0.048

The results of ^{14}C analysis of the vegetation samples are shown in Figure 17a. For the grass data from 2017 ($N=13$), the average F^{14}C value was 1.014 (SD: 0.006; SUM 0.002). According to Grubb's test, the August sample of site C13 is an outlier (possibly due to local contamination of fossil carbon). Removing this outlier, the average grass F^{14}C value for southern Sweden in 2017 was 1.015 (SD: 0.003; SUM 0.001). The crops/fodder samples from 2017 ($N=21$) showed an average F^{14}C value of 1.018 (SD: 0.005; SUM: 0.001). The mean F^{14}C value of the grass samples was not significantly different from the mean F^{14}C value of the crop/fodder samples ($p>0.05$, one-way ANOVA), see Figure 17b.

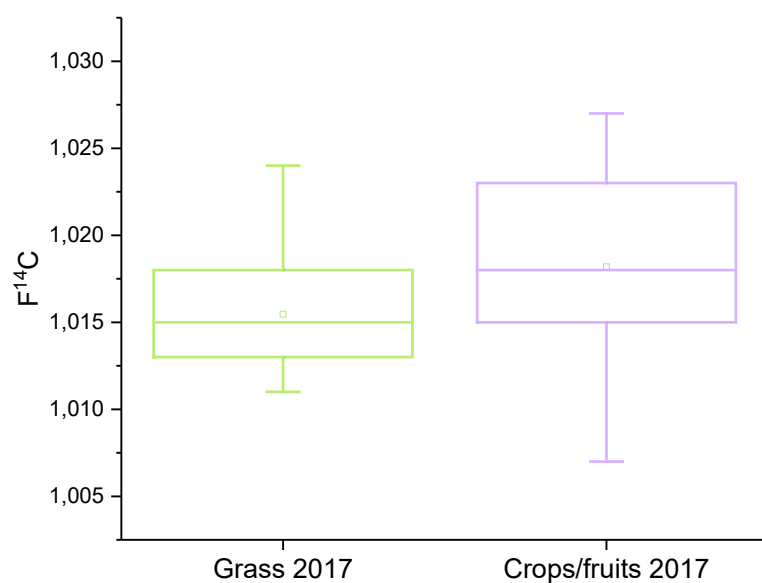
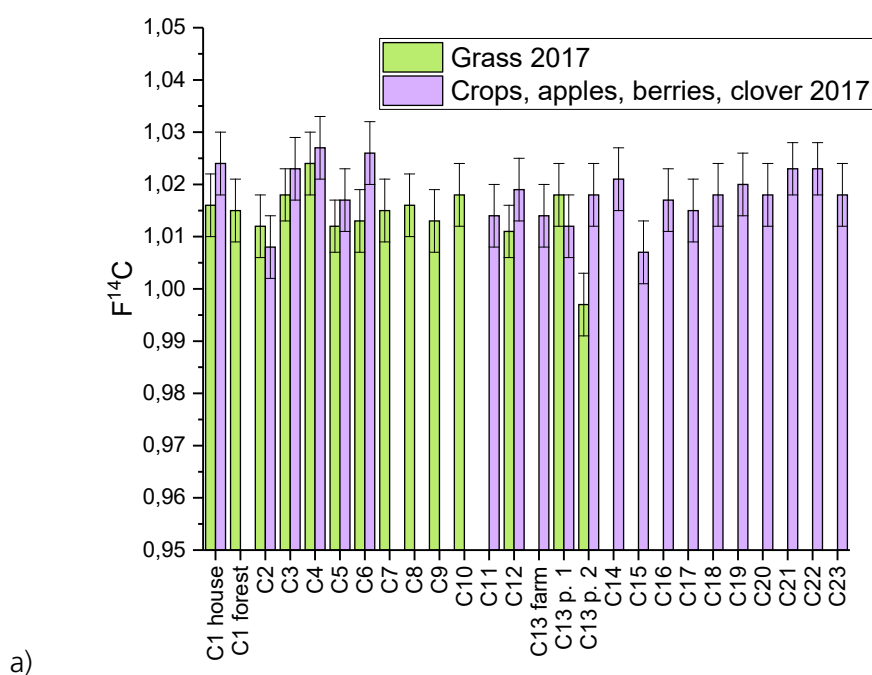


Figure 17. a) Results of the ^{14}C measurements of grass and crops/fruits from 2017. b) Box plot showing that the mean $F^{14}C$ value of grass was not significantly different from the crops/fruit data of 2017 ($p > 0.05$, one-way ANOVA).

Figure 18 shows the results of the ^{14}C measurements at the dairy farm at site C13. For comparison, the $F^{14}C$ values of vegetation from the rural and urban background sites C1 and C2 are included. As mentioned above, the grass sample from August 2017 is an outlier according to Grubb's test. Taking this into account, the two milk samples reflect the $F^{14}C$ values of the diet of the cows very well (see Figure 18).

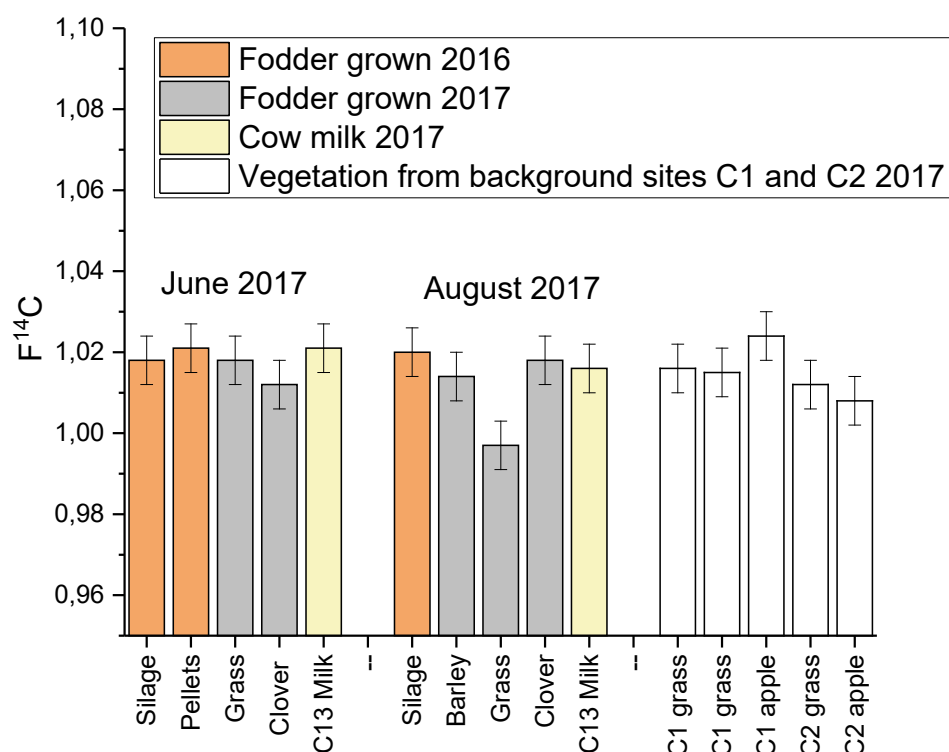


Figure 18. Results of the ^{14}C measurements at the dairy farm at site C13, compared to vegetation samples at the rural and urban background sites C1 and C2. The grass sample from August 2017 is an outlier according to Grubb's test.

The results of the moss samples are visualized in Figure 19. Compared to the grass samples at the same site (also included in Figure 19), the ^{14}C values were very similar, except at site C6 (however, the moss and grass values of site C6 overlapped within 3σ). This observation indicates that the moss sample of site C6 was older than the rest of the moss samples. The moss samples at site C1 were split into fractions: lower and upper 3 cm of 6 cm strands (C1 house), and lower, middle and upper 3 cm of 9 cm strands (C1 forest). Although not confirmed statistically, both C1 samples indicated a decreasing $F^{14}\text{C}$ value with height, implying that the lower parts of the moss samples were older than the upper parts.

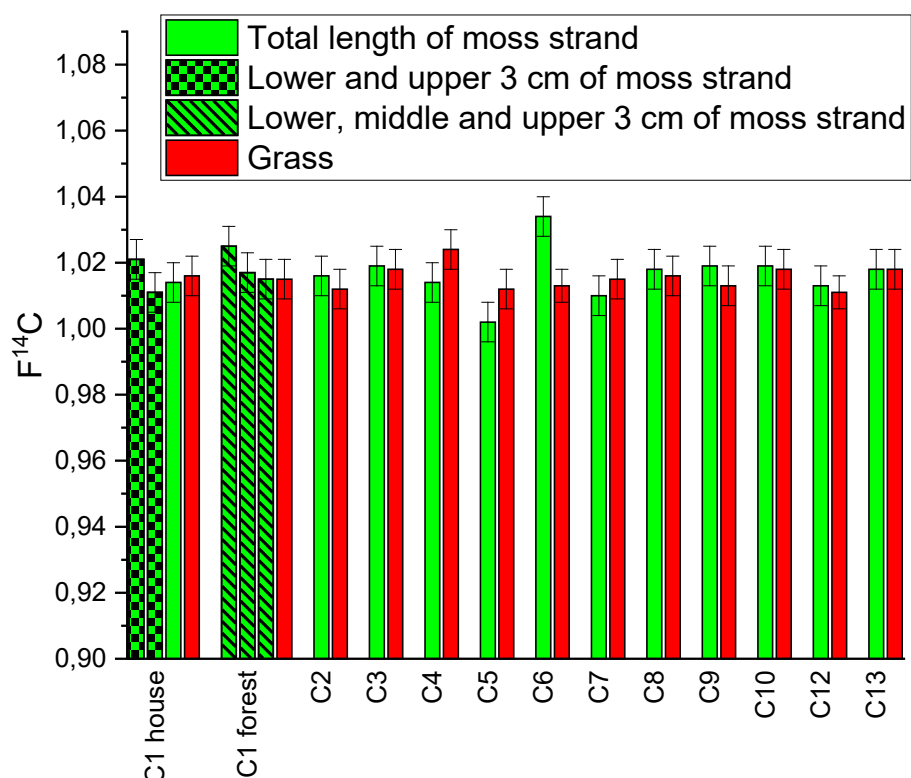


Figure 19. Results from ¹⁴C measurements of moss samples, compared to grass samples collected at the various sites.

The average F¹⁴C value for all organic samples measured ($N = 57$, tree ring samples not included) is 1.017 (SUM 0.001), corresponding to 228 Bq/kg C (using $\delta^{13}\text{C} = -25\text{‰}$, see ANNEX B4). The ¹⁴C activity concentration in various sample types is estimated in Table 6 ($\delta^{13}\text{C} = -25\text{‰}$ has been used for all samples in the calculations, performed according to ANNEX B4).

Table 6 Estimated activity concentration of ¹⁴C various sample types in southern Sweden in 2017. Values of proportion carbon are taken from Ref [35].

Material	Proportion carbon ($\frac{\text{g carbon}}{\text{kg wet weight}}$)	Activity concentration of ¹⁴ C (Bq/kg wet weight)
Cow milk	65 (62 to 69)	15 (14 to 16)
Grass or green feed	100 (40 to 160)	23 (9 to 36)
Silage	130 (65 to 180)	30 (15 to 41)
Grains	390 (360 to 430)	89 (82 to 98)
Fruits	62 (31 to 100)	14 (7 to 23)

4.4.3. Fullerene soot monitors

Figure 20 shows the number of counts registered in the ^{14}C window of the detector during 120 s as a function of measured ion beam current of $^{12}\text{C}^-$ for all fullerene soot samples. The background count rate, e.g. due to cosmic radiation, in the ^{14}C detector was estimated by linear regression to be to 2.06 counts in 120 s. This number was extracted from all ^{14}C measurements prior to calculating the $^{14}\text{C}/^{12}\text{C}$ ratio.

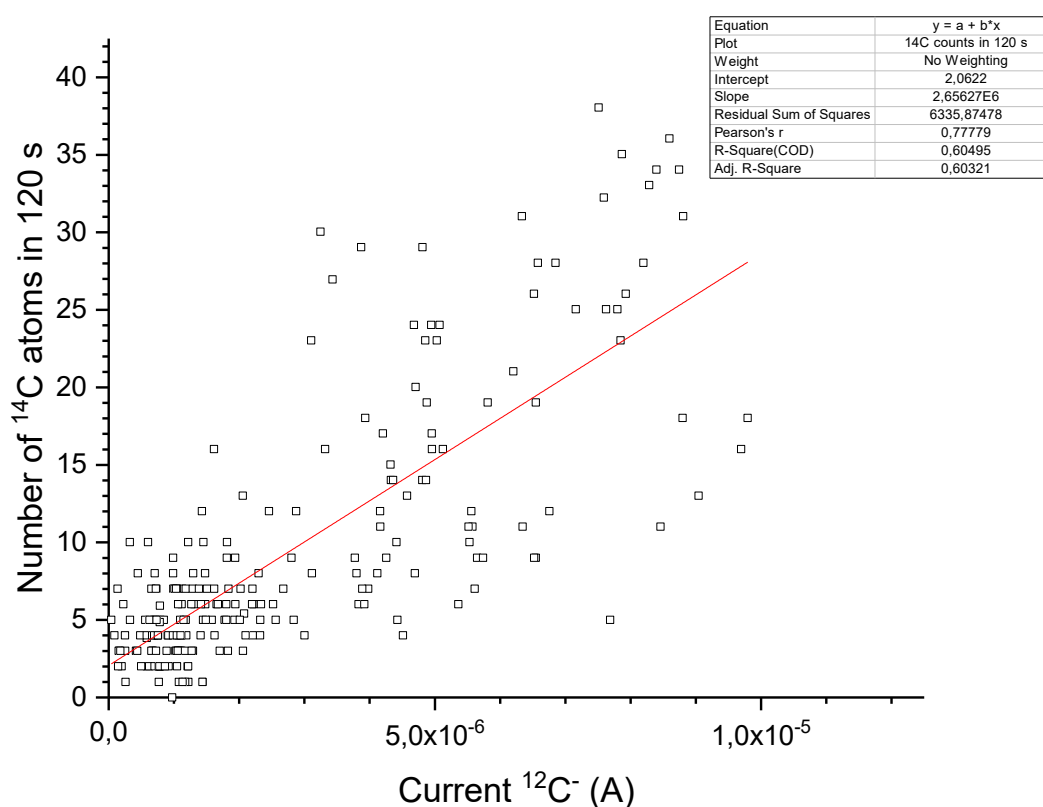


Figure 20. Number of counts registered in the ^{14}C window of the detector during 120 s as a function of measured ion beam current of $^{12}\text{C}^-$ for all fullerene soot samples.

The results of the SSAMS measurement ($^{14}\text{C}/^{12}\text{C}$ ratio corrected for background) of the 19 fullerene soot monitors are shown in Figure 21. The graph shows all ^{14}C measurements of soot monitors at the sites C1-C4, the unexposed soot (blank soot) as well as graphitized fossil carbon (Abs1 and W6C). Included in the figure is the maximum level observed value in 2009, a soot monitor exposed to ambient air for 14 days [12]. The $^{14}\text{C}/^{12}\text{C}$ ratios of clean air CO_2 in 2009 and 2017 are also included in the figure for comparison. None of the soot monitors of 2017 showed any significant degree of contamination.

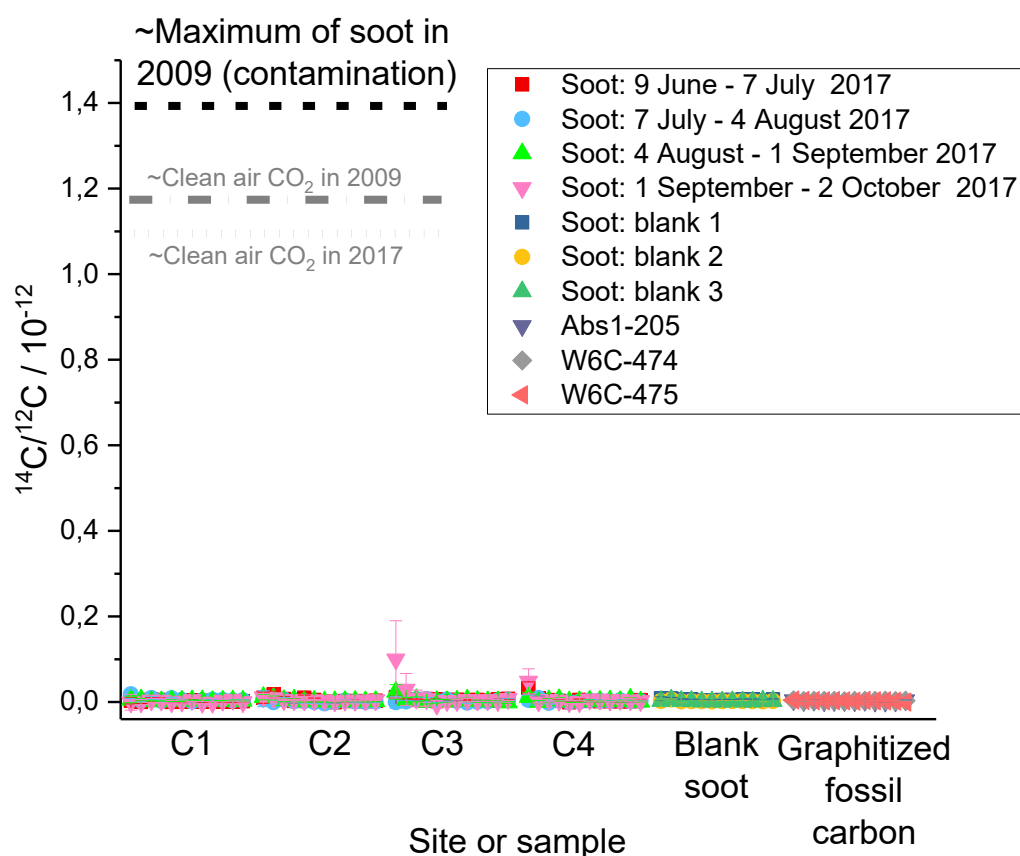


Figure 21. Measured $^{14}\text{C}/^{12}\text{C}$ ratios of soot monitors at the sites C1-C4, unexposed soot (blank soot) as well as graphitized fossil carbon (Abs1 and W6C).

Figure 22 shows the results of the fullerene soot monitors in more detail. The ratios of the main part of the samples from sites C1-C4 were very close to what is observed in unexposed fossil samples (soot blanks and graphitized carbon). The few values that display somewhat higher $^{14}\text{C}/^{12}\text{C}$ ratios are associated with large uncertainties due to the low currents of ^{12}C (see Figure 23) and very low count rates of ^{14}C at the first of the 12 measurements.

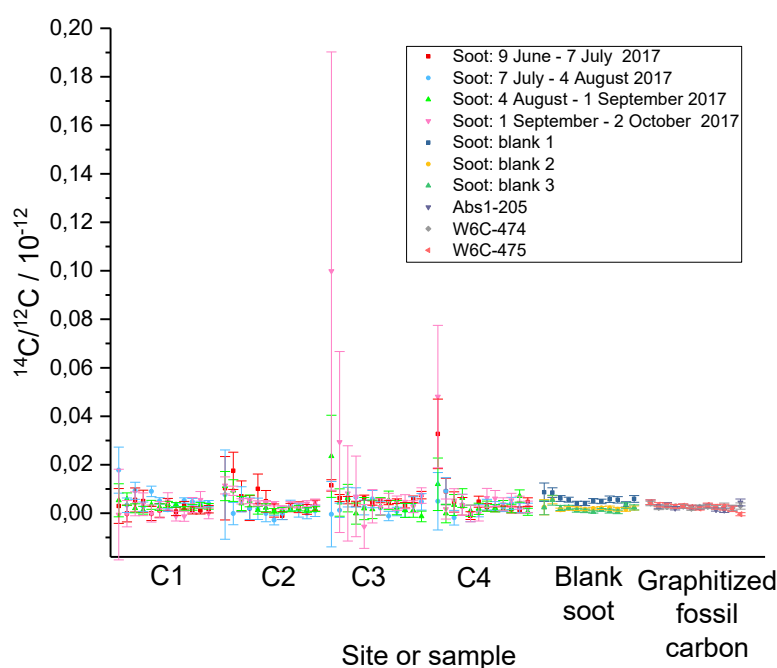


Figure 22. Measured $^{14}\text{C}/^{12}\text{C}$ ratios of soot monitors at the sites C1-C4, unexposed soot (blank soot) as well as graphitized fossil carbon (Abs1 and W6C), in more detail compared to Figure 21.

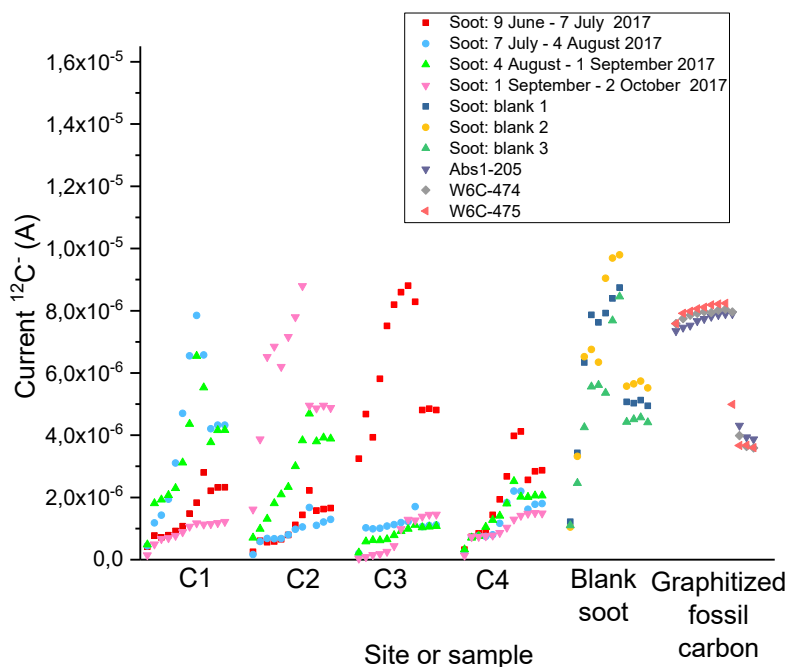


Figure 23. Current of negative ^{12}C ions measured at the high-energy side of the SSAMS system.

In conclusion, no signs of ^{14}C contamination were seen in the fullerene soot monitors exposed to ambient air during 9 June to 2 October 2017 at the measurement sites C1 (rural background,

Borrby), C2 (urban background, Lund), or ESS sites C3 (Möllegården) and C4 (Östra Odarslöv 264).

5. SUMMARY AND CONCLUSIONS

Within this work, the natural and anthropogenic radioactivity in the vicinity of the ESS site has been mapped during 2017-2018: “Zero Point of the ESS”. At the sites where sampling and measurement of gamma-emitting radionuclides were carried out, no unexpected or elevated levels of natural radionuclides or anthropogenic contamination were observed. All samples analysed for ^3H activity concentration were below, or close to, the MDA.

The sampling sites in the Lund area showed no signs of anthropogenic contamination of ^{14}C , neither for annual tree rings, vegetation samples, milk or air (the latter represented by fullerene monitors).

6. ACKNOWLEDGMENT

This work was financed by ESS under collaboration agreement ESS-0093103. The authors (Medical Radiation Physics in Malmö and Division of Nuclear Physics, Lund University) would like to express gratitude to the individuals, families and companies that have helped with providing access to the sites investigated and samples collected during this programme. The authors thank Hanna Nicklasson for extensive participation in sampling, sample preparation and measurements. Daniela Ene, ESS, is acknowledged for valuable input to the planning of the study, for support during the performance of the study, as well as for constructive reviewing of the report. We have also received input from the Swedish Radiation Safety Authority (SSM) before and during the project.

7. REFERENCES

- [1] ESS. *Assessment of environmental consequences of the normal operations of ESS facility. Part #1 Input data Source Term. Breakdown of radionuclides & Related basic information.* ESS-0028551. 2016.
- [2] SSM. Swedish Radiation Safety Authority. *Särskilda villkor för ESS-anläggningen i Lund.* Document number 13-3285, 2014.
- [3] ESS. *Collaboration Agreement ESS-0093103 Concerning "Monitoring of environmental radioactivity and radiation levels for "Zero Point" Assessment and Contributions to ESS Environmental Monitoring Plan" between European Spallation Source ERIC and Lund University.* ESS-0093103. 2017.
- [4] SSM. Swedish Radiation Safety Authority. *Underlag till placering i beredskapskategori för ESS och beredskapsplanen runt anläggningen.* Document number SSM2018-1037-4, 2018.
- [5] Adliene, D., Rääf, C., Magnusson, Å., Behring, J., Zakaria, M., Adlys, G., Skog, G., et al. *Assessment of the environmental contamination with long-lived radionuclides around an operating RBMK reactor station.* J Environ Radioact, 90(1): 68-77, 2006.
- [6] Mattsson, S., Lidén, K. *¹³⁷Cs in carpets of the forest moss Pleurozium Schreberi, 1961-1973.* Oikos: 323-327, 1975.
- [7] Mattsson, L.S. *¹³⁷Cs in the reindeer lichen Cladonia Alpestris: deposition, retention and internal distribution, 1961-1970.* Health Physics, 28(3): 233-248, 1975.
- [8] Stenström, K., Leide-Svegborn, S., Mattsson, S. *Low-level occupational ¹⁴C contamination - results from a pilot study.* Radiat Prot Dosimetry, 130(3): 337-42, 2008.
- [9] Stenström, K., Unkel, I., Nilsson, C.M., Raaf, C., Mattsson, S. *The use of hair as an indicator of occupational ¹⁴C contamination.* Radiat Environ Biophys, 49(1): 97-107, 2010.
- [10] Magnusson, Å., Stenström, K., Skog, G., Adliene, D., Adlys, G., Hellborg, R., Olariu, A., et al. *Levels of ¹⁴C in the terrestrial environment in the vicinity of two European nuclear power plants.* Radiocarbon, 46(2): 863-868, 2004.
- [11] Magnusson, Å., Stenström, K., Adliene, D., Adlys, G., Dias, C., Rääf, C., Skog, G., et al. *Carbon-14 levels in the vicinity of the Lithuanian nuclear power plant Ignalina.* Nuclear Instruments and Methods in Physics Research Section B: Beam Interactions with Materials and Atoms, 259(1): 530-535, 2007.
- [12] Skog, G. *Undersökning av förhöjda nivåer av ¹⁴C i Lund 2009-2010. Report to SSM.* Radiocarbon Dating Laboratory, Lund University. Lund. 2010.
- [13] Linderson, H. Accessed: 2018-02-01. Available from: <http://www.geology.lu.se/research/laboratories-equipment/the-laboratory-for-wood-anatomy-and-dendrochronology>.
- [14] Rundgren, M. Accessed: 2018-02-01. Available from: <http://www.geology.lu.se/research/laboratories-equipment/radiocarbon-dating-laboratory>.
- [15] Skog, G. *The single stage AMS machine at Lund University: Status report.* Nuclear Instruments and Methods in Physics Research Section B: Beam Interactions with Materials and Atoms, 259(1): 1-6, 2007.
- [16] Skog, G., Rundgren, M., Sköld, P. *Status of the Single Stage AMS machine at Lund University after 4 years of operation.* Nuclear Instruments and Methods in Physics Research Section B: Beam Interactions with Materials and Atoms, 268(7-8): 895-897, 2010.
- [17] Swedish Radiation Safety Authority. *Granskningsrapport. Granskning av ansökan om tillstånd för verksamhet med joniserande strålning.* SSM2014-127, 68, 2014.
- [18] Erlandsson, B., Mattsson, S. *Medically used radionuclides in sewage sludge.* Water, Air, and Soil Pollution, 9(2): 199-206, 1978.
- [19] Calibration certificate sheet for geometry reference source (No. NU 652). AEA Technology QSA GmbH, Gieselweg 1, 38110 Braunschweig, Germany. 2005.

- [20] Calibration certificate sheet for geometry reference source (No. RL 506). QSA Global GmbH, Gieselweg 1, 38110 Braunschweig, Germany. 2008.
- [21] Reference sheet certified reference material IAEA-330. IAEA Environmental laboratories, Vienna International Centre, P.O. Box 100, Vienna, Austria. 2009.
- [22] Reference sheet certified reference material IAEA-445. IAEA Environmental laboratories, Vienna International Centre, P.O. Box 100, Vienna, Austria 2010.
- [23] Reference sheet certified reference material IAEA-444. IAEA Environmental laboratories, Vienna International Centre, P.O. Box 100, Vienna, Austria 2010.
- [24] Reference sheet certified reference material IAEA-447. IAEA Environmental laboratories, Vienna International Centre, P.O. Box 100, Vienna, Austria 2012.
- [25] Certificates 015984, 015991, 015992, 015994 Deutscher Kalibrierdienst, DKD certificate of sources manufactured by AEA Technology QSA GmbH 2005.
- [26] Certificate of calibration – multinuclide standard solution (No. 7603; 1991-36). Eckert & Ziegler Nuclitec GmbH, 24937 Avenue Tibbitts, 91355 Valencia CA, USA.
- [27] Thomson, J. *Use and Preparation of Quench Curves in Liquid Scintillation Counting*, Application Note. Perkin Elmer Inc., Waltham Massachusetts United States.
https://www.perkinelmer.com/se/liquidsintillation/images/APP_Use-and-Preparation-of-Quench-Curves-in-LSC_tcm151-171749.pdf. 2014.
- [28] Reimer, P.J., Brown, T.A., Reimer, R.W. *Discussion: Reporting and calibration of post-bomb ^{14}C data*. Radiocarbon, 46(3): 1299-1304, 2004.
- [29] Eriksson Stenström, K., Skog, G., Georgiadou, E., Genberg, J., Johansson, A. *A guide to radiocarbon units and calculations*. Internal Report LUNFD6(NFFR-3111)/1-17/(2011). Lund University. D.o.N.P. Dep of Physics.
<http://lup.lub.lu.se/search/ws/files/5555659/2173661.pdf>. 2011.
- [30] Stenström, K., Skog, G., Nilsson, C.M., Hellborg, R., Leide-Svegborn, S., Georgiadou, E., Mattsson, S. *Local variations in ^{14}C – How is bomb-pulse dating of human tissues and cells affected?* Nuclear Instruments and Methods in Physics Research Section B: Beam Interactions with Materials and Atoms, 268(7–8): 1299-1302, 2010.
- [31] Stenström, K., Erlandsson, B., Hellborg, R., Wiebert, A., Skog, G. *Environmental levels of carbon-14 around a Swedish nuclear power plant measured with accelerator mass spectrometry*. Nuclear Instruments and Methods in Physics Research Section B: Beam Interactions with Materials and Atoms, 113(1–4): 474-476, 1996.
- [32] Levin, I., Kromer, B., Hammer, S. *Atmospheric $\Delta^{14}\text{CO}_2$ trend in Western European background air from 2000 to 2012*. 2013, 65, 2013.
- [33] Stuiver, M., Reimer, P.J., Reimer, R. Accessed: 2018-02-01. Available from: <http://calib.org/CALIBomb/>.
- [34] Tans, P., Keeling, R. *Trends in Atmospheric Carbon Dioxide*. NOAA/ESRL (www.esrl.noaa.gov/gmd/ccgg/trends/), Scripps Institution of Oceanography (scrippsco2.ucsd.edu). 2018.
- [35] IRSN. *Carbon-14 and the environment*. Available at <http://www.irsn.fr/EN/Research/publications-documentation/radionuclides-sheets/environment/Pages/carbon14-environment.aspx>. 2012. Accessed: 2018-02-01.

ANNEX A RADIATION IN THE ENVIRONMENT

Gamma emitters in the environment

A number of naturally occurring gamma-emitting radionuclides exists in the environment, emanating either from cosmogenic production or existing since or even before the formation of Earth. These radionuclides are found in terrestrial, atmospheric and aquatic biospheric systems all over the world. Although naturally occurring, their relative abundance in various ecosystems can be affected by human activities such as mineral ore mining, fresh water dwellings and use of fossil fuels. Many of these processes cause an increase in the concentration levels as well as radiation exposures to both workers and the public. One example is the concentration of radon (^{222}Rn) in the indoor environment of residential buildings which can be substantially elevated due to the type of construction material and ventilation system. In addition to these naturally occurring radionuclides, man-made gamma emitters mainly from the nuclear fuel cycle have been dispersed globally and are present in many terrestrial ecosystems. The concentration levels of these radionuclides are in most places too low to be of any health concern, but still high enough to be easily detectable with modern radiometry instrumentation.

Cosmogenic gamma emitters

The radionuclides ^3H and ^{14}C which are abundant on Earth and are both produced naturally by cosmogenic production. However, none of them emit gamma photons and are hence not detectable by gamma spectrometry. The most dominant gamma-emitting cosmogenic radionuclide is ^7Be ($T_{1/2}= 55.3$ days with a principal gamma photon at 0.429 MeV), which is produced in the atmosphere by spallation reactions between galactic cosmic rays such as neutrons and protons, and nitrogen and oxygen nuclei. The ^7Be atoms then become attached to aerosols and are mixed in the global atmosphere. The activity concentration of ^7Be in outdoor air is about 3 mBq m^{-3} [1]. The main transport route is via precipitation and the main intake route to humans is via fresh vegetables, although the resulting radiation exposure is many orders of magnitude lower than for e.g. ^{40}K and ^{210}Po . Since this radionuclide is easily washed out of the atmosphere by rain, the concentration at ground level varies considerably depending on the weather conditions in connection with the sampling event.

Another cosmogenic gamma-emitting radionuclide of importance is ^{22}Na ($T_{1/2}=2.6$ y with a principal gamma photon at 1.275 MeV), which is produced in the atmosphere by corresponding spallation reactions of galactic cosmic rays with argon nuclei. The annual radiation exposure caused by the global fallout of this nuclide is similar to that of ^7Be and can for most global populations be considered trivial compared with the radiation doses from primordial radionuclides [1].

Primordial radionuclides

Many of the radionuclides in this group were created before the earth was formed and were a part of the material that condensed to form the Earth. Hence their physical half-lives are comparable to the age of the earth, or longer. Other nuclides in this category have been produced on earth by the decay of long-lived radionuclides of stellar origin. Primordial radionuclides can therefore be divided into singly occurring radionuclides and members of a decay chain. The singly occurring primordial radionuclides decay to stable daughter products and these radionuclides generally have half-lives on the order of 10^{10} years or more. The most important one in terms of absorbed dose impact to humans and other biota is ^{40}K ($T_{1/2}=1.25 \cdot 10^9$ years) which decays through beta emission (89.3%) or electron capture (EC; 10.7%)

accompanied with an emission of a 1460.78 keV gamma ray. ^{40}K is a naturally occurring isotope of potassium. Typical concentrations of ^{40}K in human tissue range from 35 to 70 Bq kg⁻¹ resulting in annual absorbed doses in the order of 0.2 mGy y⁻¹ for an average individual.

The primordial radionuclides that decay to radioactive daughters will, in contrast to singly occurring radionuclides, form so-called decay chains or decay series (see Figure A 1). Although the radionuclide at the top of each chain is primordial, the daughters are thus continuously produced on Earth with half-lives ranging from about 10¹⁰ years to tenths of microseconds. Today there are three dominant decay chains, referred to as series; the uranium series with ^{238}U ($T_{1/2}=4.5 \cdot 10^9$ years) as a mother nuclide and ^{206}Pb as the last and stable daughter, the Thorium series with ^{232}Th ($T_{1/2}=1.4 \cdot 10^{10}$ years) as mother nuclide and ^{208}Pb as last daughter, and finally the Actinium series with ^{235}U ($T_{1/2}=0.78 \cdot 10^9$ years) as a mother nuclide and ^{207}Pb as last stable daughter. All these series include both decays through alpha emission and beta emission and are in many cases accompanied with emissions of gamma rays. The radiation dose contribution to living species on Earth from the natural series are dominated by the ^{238}U and ^{232}Th series due to their much higher isotopic abundance and the physical half-lives of some key elements in their decay chain.

One feature of these decay series is that the daughters often have shorter half-lives than the mother nuclide and thus can be expected to be found in equilibrium with each other in an undisturbed volume containing the mother nuclide. ^{238}U and ^{235}U are mainly present in the Earth's crust in the form of minerals. The abundance of uranium varies with the type of bedrock. A commonly found mineral in Sweden is granite which has an activity concentration of 37-124 Bq kg⁻¹. The average activity concentration of ^{238}U in the Earth's crust is 12-37 Bq kg⁻¹, and in water 1.2-12 mBq kg⁻¹. The population-averaged mean value of the activity concentrations of ^{238}U in soil is estimated to be 33 Bq kg⁻¹ [2]. An important daughter product is the alpha emitter ^{226}Ra ($T_{1/2}=1600$ y), which also emits a gamma ray at 0.186 MeV and can therefore be assessed by gamma spectrometry. Similar concentration values as for ^{238}U are found in both soil and water.

Thorium is found in large quantities in the Earth's crust, for example, in minerals such as thorite (ThSiO_4), and thorianite ($\text{ThO}_2 + \text{UO}_2$). The population averaged mean values of the activity concentration of ^{232}Th in soil is 45 Bq kg⁻¹ [2]. As for the ^{226}Ra of the ^{238}U series, the daughter nuclide ^{228}Ra is important in terms of radiation dose due to the affinity of the element to be incorporated into bone structure. In contrast to ^{226}Ra , ^{228}Ra does not emit any significant gamma rays, and is often assumed to be in equilibrium with its alpha-emitting mother ^{232}Th and with its daughter ^{228}Ac which has many gamma lines that can be assessed by gamma spectrometry. Hence the activity concentration in environmental samples of ^{232}Th and ^{228}Ra can indirectly be determined by assessing the ^{228}Ac concentration.

The concentrations of the remaining daughter nuclides of ^{238}U and ^{232}Th series are in the same order of magnitude as their mother nuclides provided that equilibrium is not disturbed. However, all decay series contain decay steps involving the noble gas radon (Rn). In the ^{238}U decay series, ^{226}Ra decays to ^{222}Rn ($T_{1/2}=3.8$ days), which is substantially longer than the radon daughters of the two other series, 55 and 3.96 s, for ^{220}Rn and ^{219}Rn , respectively. Due to the extremely high mobility of noble gases, the ^{222}Rn atom can migrate up to 1 m in a geological matrix during its short half-life, thereby creating a disruption of the equilibrium of the ^{238}U series. The Earth's crust will thus continuously inject radon daughters to water beds and to the atmosphere close to the ground, a process referred to as radon exhalation. This exhalation in turn causes a substantial redistribution of on a global scale of its daughter nuclides, of which ^{210}Pb ($T_{1/2}=22.3$ years) and ^{210}Po ($T_{1/2}=138$ days) are the most important in terms of radiation dose to living species. Typical ^{210}Pb and ^{210}Po concentration in soil is 20 –240 Bq kg⁻¹, depending on

annual precipitation at the site [3]. However, these levels decrease rapidly with depth and reaches the levels that correspond with the ^{238}U concentration in the local bedrock. The concentrations of ^{210}Pb and ^{210}Po in soil vegetation are similar to that in soil, but are also dependent on the direct contamination from the atmospheric deposition of the two radionuclides.

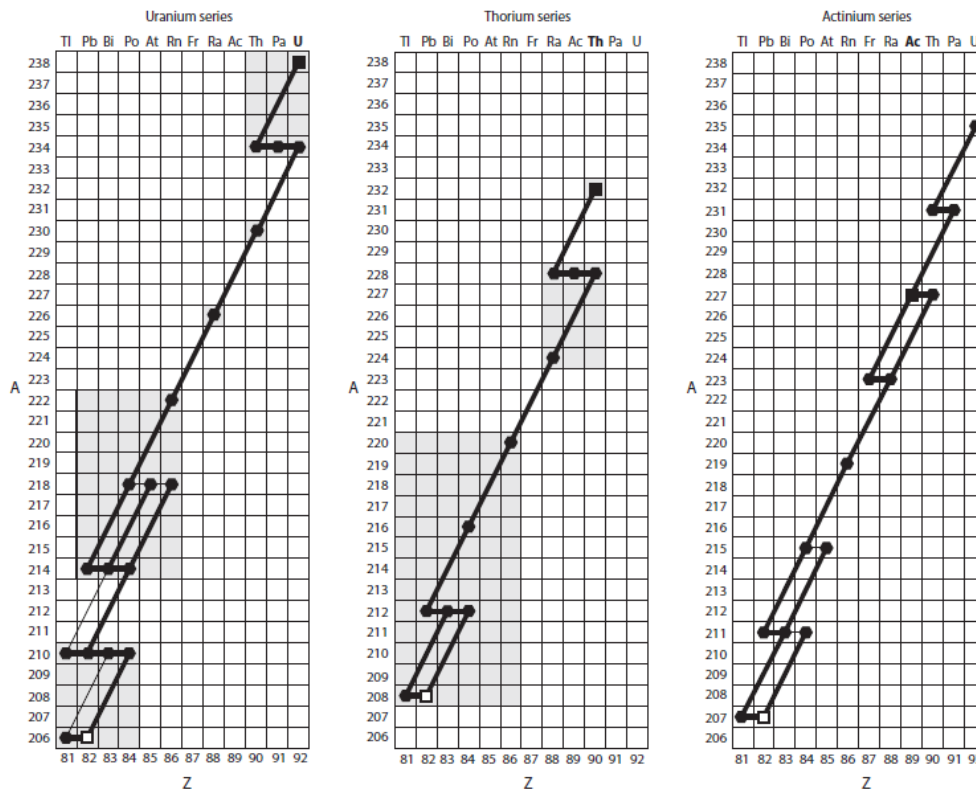


Figure A 1. Decay chart for the three naturally occurring decay series [4]. Sub-series, in which the radionuclides have similar properties regarding transport in the environment, are indicated in grey shading for the uranium and thorium series. The first at the last nuclide in the sub-series tend to have the same activity. Each decay chain ends with a stable isotope of lead, indicated by an open symbol.

Man-made gamma-emitting radionuclides in the environment

The principal inflow of anthropogenic radionuclides to the environment have come from the global fallout of nuclear weapons tests in the 1950s and 60s, together with operative and accidental releases from the nuclear power industry (e.g. the Sellafield releases in 1970s and the Chernobyl accident release in 1986).

The nuclear weapons fallout has resulted in a global deposition of gamma-emitting fission product ^{137}Cs ($T_{1/2}=30.2$ years with principal gamma photon of 0.662 MeV) ranging from 1-3 kBq m^{-2} , depending on the local annual precipitation and the geographical latitude. Other important fission products are the pure beta emitter ^{90}Sr ($T_{1/2}=28$ years) and the short-lived ^{131}I ($T_{1/2}=8.02$ days). In 1986 the atmospheric injection of the Chernobyl release resulted in many countries receiving more than 100 kBq m^{-2} of ^{137}Cs , as well as other short-lived fission products (again ^{131}I). In south of Sweden this deposition was, more modest, ranging from 1-2 kBq m^{-2} . These depositions will today result in typical soil concentrations of ^{137}Cs ranging from 10-

100 Bq kg⁻¹. In leafy vegetation and grass the corresponding values are less than 10 Bq kg⁻¹. In moss and lichens, concentrations may exceed these values substantially due to their higher efficiency in retaining atmospheric depositions [5, 6].

Other important sources of man-made gamma-emitting radionuclides are the operational releases from nuclear power plants. In Sweden the operational releases of gamma emitters from the light water reactors are principally through water releases and considerable radionuclide concentrations of neutron activation products such as ⁶⁰Co ($T_{1/2}$ =5.27 years), ⁵⁸Co ($T_{1/2}$ =70.7 days), ⁵⁴Mn ($T_{1/2}$ =312 days), ⁶⁵Zn ($T_{1/2}$ =244 days) and ¹¹⁰Ag^m ($T_{1/2}$ =250 days) have been found in species in shallow waters along the Swedish coasts, following a power law relationship with distance from the NPP site (e.g. [6-9]). In terrestrial bioindicators with high efficiency for atmospheric retention, such as sewage sludge and moss, detectable amounts of activation products like ⁶⁰Co have been found in the environment around Swedish as well as foreign nuclear power plants [10-12].

Gamma-emitting radiopharmaceuticals, such as ¹³¹I ($T_{1/2}$ =8.02 days), that are administered to in-patients in hospital will result in detectable amounts of these nuclides in sewage sludge and in shallow water species close to water reprocessing plants. Temporary peaks in ¹³¹I concentrations in *Fucus* close to the Barsebäck nuclear power plant were found many years after shut-down indicating the importance of this type of man-made source and was of considerable concern for the industry as these findings were erroneously linked with their activities.

Tritium in the environment

Tritium ($T_{1/2}$ =12.3 years, decay mode: beta (β^-), $E_{\max}(\beta^-)$ =18.6 keV, $E_{\text{mean}}(\beta^-)$ =5.7 keV) is produced by neutron activation in vast amounts in nuclear reactors and can also be formed in target materials and surrounding cooling media in particle accelerators, like the ESS. However, tritium also occurs naturally in the environment since cosmic-ray induced slow and fast neutrons interact with certain elements in atmospheric gases, e.g. nitrogen: (¹⁴N+n→¹²C+³H). Almost all (~99%) of the tritium produced naturally is oxidized to water (HTO) in the atmosphere, resulting in a cosmogenic background level of tritium is between 0.1 and 0.6 Bq l⁻¹ of water [13].

The annual natural production of tritium is about 10¹⁷ Bq, resulting in a global inventory of tritium of about 10¹⁸ Bq [2, 14]. The predominant form is as tritiated and gaseous water (HTO) (and to a small fraction of gaseous tritium (HT)), which take part in the hydrological cycle [2, 14]. Environmental free tritium is thus extremely mobile in the environment. The remaining fraction is organically bound tritium (OBT) which has been incorporated in organic compounds in living matter. The OBT can be either exchangeable (if bound to oxygen, sulphur or nitrogen) or non-exchangeable (if covalently bound to carbon). The fraction of OBT compared to total tritium varies considerable between various biological matrices [13]. The OBT fraction is of special interest due to the longer residence time of OBT than HTO in the body, effecting dose as well as risk. For globally dispersed tritium the dominant pathways are drinking water and food (HTO as well as OBT), and UNSCEAR estimates a global individual average annual dose of 0.01 μSv year⁻¹.

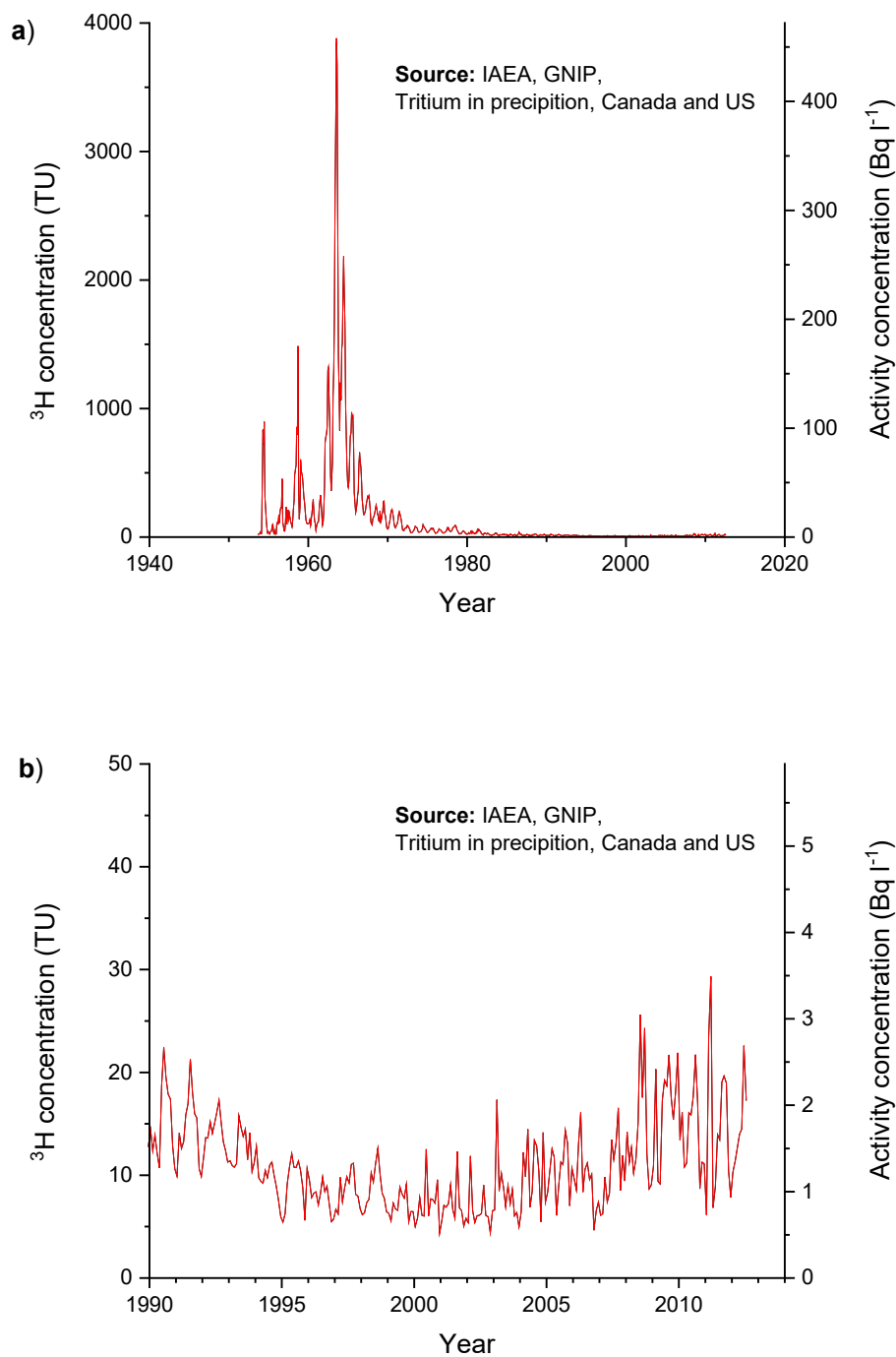


Figure A 2. Tritium concentration in precipitation in Canada and the US [15] a) during the bomb-pulse era, b) from 1990 to 2012. 1 TU = 1 Tritium Unit, which equals 1 tritium atom per 10^{18} ^1H atoms, corresponding to 0.119 Bq l^{-1} of water. Seasonal variations are e.g. due to the “spring leak”, resulting from the exchange of tropospheric and stratospheric air masses during winter and spring, see [16] and references therein.

The anthropogenic production of tritium mainly stems from nuclear weapons tests using fusion components (so-called hydrogen bombs) in the 1960s, adding $\sim 2 \cdot 10^{20}$ Bq tritium worldwide [17]. By 1963 the tritium activity concentration in rainwater was about three orders of magnitude higher than prior to the tests [13], see Figure A 2a [15]. Today (2018) about 5% of this tritium (i.e. in the same order of magnitude as the natural global inventory) remains in the global water circulation, and the tritium activity levels in rainwater are now in the order of single Bq l⁻¹ or less, as shown in Figure A 2b [15]. Recent data from rivers in south of France report HTO concentrations of 0.12 ± 0.11 to 0.86 ± 0.15 Bq l⁻¹ [16].

In some countries, tritium is produced in industrial nuclear reactors in substantial amounts for military as well as civil purposes. Tritium commonly serves as tracer in radiolabelled compounds in hospitals and research laboratories. Tritium is also used in neutron generators in some nuclear physics laboratories. The same deuterium-tritium (DT) reaction is also used in fusion test-reactors. Furthermore, tritium is used in industrial applications such as luminous objects. Although the releases from these applications are negligible compared to the global inventory, they may give rise to significant excess of tritium in the local environment and biota [14, 18].

The nuclear power industry is a large source of anthropogenic environmental tritium. The annual total amount of tritium released from nuclear power industry is several orders of magnitude lower than that from nuclear weapons' tests, and primarily originates from deuterium enriched (heavy water) moderated nuclear reactors and from fuel reprocessing plants. A typical tritium release rate from a 1 GW_{el} heavy-water reactor is $7.4 \cdot 10^{14}$ Bq year⁻¹ and $1.8 \cdot 10^{14}$ Bq year⁻¹ as gaseous and liquid effluents, respectively [19]. Tritium releases from light-water reactors is usually at least a factor of 10 less than for heavy-water reactors [19]. For fuel reprocessing plants, typical release rates are in the order of 10^{16} Bq year⁻¹ [20]. Excess activity of tritium can be found in the surroundings of nuclear facilities: e.g., in the lower Rhone River 95% of the observed tritium (up to 10 Bq l⁻¹ of water) originates from nuclear facilities [21].

Environmental tritium contamination has also occurred after incidents at tritium production facilities as well as major accidents nuclear power plants [14]. In the literature, incidental releases up to the order of 10^{16} Bq are reported from the US [14]. The Chernobyl as well as the Fukushima accident resulted in highly elevated environmental tritium levels: e.g. water in a plant collected 20 km from the Fukushima site one month after the accident in 2011 had 100 times higher tritium activity (167 Bq l⁻¹) than background water (<1.5 Bq l⁻¹) [22].

Examples of tritium measurements in Sweden

The Swedish Radiation Safety Authority (SSM) collects water samples twice a year at six Swedish waterworks since year 2001 [23]. The tritium activity concentrations are often below the detection limit of a few Bq l⁻¹, as shown in Figure A 3 (data from two of the waterworks; "< value" refers to values lower than the detection limit).

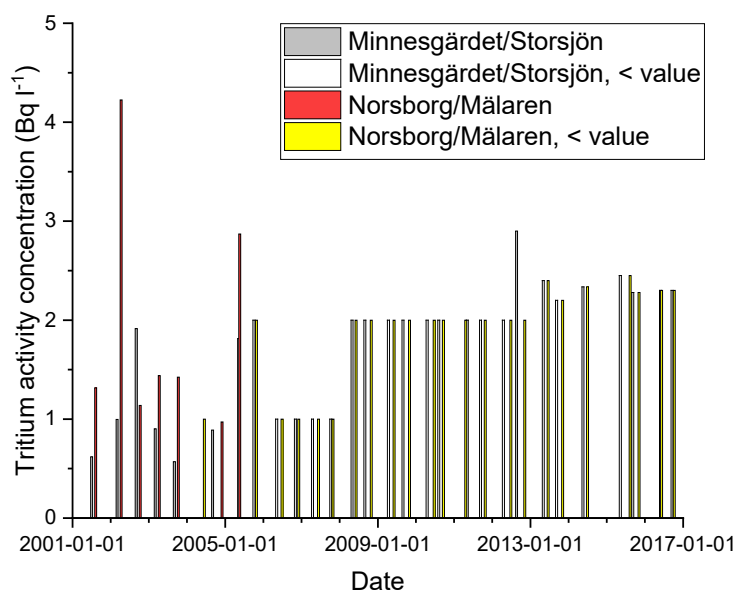


Figure A 3. Tritium activity concentration in drinking water [23].

SSM also monitors tritium in surface sea water at six Swedish stations since 2009 [24]. These measurements are part of the national programme for the environmental control at the nuclear facilities [24]. Data from two of these stations, Ringhals in Kattegatt and Fjällbacka in Skagerak, are shown in Figure A 4. The Kattegatt station (R35) is located 8.2 km from the release point of cooling water from Ringhals nuclear power plant [25], while the Skagerak station lies approximately 160 km north of Ringhals. Most data in Figure A 4 are below the detection limit for tritium of the instruments used (a few Bq l⁻¹).

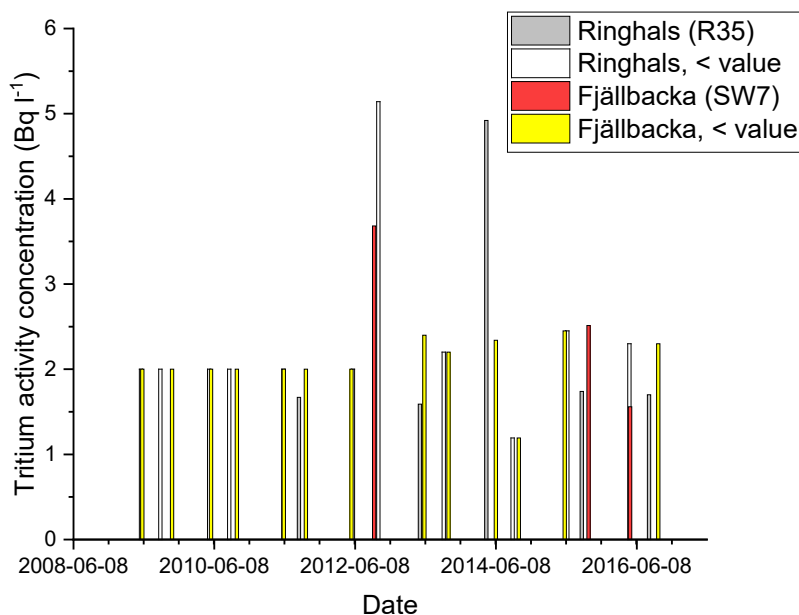


Figure A 4. Tritium activity concentration in sea water [24].

^{14}C in the environment and previous measurements in the Lund area

^{14}C is a long-lived beta-emitting radionuclide ($T_{1/2} = 5730$ years, decay mode: beta (β^-), $E_{\max}(\beta^-) = 156$ keV, $E_{\text{mean}}(\beta^-) = 49.5$ keV) that is produced naturally in the upper atmosphere when thermal neutrons – originating from spallation reactions of atmospheric gases induced by cosmic radiation – interact with atmospheric nitrogen ($^{14}\text{N} + n \rightarrow ^{14}\text{C} + p$). ^{14}C is mainly incorporated into atmospheric CO_2 , and thus takes part in the global carbon cycle. The natural abundance of ^{14}C is approximately $10^{-10}\%$ of total carbon ($226 \text{ Bq (kg C)}^{-1}$, or $F^{14}\text{C} \approx 1$ (for definition of $F^{14}\text{C}$ see [26, 27]). The main transfer pathway of naturally produced ^{14}C to man is through ingestion leading to an effective dose rate of about $12 \mu\text{Sv year}^{-1}$ [14].

The ^{14}C concentration is under influence of anthropogenic activities, which may decrease or increase the specific activity of carbon, globally as well as locally [28]. Atmospheric testing of nuclear weapons during the last century temporarily doubled the ^{14}C concentration in the atmosphere, as shown in Figure A 5. The data in Figure A 5 have been collected at sites representing a minimum of local human interference (clean-air) [29-31] and environmental ^{14}C data is usually compared to this clean air data. After the Limited Test Ban Treaty, the ^{14}C specific activity of atmospheric carbon dioxide has decreased due to absorption into the oceans and biosphere, and also due to dilution caused by the increasing CO_2 -concentration of the atmosphere (mainly caused by fossil fuels, which are free from ^{14}C).

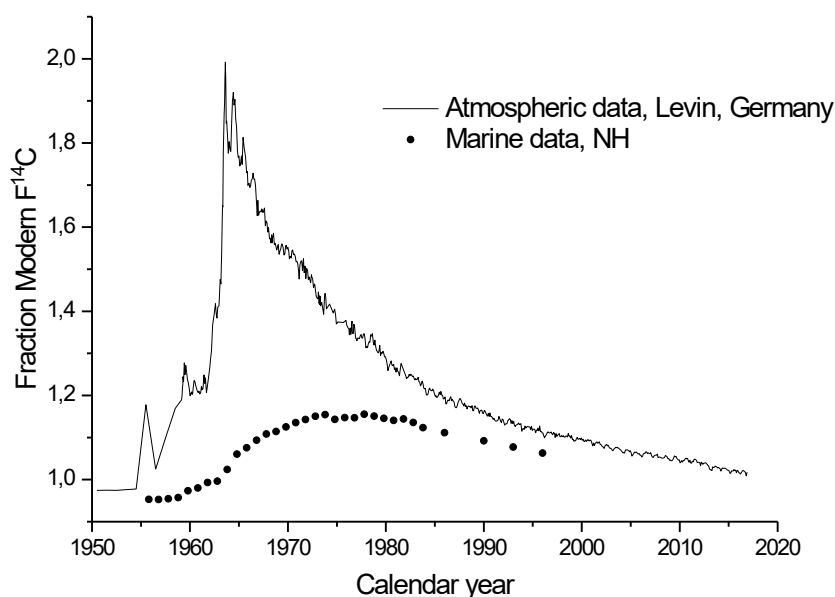


Figure A 5. ^{14}C in atmospheric CO_2 and oceans representative for the Northern Hemisphere, expressed in units of Fraction Modern, $F^{14}\text{C}$ [26]; $F^{14}\text{C}$ is approximately 1.0 before the nuclear weapons tests, corresponding to the natural $^{14}\text{C}/^{12}\text{C}$ ratio of about $10^{-10}\%$. Atmospheric data are taken from the CaliBomb home page [31] including data from Levin and Kromer [29] and Levin, Kromer et al. [30]. Marine data are from Kalish, Nydal et al. [32].

Local fluctuations in the specific activity of carbon can be caused by local emissions of combustion of fossil fuels (lowering the specific activity, known as the local Suess effect). The magnitude of the suppression in $F^{14}\text{C}$ values of vegetation in heavily industrialized regions is in

the order of some percent (see e.g. [28, 33]). The opposite effect can be observed close to nuclear power plants as well as industries and research facilities using ^{14}C as a tracer [28].

Typical release rates of ^{14}C from nuclear power reactors are about 200 GBq year⁻¹ from light-water moderated pressurized water reactors (LWR-PWR), mainly as airborne hydrocarbons; about 300 GBq year⁻¹ from light-water moderated boiling water reactors (LWR-BWR), mainly as airborne CO₂; about 2500 GBq year⁻¹ from a heavy-water reactor (HWR), predominantly as CO₂ [19]. $F^{14}\text{C}$ values in vegetation within a few km from LWRs typically show a maximum ^{14}C excess of 10% (see [28, 34] and references therein). Near HWRs significantly higher values have been observed (see [28, 34] and references therein). An extreme example is reported from Pickering Nuclear Generating Station (PNGS, Canada), a large HWR facility: ^{14}C concentrations of about 13 kBq (kg C)⁻¹ ($F^{14}\text{C} \approx 57.6$) have been found in fruit close to the facility in year 1992 [35]. Measurements at larger distances from PNGS have shown $F^{14}\text{C} > 6$ at 2 km from the facility (year 1998), and about 7% excess at a distance of 100 km ($F^{14}\text{C} = 1.20 \pm 0.03$) [28].

The local contamination of ^{14}C found in the surroundings of research facilities and radiolabelling laboratories is usually site-specific (see examples in [28]) and varies with time. E.g., ^{14}C concentrations of > 60 kBq (kg C)⁻¹ have been found in soils (corresponding to $F^{14}\text{C} \approx 290$) close to a company performing radiolabelling [36]. Also plants showed > 100 times clean-air ^{14}C levels [36]. Previous measurements at the research facilities show local ^{14}C values in vegetation of $F^{14}\text{C} > 10$ (in a tree ring from 1985 at the Rossendorf research centre, Germany) [28]. Measurements of grass, moss and soil at Jülich research centre (Germany) in 2004 showed very local contamination within the research facility area: some samples were uncontaminated, others showed an excess of up to 36% ($F^{14}\text{C} > 1.4$) above clean air in 2004 [28].

Also the research-intensive city of Lund hosts several potential anthropogenic sources of ^{14}C . In 2009, a contamination was observed in Lund: chestnut leaves in the university area showed excess ^{14}C of 25% above clean air values (i.e. $F^{14}\text{C} = 1.30$ compared to clean air $F^{14}\text{C} = 1.05$ in 2009) [37]. Measurements performed in 2010 led to the conclusion that a pharmaceutical company probably was the source of the contamination [37].

Long-lived spallation and activation products in accelerator driven systems

A facility that operates a high energy accelerator with large beam current, like ESS, has many features common with a nuclear power plant. However, differences are also large. The ESS-facility will operate at a mean power of 5 MW that is hundreds of times lower than the power in a nuclear plant for energy production (see Table A 1 for some ESS parameters). This means that the total amount of activity involved will be proportionally smaller. In a reactor which uses uranium as fuel, the storage of waste with long-lived activity is a large problem while in the proton irradiation of ESS, the half-lives of the produced radionuclides are considerably shorter. On the other side, the radionuclides in a nuclear plant are restricted mainly to the core, while in ESS it will be more distributed. The target with its different components, tungsten wheel, cooling media, reflector, moderator and windows will have the highest activity, but magnets bending and spreading the beam will also be highly activated. For many of the radionuclides produced at ESS, we lack experience of its behaviour in the facility, and in premises and surroundings. More research is needed how to measure and analyse radionuclides that will be generated at ESS.

Table A 1. Some ESS parameters [38]

Parameter	Value
Average beam power	5 MW
Proton kinetic energy	2.0 GeV
Pulse repetition rate	14 Hz
Average pulse current	62.5 mA
Macro-pulse length	2.86 ms

Spallation products

The radionuclide inventory induced by high-energetic protons differs strongly from the inventory of nuclear reactors. Elements from nearly the whole periodic system with a lower mass number than the target element tungsten are produced by spallation, fragmentation, and high-energy fission processes, this means e.g. isotopes of Ta, Hf, Lu, Yb, Tm, Er, Ho, Dy, Tb, Gd, Eu, Sm, Pm, ..., Cs, I, ... Sr, Mn. Moreover, species with higher atomic number than the target element are formed as well, due to compound nucleus reactions of stable tungsten isotopes. Next to such primary reactions, also reactions of tungsten with high energetic secondary particles like helium and tritium, as well as (p,xn) reactions of *in-situ* generated long-lived products with a higher atom number may have an impact on the final radionuclide spectrum. Theoretical predictions of the residue radionuclide inventory are difficult, due to the complexity of the involved nuclear reactions.

Experimental data are needed in order to benchmark and improve theoretical high-energy models and Monte Carlo calculation codes. Investigations should primarily focus on radionuclides with half-lives longer than several months, considering issues of disposal and final storage as well as radiological accident scenarios. Important radionuclides could be investigated based on the following selection criteria [39].

1. Radionuclides with high energetic photons and half-lives up to 500 years have to be considered, due to their major contribution to the total activity and dose rate of the radioactive waste, even after several years of cooling time. Such candidates are [40, 41]: ^{173}Lu ($T_{1/2}=1.37$ years), $^{172}\text{Hf}/^{172}\text{Lu}$ ($T_{1/2}=1.87$ years), ^{133}Ba ($T_{1/2}=10.5$ years), ^{125}Sb ($T_{1/2}=2.77$ years), $^{102\text{m}}\text{Rh}$ ($T_{1/2}=2.9$ years), ^{101}Rh ($T_{1/2}=3.3$ years) and ^{60}Co ($T_{1/2}=5.27$ years).
2. Radionuclides decaying by alpha emission: ^{148}Gd ($T_{1/2}=74.6$ years), ^{150}Gd ($T_{1/2}=1.79 \cdot 10^6$ years), ^{154}Dy ($T_{1/2}=3 \cdot 10^6$ years) and ^{146}Sm ($T_{1/2}=1.03 \cdot 10^8$ years) [40, 41] are of essential importance, due to their radiotoxic effects.
3. Attention should also be paid to radionuclides of volatile species like ^{125}I ($T_{1/2}=60.1$ days) and ^{129}I ($T_{1/2}=1.57 \cdot 10^7$ years) due to their high inhalation probability and thyroid uptake in case of radiological accident scenarios.
4. High power spallation targets are a potential source also of other rare and very long-lived radionuclides like ^{44}Ti ($T_{1/2}=60.40$ years), ^{26}Al ($T_{1/2}=7.16 \cdot 10^5$ years) and ^{53}Mn ($T_{1/2}=3.7 \cdot 10^6$ years), ^{182}Hf ($T_{1/2}=9.0 \cdot 10^6$ years) and ^{60}Fe ($T_{1/2}=2.60 \cdot 10^6$ years).

Activation products

The residual activity induced in particle accelerators is a serious issue from the point of view of radiation safety as the long-lived radionuclides produced by fast or moderated neutrons and impact protons cause problems of radiation exposure for staff involved in the maintenance work

and when decommissioning the facility. The dominant activity after shut down results from ^{187}W , ^{185}W and ^{181}W [41]. To accurately estimate the radiological consequences of beam loss during acceleration and associated activation of components, concrete and air are difficult, if even possible, and an (conservative) assumption has to be the input in the calculations.

The activation of the magnets and collimators in the high energy beam transport line of the ESS due to the backscattered neutrons from the target and also due to the direct proton interactions and their secondaries has been estimated [42]. The result includes the production of any radionuclide that decays emitting gamma rays and also that has a lifetime longer than 24 hr. Shorter lived radionuclides, like ^{24}Na can pose a safety concern if the tunnel has to be accessed in emergency situations, but the study was limited to include only the radionuclides that live longer than 24 h: ^7Be , ^{46}Sc , ^{44}Ti , ^{51}Cr , ^{54}Mn , ^{59}Fe , ^{56}Co , ^{57}Co , ^{58}Co , ^{60}Co , ^{65}Zn , ^{75}Se , ^{84}Rb , ^{85}Sr , ^{88}Y , ^{95}Zr , ^{94}Nb , ^{95}Nb , ^{106}Ru , ^{109}Cd , ^{111}In , ^{113}Sn , ^{125}Sn , ^{124}Sb , ^{125}Sb , ^{125}I , ^{132}Cs , ^{134}Cs , ^{137}Cs , ^{133}Ba , ^{139}Ce , ^{141}Ce , ^{144}Ce , ^{152}Eu , ^{154}Eu , ^{153}Gd , ^{160}Tb , ^{161}Tb , ^{170}Tm , ^{169}Yb , ^{172}Hf , ^{182}Ta , ^{185}Os , ^{192}Ir , ^{198}Au , ^{199}Au , ^{203}Hg , ^{210}Pb , ^{207}Bi , ^{228}Th , ^{239}Np , ^{241}Am , and ^{243}Am . One of the factors that contribute to the production of these radionuclides inside the magnets is the direct impact of the proton beam. When proton beam losses occur, the protons interact with the beam pipe producing hadronic and electromagnetic showers. Also, when the protons interact with the magnets they will produce additional secondary radiation. The main factor proved to be the backscattered neutrons, the particle collimator placed in front of the target being the worst affected.

References

- [1] UNSCEAR. United Nations. *Sources and effects of ionizing radiation, Vol.I: Sources of ionizing radiation, Annex B*. 2008.
- [2] UNSCEAR. United Nations. *Sources and effects of ionizing radiation. UNSCEAR 2000 report to the General Assembly, with scientific annexes. Volume I: Sources*. 2000.
- [3] Persson, B.R., Holm, E. *Polonium-210 and lead-210 in the terrestrial environment: a historical review*. Journal of Environmental Radioactivity, 102(5): 420-429, 2011.
- [4] Isaksson, M., Raaf, C.L., *Environmental radioactivity and emergency preparedness*. CRC Press, 2017.
- [5] Mattsson, S., Lidén, K. *^{137}Cs in carpets of the forest moss *Pleurozium Schreberi*, 1961-1973*. Oikos: 323-327, 1975.
- [6] Adliene, D., Rääf, C., Magnusson, Å., Behring, J., Zakaria, M., Adlys, G., Skog, G., et al. *Assessment of the environmental contamination with long-lived radionuclides around an operating RBMK reactor station*. J Environ Radioact, 90(1): 68-77, 2006.
- [7] Mattsson, S., Finck, R., Nilsson, M. *Distribution of activation products from Barsebäck nuclear power plant (Sweden) in the marine environment. Temporal and spatial variations as established by seaweed*. Environmental Pollution Series B, Chemical and Physical, 1(2): 105-115, 1980.
- [8] Rääf, C., Hubbard, L., Falk, R., Ågren, G., Vesanen, R. *Transfer of ^{137}Cs from Chernobyl debris and nuclear weapons fallout to different Swedish population groups*. Science of the total environment, 367(1): 324-340, 2006.
- [9] Zakaria, M., Rääf, C., Mattsson, S. *The 2002/2003 radionuclide concentration in the marine environment at various distances from the Barsebäck nuclear power plant*. Radioprotection, 43(3): 429-438, 2008.
- [10] Erlandsson, B., Ingemansson, T., Mattsson, S. *Comparative studies of radionuclides from global fallout and local sources in ground level air and sewage sludge*. Water, Air, and Soil Pollution, 20(3): 331-346, 1983.
- [11] Ingemansson, T., Erlandsson, B., Mattsson, S. *Studies of activation products in the terrestrial environments of three Swedish nuclear power stations*. Environmental Pollution Series B, Chemical and Physical, 5(1): 17-33, 1983.

- [12] Mattsson, S., Ingemansson, T., Erlandsson, B. *The ^{60}Co concentration in ground level air at various distances from a nuclear power station*. Atmospheric Environment (1967), 17(4): 853-858, 1983.
- [13] IRSN. *Tritium and the environment*. Available at <http://www.irsn.fr/EN/Research/publications-documentation/radionuclides-sheets/environment/Pages/Tritium-environment.aspx>. 2012. Accessed: 2018-02-01.
- [14] UNSCEAR. United Nations. *Sources, effects and risks of ionizing radiation. UNSCEAR 2016. Report to the General Assembly, with Scientific Annexes. Annex C. Biological effects of selected internal emitters - tritium*. 2016.
- [15] IAEA/WMO. *Global Network of Isotopes in Precipitation. The GNIP Database*. Accessible at: <http://www.iaea.org/water>. Accessed: 2018-02-02.
- [16] Ducros, L., Eyrolle, F., Vedova, C.D., Charmasson, S., Leblanc, M., Mayer, A., Babic, M., et al. *Tritium in river waters from French Mediterranean catchments: Background levels and variability*. Science of The Total Environment, 612(Supplement C): 672-682, 2018.
- [17] Eyrolle, F., Ducros, L., Le Dizès, S., Beaugelin-Seiller, K., Charmasson, S., Boyer, P., Cossonnet, C. *An updated review on tritium in the environment*. Journal of Environmental Radioactivity, 181(Supplement C): 128-137, 2018.
- [18] Brunner, P., Schneider, P., Scheicher, H., Seyerl, G., Kurnik, P., Ennemoser, O., Ambach, W. *Tritium intake by exposure to plastic case watches*. Health Physics, 70(4): 484-487, 1996.
- [19] IAEA. International Atomic Energy Agency. *Management of waste containing tritium and carbon-14. Technical report series no 421*. 2004.
- [20] Fiévet, B., Pommier, J., Voiseux, C., Bailly du Bois, P., Laguionie, P., Cossonnet, C., Solier, L. *Transfer of tritium released into the marine environment by French nuclear facilities bordering the English channel*. Environmental Science & Technology, 47(12): 6696-6703, 2013.
- [21] Eyrolle-Boyer, F., Antonelli, C., Renaud, P., Tournieux, D. *Origins and trend of radionuclides within the lower Rhône River over the last decades*. Radioprotection, 50(1): 27-34, 2015.
- [22] Kakiuchi, H., Akata, N., Hasegawa, H., Ueda, S., Tokonami, S., Yamada, M., Hosoda, M., et al. *Concentration of ^3H in plants around Fukushima Dai-ichi nuclear power station*. Scientific reports, 2: 947, 2012.
- [23] SSM. *Miljödatabasen/Dricksvatten*. Accessed: 2018-05-29. Available from: <https://www.stralsakerhetsmyndigheten.se/omraden/miljoovervakning/sokbara-miljodata/miljodatabasen/dricksvatten/>.
- [24] SSM. *Miljödatabasen/Havsvatten*. Accessed: 2018-05-29. Available from: <https://www.stralsakerhetsmyndigheten.se/omraden/miljoovervakning/sokbara-miljodata/miljodatabasen/havsvatten/>.
- [25] Lindén, A.-M. The Swedish Radiation Safety Authority. 2004:15 *Omgivningskontrollprogram för de kärntekniska anläggningarna, revision*. ISSN 0282-4434, 2004.
- [26] Reimer, P.J., Brown, T.A., Reimer, R.W. *Discussion: Reporting and calibration of post-bomb ^{14}C data*. Radiocarbon, 46(3): 1299-1304, 2004.
- [27] Eriksson Stenström, K., Skog, G., Georgiadou, E., Genberg, J., Johansson, A. *A guide to radiocarbon units and calculations*. Internal Report LUNFD6(NFFR-3111)/1-17/(2011). Lund University. D.o.N.P. Dep of Physics. <http://lup.lub.lu.se/search/ws/files/5555659/2173661.pdf>. 2011.
- [28] Stenström, K., Skog, G., Nilsson, C.M., Hellborg, R., Leide-Svegborn, S., Georgiadou, E., Mattsson, S. *Local variations in ^{14}C – How is bomb-pulse dating of human tissues and cells affected?* Nuclear Instruments and Methods in Physics Research Section B: Beam Interactions with Materials and Atoms, 268(7–8): 1299-1302, 2010.
- [29] Levin, I., Kromer, B. *The tropospheric $^{14}\text{CO}_2$ level in mid latitudes of the Northern Hemisphere (1959-2003)*. Radiocarbon, 46: 1261-1271, 2004.

- [30] Levin, I., Kromer, B., Hammer, S. *Atmospheric $\Delta^{14}\text{CO}_2$ trend in Western European background air from 2000 to 2012*. 2013, 65, 2013.
- [31] Stuiver, M., Reimer, P.J., Reimer, R. Accessed: 2018-02-01. Available from: <http://calib.org/CALIBomb/>.
- [32] Kalish, J., Nydal, R., Nedreaas, K., Burr, G., Eine, G. *A time history of pre- and post-bomb radiocarbon in the Barents Sea derived from Arcto-Norwegian cod otoliths*. Radiocarbon, 43: 843-845, 2001.
- [33] Rakowski, A., Kuc, T., Nakamura, T., Pazdur, A. *Radiocarbon Concentration in the Atmosphere and Modern Tree Rings in the Kraków Area, Southern Poland*. Radiocarbon, 46(2): 911-916, 2004.
- [34] IRSN. *Carbon-14 and the environment*. Available at <http://www.irsn.fr/EN/Research/publications-documentation/radionuclides-sheets/environment/Pages/carbon14-environment.aspx>. 2012. Accessed: 2018-02-01.
- [35] Milton, G.M., Kramer, S.J., Brown, R.M., Repta, C.J.W., King, K.J., Rao, R.R. *Radiocarbon dispersion around Canadian nuclear facilities*. Radiocarbon, 37(2): 485-496, 1995.
- [36] Leprieux, F., Linden, G., Pasquier, J. *Radioecology and health impact of the carbon-14 contamination on the Ganagobie site (Provence, France)*. Radioprotection, 38(1): 13-28, 2003.
- [37] Skog, G. *Undersökning av förhöjda nivåer av ^{14}C i Lund 2009-2010. Report to SSM*. Radiocarbon Dating Laboratory, Lund University. Lund. 2010.
- [38] Garoby, R., Danared, H., Alonso, I., Bargallo, E., Cheymol, B., Darve, C., Eshraqi, M., et al. *The European Spallation Source Design*. Physica Scripta, 93(1): 014001, 2017.
- [39] Lorenz, T., Dai, Y., Schumann, D. *Analysis of long-lived radionuclides produced by proton irradiation in lead targets- γ -measurements*. Radiochimica Acta, 101(10): 661-666, 2013.
- [40] ESS. *Assessment of environmental consequences of the normal operations of ESS facility. Part #1 Input data Source Term. Breakdown of radionuclides & Related basic information*. ESS-0028551. 2016.
- [41] Mora, T., Sordo, F., Aguilar, A., Mena, L., Mancisidor, M., Aguilar, J., Bakedano, G., et al. *An evaluation of activation and radiation damage effects for the European Spallation Source Target*. Journal of Nuclear Science and Technology: 1-11, 2017.
- [42] Bungau, C., Bungau, A., Cywinski, R., Barlow, R., Edgecock, T.R., Carlsson, P., Danared, H., et al. *Induced activation in accelerator components*. Physical Review Special Topics-Accelerators and Beams, 17(8): 084701, 2014.

ANNEX B **MATERIALS AND METHODS**

ANNEX B1 ASSESSMENT OF *IN SITU* AND MOBILE GAMMA SPECTROMETRY AND AMBIENT DOSE EQUIVALENT

Purpose

The purpose of this appendix is to describe the methods applied for *in situ* high-resolution gamma spectroscopy and the assessment of the ambient dose equivalent rate and its variability (stationary, by foot and by car) for the project entitled "Monitoring of environmental radioactivity and radiation levels for "Zero Point" assessment and contributions to ESS environmental monitoring plan" (contract ESS-0093103).

Applicability

This description (procedure) is applicable to general measurements outdoor (free in air) of the photon radiation from natural occurring and anthropogenic radionuclides. The procedure is applicable to future assessments of the radiation environment from gamma-emitting radionuclides and its variability around ESS, enabling assessment of the radiological impact of ESS.

Methodological outline

After signing the contract, suitable sites were selected (to cover all directions around the site; to stay untouched for long time periods; to be representative and reflect the current population density (approximately within 1500 m of the ESS site)). At the sites where *in situ* high-resolution gamma spectroscopy was carried out, soil samples were also collected. In order to illustrate the variability in the radiation fields within and between these sites, gamma spectrometry mapping was also carried out by foot and car in combination with stationary measurements of the ambient dose equivalent rate at the sites.

At the majority of the sites of the stationary measurements (i.e. *in situ* gamma spectrometry and assessment of the ambient dose equivalent rate), the measurements started directly and continued during the soil samplings and parallel measurements. The total measurement time varied between 1 to 2 hours.

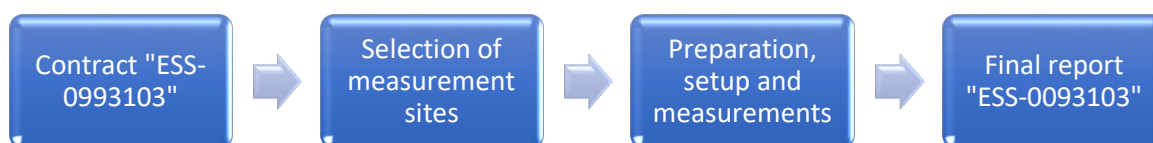


Figure B1. 1. Flow of actions for achieving the point zero measurements of *in situ* gamma spectrometry and ambient dose equivalent.

Methodological details

Planning	
<p>In the close vicinity of the ESS site, 24 sites were selected for combined measurements of <i>in situ</i> high-resolution gamma spectrometry, mapping of the ambient dose equivalent, and soil sampling. These sites were selected as described in detail in section 2.1.</p> <p>The majority of the stationary and mobile spectrometric assessments were carried out at private or company owned gardens in the vicinity of the ESS facility and at the one church closest to ESS (Site 7). Slightly further away, but also included, were two sites in the Northern inhabited parts of Lund city (Sites 23 and 45).</p> <p>In addition, a detailed survey was carried out by car-borne measurements on the streets enclosing the about 2 km radius area around ESS to provide an overview of the dose rate variability in the area.</p>	
Output	Representative locations for future re-assessments of the temporal changes in the radiation environment after commissioning of ESS, enabling dose estimations relevant for today's population density in the area.
General aspects on the measurements	
<p>At specific sites, <i>in situ</i> high-resolution gamma spectrometry (using High Purity Germanium detectors, HPGe) was carried out in combination with soil sampling (and when possible also grass) as well as measurements of the ambient dose equivalent rate. The ambient dose equivalent rate was determined with stationary detectors at the sites and its variability was determined with backpack configured detector systems.</p> <p><i>In situ high-resolution gamma spectrometry</i></p> <p>Field gamma spectrometry measurements were carried out using HPGe detectors (ORTEC, USA), mainly a 123% but also a 26.10% (relative efficiencies). Using either of these two, the HPGe detector was positioned on a tripod in the centre of the selected surfaces, where the ground was as flat as possible, with the crystal at a distance of 1 m above the ground. The surface was selected so that it was at least 30 meters from any buildings or topography that might shield the detector's field of view (at a distance of 30 m, ~1% of the 662 keV photons from ¹³⁷Cs reach the detector).</p> <p>In private gardens and backyards, it might not always be possible to put the detector 30 m from the main house or other buildings. In such situations, the detector was positioned as far away as possible from such buildings and where a flat surface could be found. The selected position of the HPGe detector defined the centre of the surface for further measurements and samplings. The measurement time of the HPGe detector for <i>in situ</i> gamma spectrometry was >1 h.</p>	

Selection of
measurement
sites

Preparation,
setup and
measurements

Mobile gamma spectrometry

In parallel with the stationary HPGe measurements, foot-borne mapping (with about 1-2 m between the walking lines) of the ambient dose equivalent rate, $\dot{H}^*(10)$ ($\mu\text{Sv h}^{-1}$), over the surface of the site, was carried out with a (76.2 mm \times 76.2 mm) LaBr₃:Ce based back-pack radiation detection system. This system is based on the SSM developed CEMIK system with Nugget software [1]. Using this system, the total gamma dose rate as well as individual spectra, were acquired each 1-3 seconds and stored together with the GPS coordinates. Similarly, car borne measurements of the ambient dose rate was carried out using two 3 litre NaI(Tl) detectors mounted in the car. This mapping was carried out on the available roads near the ESS facility.

Stationary assessment of the ambient dose rate

In addition, the ambient dose equivalent rate was acquired using a tripod-mounted detector based on a ZnS scintillation dose rate probe (detector based on a 75 mm \times 75 mm organic scintillator; Automess, Probe 6150AD-b). This detector was positioned at four different points around the same central position as the HPGe detector, at a height of 1 m above the ground. For each of these four points, the ambient dose equivalent rate was averaged over time (10-20 minutes), and an average dose rate was calculated for the entire surface/site. The average variability of the dose rate was calculated based on the gamma dose rate variation as determined with the foot-borne back-pack system at each of individual surfaces/sites.

Output	Gamma spectra from the majority of the sites close to the ESS facility as well as careful mapping of the ambient dose equivalent rate and the dose rate variability within and between these sites. Provides for reproducible and comparable assessments in the future.
---------------	---

Special precautions

During *in situ* gamma spectrometry, it is important that any persons do not obscure the detector field of view, in order to avoid shielding or influencing the radiation fields. Further, it is also important to protect the detector (including the tripod) from any possible contamination on the ground by using e.g. plastic bags over the detector and cleaning of the tripod between the sites. If the equipment is observed or is expected to be contaminated, it is important to evaluate this further in a low-background room, followed by proper procedures.

Preparation,
setup and
measurements

When evaluating the mobile (by foot or by car) mappings of the radiation fields, it may be important to also consider variations in topography, surface material and other obscuring objects such as buildings etc. Such variations can influence the results, as compared to a perfectly flat, open and homogenous surface.

Output	Reduces the risk of contaminating the detectors and the equipment and reduces the risk of misinterpreting the results.
---------------	--

Output

The output of the procedure provides representative sites for follow up of the temporal changes in the radiation environment after commissioning the ESS, enabling dose estimations relevant for today's population density in the area.

Gamma spectrum from the majority of the sites close to the ESS facility as well as careful mapping of the ambient dose equivalent rate at the various sites, including its variability within and between these sites.

The procedure reduces the risk of contamination of the equipment and misinterpretation of the results and provides for reproducible assessments in the future.

References

- [1] Karlberg, O. *Manual och teknisk beskrivning av CEMIK-systemet och NuggetW version 3.2*. 2007.

ANNEX B2 SAMPLING, SAMPLE PREPARATION AND LABORATORY MEASUREMENTS USING HIGH-RESOLUTION GAMMA SPECTROMETRY

Purpose

The purpose of this appendix is to describe the sampling, sample preparation and measurement of the environmental sample activity concentration using laboratory gamma spectroscopy for the project entitled "Monitoring of environmental radioactivity and radiation levels for zero point assessment and contributions to ESS environmental monitoring plan" (contract ESS-0093103).

Applicability

This description (procedure) is applicable to environmental samples measured at the environmental radioactivity laboratory in Malmö using high-resolution gamma spectroscopy. The procedure is applicable to future measurements of gamma-emitting radionuclides in various samples collected from the Lund area to monitor the radiological impact of ESS.


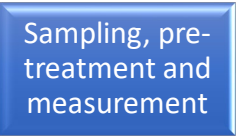
Methodological outline

Firstly, suitable sampling and measurement sites were selected to cover all directions around the ESS site (see details in Section 2). After that, sample types collected for analysis of the activity concentration by gamma spectrometry included soil, bioindicators, grass, crops, milk and sewage sludge. Prior to the measurements, the samples (except the milk) were pre-treated by homogenising the sample and by drying them at 70 °C (during several hours) to reduce the water contents. The prepared samples were then distributed in special sample beakers and the radionuclide concentration was measured by means of well-shielded High-Purity Germanium (HPGe) detectors. After evaluating the spectrums, the results are presented in a final report.



Figure B2. 1. Flow of actions for achieving the point zero measurements of the gamma activity concentration in various types of samples by laboratory analysis in HPGe detectors.

Methodological details

Planning	
<p>Several sampling sites in the close vicinity of the ESS site (within approximately 1500 m in various wind directions) were selected as well as some sites at larger distances than 1500 m from the ESS site.</p> <p>Soil and grass samples were collected at the majority of the sites when <i>in situ</i> gamma spectrometry was carried out. Soil reflects the history of previously deposited radionuclides on the ground such as ^{137}Cs. The radionuclide concentration in soil together with the radionuclide concentration in grass provide important information on both the external radiation exposure at the sites, as well as how fixed the radionuclides are in the soil.</p> <p>Bioindicators such as moss and spruce needles have since long been used as an important tool for determining radionuclides in the environment. Bioindicators representative for the area were collected both close to the ESS site (<1500 m) and further away.</p> <p>Crops is an important pathway of transfer of various pollutants to humans. Samples of various crops were therefore collected at the farmlands (Site 36) north of ESS. Other farmlands should also be considered after establishing contact with the owners of these.</p> <p>There are currently few dairy farms close to ESS. However, as milk is an important pathway of transfer from ground deposited radionuclides to humans, milk was sampled from one farmer with dairy cows (Site 22).</p> <p>Sewage sludge is an indicator of the collective radionuclide concentration in the human population in the catchment area of sewage treatment facility and may to a certain extent also reflect the wash-off of ground surfaces in the catchment area. Hence, samples of sewage sludge were collected at the sewage treatment facility in Lund (Site 35), Källby VA Syd.</p>	
	
Output	Representative sampling locations and types of samples for assessment of the background radionuclide concentration relevant for gamma dose estimations.
General aspects on sampling	
<p>Gloves should be worn (when possible) during sampling, especially when in direct contact with the sample itself. At the site, each sample taken must be carefully documented and marked in temporary containers e.g. double sets of plastic bags. The site itself should be documented by its GPS coordinates, photographs from different directions and preferably also at various distances to include ambient information that might be of importance for the future.</p> <p>Between samplings, it is important to carefully clean the sampling probe, e.g. the tube for soil samplings and the scissors for grass samplings. Likewise, it is important to clean the tools used in the laboratory during sample preparation between the handling of different samples. When sampling soil with the STS (see below), special plastic sheets are inserted in the soil-sampling</p>	
	

probe to further reduce the contact between the sample and the probe. These sheets can easily be cleaned in the field and re-used to avoid cross contamination between samples. The EPS sampler (see below) does not have such sheets and must therefore be cleaned with water/paper between samplings.

If there is a suspicion that the samples are contaminated, additional precautions must be taken.

The information collected during the sampling must as soon as possible be digitalised, stored and secured.

Output	Reduction of risk of cross-contamination between samples. Minimizes risk of loss of data.
---------------	---

Sampling and sample preparation

Soil

Soil samples were collected using two different methods. One method uses a split tube sampler (STS, see Figure B2. 2), consisting of an aluminium tube with an inner diameter (\varnothing) of 53 mm and a total length of 400 mm. The STS is brought down into the soil by a dedicated hammer, to a depth of at least 20 cm. This is repeated at each of the five positions at each site. The individual soil cores are then divided into different sections, corresponding to various depth layers: the first is the vegetation and litter, followed by different soil layers from 0.0-2.5, 2.5-5.0, 5.0-7.5, 7.5-10.0, 10.0-15.0, 15.0-20.0 cm and >20 cm, the latter being of indefinite size (normally between 2-5 cm). Each depth layer from the five cores is mixed and put into eight different plastic bags marked with site, date and the corresponding layer depth in cm. This results in eight bags with five subsamples (core fragments) in each bag. The bags are then sealed until the samples are prepared in the laboratory. The STS soil samples are weighed fresh (wet weight, w.w.) in the laboratory, layer by layer, and then put onto individual aluminium trays. The information about the sample is registered in the laboratory protocol together with other information relevant to the sample and the sample site. Each sample is given a serial number that is written on the aluminium tray. The trays are then put in a heating cabinet at 70 °C until the soil is dry (a couple of hours). In order to avoid clustering of the soil, which are hard to separate when dry (for the specific clay soil outside Lund), the samples are continuously crumbled and homogenised during the drying process. The higher the clay contents of the soil the shorter heating periods between the repeated crumbling of the sample. When the sample is completely dry, the sample weight is determined (dry weight, d.w.) and registered in the laboratory protocol. Each sample, corresponding to different depth layers, are homogenised and put into dedicated 200 ml sample beakers (60 ml for the vegetation/litter). The sample serial number, weight and sampling date are written on the lid of the sample beaker. The sample is then measured in a lead shielded HPGe detector for at least 20 h, after which it is stored.

Sampling, pre-treatment and measurement

The other method applied for soil sampling utilises a sampler standardised for the Swedish radiological and nuclear emergency preparedness (emergency preparedness sampler, EPS, see Figure B2. 2) that generates a ~70 mm deep and $\varnothing=65$ mm core of soil. These soil samples are referred to as EPS cores. Images of these two soil sampling tools, the STS and the EPS, are shown in Figure B2. 2 below. The EPS samples are easily taken by pressing the tool down in to

the ground by foot. The EPS soil core is then directly, at the site, inserted into a 200 ml sample beaker, dedicated for the purpose.

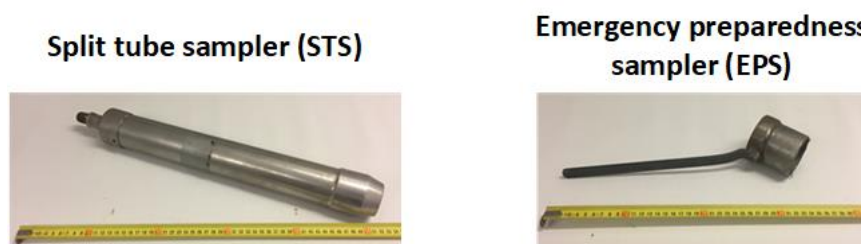


Figure B2. 2. Images of the soil samples: to the left is the assembled split tube sampler, and to the right is the emergency preparedness sampler.

When the samples arrive to the laboratory, the weight of the EPS soil cores is determined after which they are assigned a unique serial number. The serial number, site, weight and sampling date is noted on the lid of the sample beaker. The information is also registered in the laboratory protocol, together with other relevant information to the sample and the sample site. When the samples have been catalogued, they are measured in a lead-shielded HPGe detector for at least 20 h. The acquired data then represents the fresh weight concentration of gamma-emitting radionuclides. After the sample has been measured, it is dried prior to storage, by heating the sample in a heating cabinet at 70 °C for a few hours.

At each site, two sets of dedicated ropes are placed around the HPGe detector (with the HPGe detector as the centre of Figure B2. 3); one forming an isosceles triangle around the tripod and one forming a larger square around the triangle. This method was introduced in order to achieve a high reproducibility for the two methods of soil samplings at the various sites.

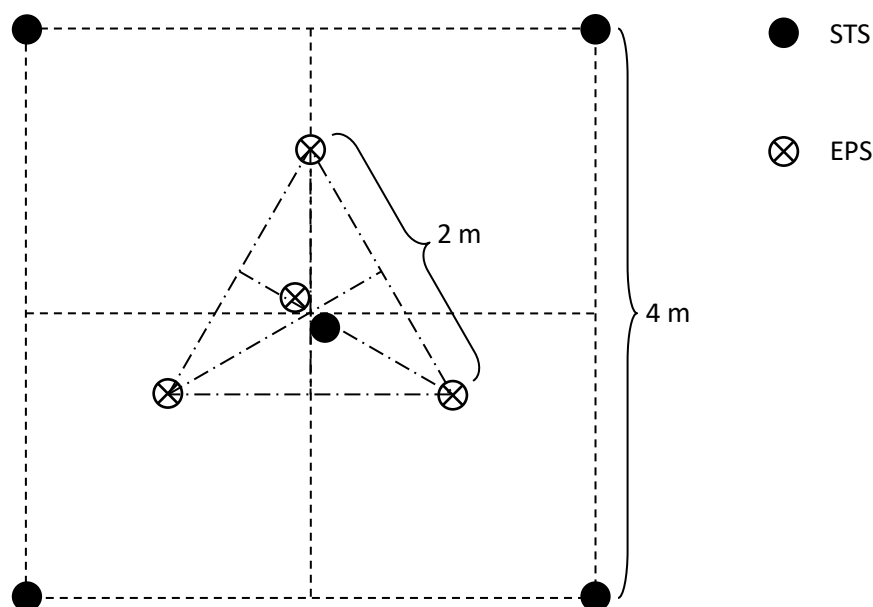


Figure B2. 3. STS (deep soil cores, > 20 cm) and EPS (surface soil cores, 7 cm) sampling strategy at the sites.

The STS samples are taken in the four corners of a square and one that is taken directly under the HPGe detector in the centre of the surface (Figure B2. 3). The EPS samples are taken at

the three corners of the triangle enclosed by the STS square and one that is taken directly under the HPGe detector (Figure B2. 3).

Bioindicators

Various bioindicators (moss, spruce needles, lichen), depending on availability, were collected in the vicinity of ESS. The samples were dried in a heating cabinet at 70 °C and then put into the most suitable plastic beaker geometry for measurement of the gamma-emitting radionuclide contents in the same way as with samples of soil.

Crops

The workers at Svenstorp's county estate were informed by LU to collect crops during harvesting of the fields close to ESS. They were instructed that after collecting the harvest from a specific field, a sub-sample of approximately 1.5 kg should be allocated for LU. In total, ten samples of barley, rape, and wheat were collected.

At the laboratory in Malmö, the weight of each sample was determined after which they were dried at 70 °C in a heating cabinet. After eliminating the water contents of the samples the sample weight was determined once again. The dried samples were then put into 200 ml plastic sample beakers (one per sample fraction, i.e. ten samples). Then the activity concentration of gamma-emitting radionuclides was determined by high-resolution gamma spectrometry in a well-shielded HPGe detector system for at least 20 h.

Grass

Grass was collected at various sites over a surface corresponding to 1 m². The grass was cut ~3 cm above ground (soil level), in order to make sure that only the green part of the grass was included in the sample *i.e.* no parts of the root system or soil. If the grass was short, a larger area was used in order to collect enough material. However, grass was always sampled from areas in multiples of 1 m². After sampling the grass in big plastic bags, the grass was dried in a heating cabinet at 70 °C. The dried grass was then grinded, in order to increase the density of the sampled grass, after which the sample was put into either a 60 ml or a 200 ml sample beaker. The individual samples were then measured in a lead shielded HPGe detector for at least 20 h, to obtain the activity concentration of gamma-emitting radionuclides per d.w., after which the samples were stored.

Milk

Milk was sampled at one dairy farm by collecting representative milk samples from the milk storage tank. During the two collections, five litres (five individual one-litre bottles) were collected. The HPGe gamma measurement was performed in 200 ml beakers with similar acquisition time as for the other types of samples. The milk was not prepared in any way before the measurements. In addition, at this farmer, forage was also sampled and analysed for gamma-emitting radionuclides, as a pathway for radionuclides to the cows.

Sewage sludge

Every month the staff at Källby sewage treatment facility in Lund collected sub-samples of sewage sludge. During operation of the sludge centrifuge (a few times per week), a small portion was taken and stored in a freezer. At the end of the month, an amount of 1-1.5 l of sludge was acquired for later transport to Malmö. The monthly samples were divided in two portions, one for gamma spectrometry analysis and one for analysis of ³H. The one part for gamma measurement was first dried in a heating cabinet at 70 °C after which it was

homogenised and put into a 200 ml sample beaker for HPGe gamma spectroscopy measurement.

Laboratory high-resolution gamma spectrometry

For the assessment of the radionuclide concentration in the various samples, three different gamma spectrometers are used. All of them are based on HPGe crystals (ORTEC, USA) inserted into lead shielded cavities, but with varying relative efficiencies: detector 4: 55%; detector 5: 92.5%; detector 7: 100%.

The recorded gamma spectra are evaluated using an in-house evaluation sheet (cross-checked with the detector software evaluation program, Gamma Vision 7.1™ and used for reporting to e.g. IAEA and SSM), in order to have full control of all the steps in the evaluation of each individual gamma line. Using this sheet, the minimum detectable activity concentration (MDA) is based on the definitions by Currie [1] summarised by the following equation:

$$MDA = \frac{2.71 + 4.65 \cdot \sigma_{NBkg}}{t \cdot \varepsilon \cdot n_\gamma} \quad (\text{Eq. B2.1})$$

where σ_{NBkg} is the uncertainty of the net counts within a channel interval around a specific gamma energy of the current spectrum calculated by GammaVision, t is the live time of the current measurement, ε is the absolute efficiency of the sample geometry at the specific energy and n_γ is the branching ratio of the decay.

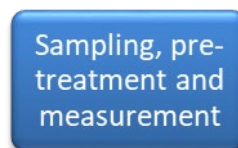
For the naturally occurring radionuclides, e.g. the radon daughters, a background is present. This background is obtained by acquiring background spectra (with measurement time t_{bkg}), where photo-peaks are localized, identified and quantified. The statistical uncertainties in the peak present in the background is σ_{NBkg} , thus giving the equation:

$$MDA = \frac{2.71 + 4.65 \cdot \sqrt{(2 \cdot \sigma_{Net} - \sqrt{G})^2 + \left(\sigma_{NBkg} \cdot \sqrt{\frac{t}{t_{bkg}}} \right)^2}}{t \cdot \varepsilon \cdot n_\gamma} \quad (\text{Eq. B2.2})$$

where σ_{Net} is the uncertainty in net counts in the channel interval in the current spectrum reported by GammaVision. G is the gross number of counts in the channel interval.

Output	Gamma spectra of the measured samples and the corresponding radionuclide concentrations of gamma emitters.
---------------	--

Storage of samples	
<p>All samples collected are stored for future analysis (in dried form, except for milk). Each sample is stored at room temperature in the sample beaker that was used during the measurement, sealed in a plastic bag (the milk samples are stored in a freezer).</p> <p>For all samples with excess sample material, the material is stored at Lund University.</p>	
Output	The procedure guarantees that sample material from prior the start of ESS is available for future measurements.



Output

The output of the procedure is the activity concentrations, and spectra, of gamma-emitting radionuclides in soil, bioindicators, crops, grass, milk and sewage sludge. Re-analysis of the samples collected is possible.

References

- [1] Currie, L.A. *Limits for qualitative detection and quantitative determination. Application to radiochemistry*. Analytical chemistry, 40(3): 586-593, 1968.

ANNEX B3 SAMPLING, SAMPLE PREPARATION AND MEASUREMENTS OF ^3H ACTIVITY CONCENTRATION USING LIQUID SCINTILLATOR COUNTING

Purpose

The purpose of this appendix is to describe the sampling, sample preparation and measurement of the activity concentration of ^3H using liquid scintillation counting (LSC) analysis for the project entitled "Monitoring of environmental radioactivity and radiation levels for zero point assessment and contributions to ESS environmental monitoring plan" (contract ESS-0093103).

Applicability

The description (procedure) is applicable to various environmental samples measured at the Lund University laboratory at the Medical Radiation Physics group in Malmö using LSC. The procedure is applicable to future measurements of tritiated water (HTO) in various samples collected from the Lund area to assess the radiological impact of ESS. The current method does not allow measurement of the organically bound tritium.

Methodological outline

For the background mapping of ^3H , samples of water, sewage sludge, milk and sugar beet have been sampled, measured and analysed.



Figure 3. 1. Flow of actions for achieving the zero point measurements of the ^3H activity concentration in various types of samples by laboratory LSC analysis.

Each sample measured for the ^3H concentration in the LSC is prepared according to a procedure that was developed during the ESS-0093103 contract period (as provided below). The milk, sewage sludge and sugar beet were freeze dried in order to extract water from the samples, prior to the chemical pre-treatment and LSC analysis. After evaluation of raw data, the results are presented in a final report.

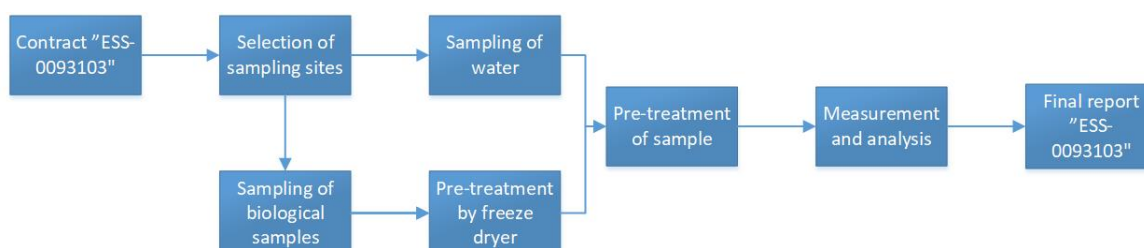


Figure B3. 1. Details of the workflow of the ^3H procedure.

Methodological details

Selection of sampling sites	
<p>Several sampling sites were selected in the close vicinity of the ESS site. The sites were selected as described in detail in Section 2.</p> <p>Water was sampled at some locations within the fenced area of the ESS facility, including samples of ground water and surface water (see Section 2.2). Ground water was sampled in the existing drill holes on the ESS site (Site 31), as well as in the close vicinity of the ESS site (Sites 4, 32). Surface water was collected from the existing ponds located within and around the site perimeter (Sites 31, 33, 34, 35). In addition, water samples were collected in some private wells (although not all of them were in operation), in households within the approximately 1500 m radius from ESS (Sites 24, 37, 38), as well as from the five water outlet ponds at Källby sewage treatment facility in Lund (Site 35). Sewage sludge is an indicator of the collective radionuclide concentration in human population in the catchment area of the sewage treatment facility. To a varying degree the sludge also contains radionuclides from runoff and from household and processed water.</p> <p>Milk was sampled from one farmer (Site 22) with dairy cows. Although there are currently few dairy farms close to ESS, milk is an important pathway of transfer to humans from ground deposited radionuclides.</p> <p>Sugar beet was the only bioindicator (at this stage) that was analysed for ^3H activity concentration (sampled at Site 46).</p>	
Output	Representative sampling locations for determination and follow up of ^3H activity concentration in water, sewage sludge, milk and sugar beet, for ^3H background dose estimates to representative persons.
General aspects on sampling	
<p>It is recommended to wear gloves during sampling, especially when in direct contact with the sample itself. At the site, each sample taken must be carefully documented and marked in temporary containers that are carefully sealed. To avoid cross contamination, special precaution should be taken when several samples are taken and when a ^3H contamination is suspected.</p> <p>Special sampling tools are required for sampling of surface water (a long enough rod to reach out in the water without disturbing it) and ground water (a long enough rope to reach the water level).</p> <p>The site itself should be documented by its GPS coordinates, photographs from different directions and preferably also at various distances to include ambient information that might be of importance for the future.</p> <p>Between samplings, it is important to carefully clean the sampling probe, e.g. by washing of the sampler with clean water.</p>	

Selection of
sampling sites

Sampling, pre-
treatment and
measurement

The information collected during the sampling must be digitalised as soon as possible and after that stored and secured.

Output	Reducing the risk of cross-contamination between samples. Guarantees sampling locations for the future. Minimizes the risk of loss of data.
---------------	---

Sampling and sample preparation

Pre-treatment of the samples

The water was sampled in 200 ml plastic beakers which were kept in a refrigerator until preparation. To reduce quenching and remove ions from the sample, about 2 g of a mixture of cation and anion exchange resin (DOWER 50WX8 and DOWER 1X8) was added to about 15 ml of the sample. The vials were then shaken for about 10 minutes and then filtered using a paper filter.

Sampling, pre-treatment and measurement

Water from the sludge, milk and beet samples was extracted using freeze-drying. For increased efficiency of the method, the milk was poured into small aluminium foil trays and frozen at -18 °C before placed in the freeze dryer. The sludge and the beet were frozen directly after being collected. Using a hammer, the sludge was crushed to smaller pieces and placed in an aluminium tray. The freeze dryer process started in the morning and was turned off at the end of the day. In the following morning, the extracted water from the sample was retrieved from the condenser of the freeze dryer.

The mass of the samples was measured before and after the freeze-drying process. To extract all water from the sludge, the samples were placed in a drying cabinet until they were completely dry. Thereafter, the mass and water content were determined.

The method was tested using a tritium tracer to establish the freeze-drying yield. It shall be noted that only the water fraction is measured in this method and not the organically bound tritium in the solid residue.

^3H analysis using liquid scintillator counting

For the majority of the samples, 5 ml of water were mixed with 10 ml of Ultima Gold LLT scintillation cocktail (Perkin Elmer) in a 20 ml polyethylene vial (for a few of the sewage samples 10 ml of water was used). Samples were then shaken for 10 min and stored in the dark for 48 hours to decrease chemical quenching before measurement. The samples were then measured in a Beckman LS 6500 multi-purpose LSC during 120 or 240 minutes and evaluated using a dedicated user programme (the 10 ml water samples were measured for 120 minutes 5-15 times). A sample of deep well water (Grevie-Bulltofta verket, VA Syd) with a well-documented low tritium concentration was used as background and Horrocks's method was used for quenching correction.

Uncertainty estimate

The uncertainty in the results is dominated by the statistical uncertainty in the count rates of the sample and background. Uncertainties introduced in volume and efficiency measurements are negligible compared to the statistical uncertainty in the number of counts. The activity of the reference solution (TRY44 number R8/12/123 by Eckert and Ziegler, Germany) has a reported uncertainty of 0.75% (1 standard deviation).

The total calculated uncertainty (σ_{calc}) in the activity concentration considers the uncertainty of the sample as well as the background:

$$\sigma_A^2 = \left(\frac{\partial A}{\partial cpm_s} \right)^2 \cdot \sigma_{cpm_s}^2 + \left(\frac{\partial A}{\partial cpm_b} \right)^2 \cdot \sigma_{cpm_b}^2 \quad (\text{Eq. B3.1})$$

Thus,

$$\sigma_A = \frac{1}{60 \cdot V} \left(\left(\frac{\sigma_{cpm_s}}{E_s} \right)^2 + \left(\frac{\sigma_{cpm_b}}{E_b} \right)^2 \right)^{0.5} \quad (\text{Eq. B3.2})$$

The statistical uncertainty in counts ($cpm \cdot t$) of a measurement equals $(cpm \cdot t)^{0.5}$, thus:

$$\sigma_{cpm} = \frac{(cpm \cdot t)^{0.5}}{t} = \left(\frac{cpm}{t} \right)^{0.5} \quad (\text{Eq. B3.3})$$

and

$$\sigma_A = \frac{1}{60 \cdot V} \left(\frac{cpm_s/t_s}{E_s^2} + \frac{cpm_b/t_b}{E_b^2} \right)^{0.5} \quad (\text{Eq. B3.4})$$

Minimum detectable activity

The minimum detectable activity, MDA, is defined according to [1]:

$$MDA = \frac{3.29 \cdot \sqrt{\left(\frac{cpm_b}{t_s} \right) + \left(\frac{cpm_b}{t_b} \right) + \left(\frac{2.71}{t_s} \right)}}{60 \cdot E \cdot V} \quad (\text{Eq. B3.5})$$

where cpm_b is the count rate of the background (counts per minute), t_s is the measurement time of the sample (min), t_b is the measurement time of the background (min), E is the efficiency and V is the sample volume (l). The background count rate was established using deep well water with a well-documented low tritium level. The counting time was set to 120 or 240 minutes depending on the current number of samples. The relatively short counting times gave MDA values of about 29 and 14 Bq l⁻¹, respectively. This counting time provides results rapidly with MDA levels well below the limit of 100 Bq l⁻¹ in drinking water set by the National Food Agency [2]. The MDA was further decreased by extending the counting time for a few of the sewage sludge samples, giving an MDA of 2.6-3.4 Bq l⁻¹.

Output	Activity concentration of tritiated water in various types of samples.
Storage of samples	
<p>An overview of storage procedures for ^3H samples is provided in [3]. For the present program, the water samples are stored in air tight and closed containers. Organic samples are stored in closed containers in a freezer. Residual parts of samples, fractions not prepared and analysed, are stored in closed containers in a freezer.</p>	
Output	<p>The samples collected are possible to re-analyse in the future. However, when the sample comes in contact with any other material such as the container or the atmosphere, the tritium content may change. A re-analyse of a background sample is thus of limited value.</p>

Sampling, pre-treatment and measurement

Output

Representative sampling locations for determination and follow up of ^3H activity concentration in water, sewage sludge, milk and sugar beet, for background ^3H dose estimates to representative persons.

Reducing the risk of cross-contamination between samples. Guarantees sampling locations for the future. Minimizes the risk of loss of data.

^3H activity concentration for the sampled matrices.

References

- [1] Currie, L.A. *Limits for qualitative detection and quantitative determination. Application to radiochemistry*. Analytical chemistry, 40(3): 586-593, 1968.
- [2] Livsmedelsverket. *Vägledning till livsmedelsverkets föreskrifter (SLVFS 2001:30) om dricksvatten*. 2016.
- [3] Kim, D., Croudace, I.W., Warwick, P.E. *The requirement for proper storage of nuclear and related decommissioning samples to safeguard accuracy of tritium data*. Journal of hazardous materials, 213: 292-298, 2012.

ANNEX B4 SAMPLING, SAMPLE PREPARATION AND MEASUREMENTS OF ^{14}C

Purpose

The purpose of this appendix is to describe the sampling, sample preparation and measurement of the ^{14}C concentration in tree rings, vegetation and milk using accelerator mass spectrometry for the project entitled “Monitoring of environmental radioactivity and radiation levels for zero point assessment and contributions to ESS environmental monitoring plan” (contract ESS-0093103).

Applicability

The description (procedure) is applicable to environmental samples measured with respect to ^{14}C at the Single Stage Accelerator Mass Spectrometry (SSAMS) facility in Lund [1, 2]. The fundamentals of the procedure are applicable to future measurements of ^{14}C in the Lund area to assess the radiological impact of ESS.

Sampling and measurement of ^{14}C in environmental samples

Methodological outline

The general methodology for the ^{14}C mapping is shown in Figure B4. 1. Suitable sampling sites were selected (rural background, urban background, sites around ESS (approximately within 1500 m of the ESS site)) as given in Table 2. Sample types collected included tree rings, vegetation (grass, moss, fruits, crops, berries) and milk. Organic samples (tree rings, vegetation and milk) were pretreated, graphitized and measured by the SSAMS facility. Fullerene soot monitors were used to display airborne contamination of ^{14}C (including other compounds than CO_2 in ambient air). After evaluation of raw data, the results were presented in Section 4.4. Parts of all organic samples were stored in dried form.

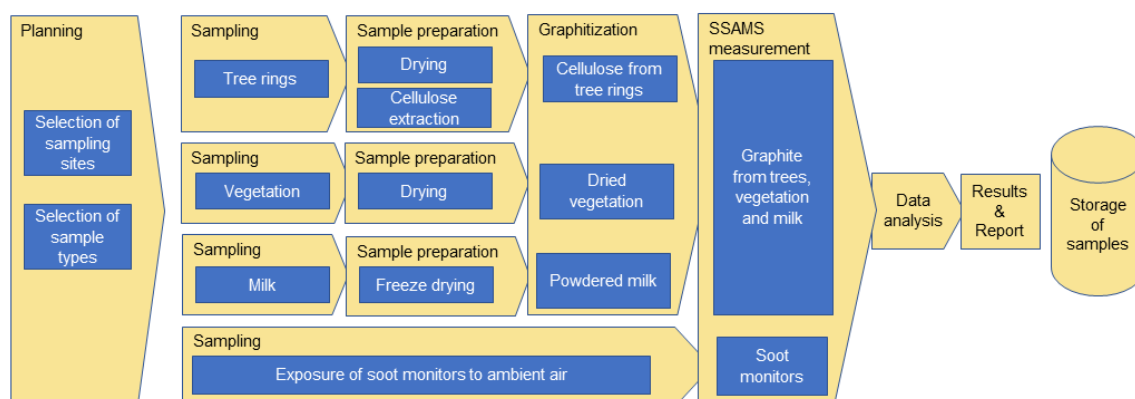
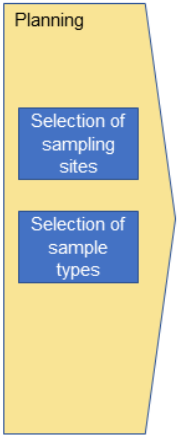
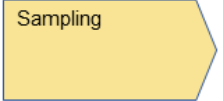



Figure B4. 1. General methodology for ^{14}C .

Methodological details

Planning	
<p>The selection of the 23 sampling sites, including the rural and urban background sites, is described in detail in section 2.4. The motivation of sample types is also stated in this section.</p>	
	
Output	Representative sampling locations, including urban and rural background sites, and sampling materials relevant for dose assessment.
General aspects on sampling	
<p>Gloves were worn during sampling. All sampling was photographically documented, and GPS coordinates were noted. All data were stored at multiple locations.</p>	
	
Output	Reduction of risk of cross-contamination between samples. Guarantee of sampling locations for the future. Minimizing risk of loss of data.

Sampling and sample preparation of tree rings	
<p>A tree borer (250 mm, EDUCATION/SCIENCE COLLECTION P, VWR 763-0191) was used to collect several drill cores from one well-grown tree at each site (spruce, fir or pine tree), see Figure B4.2. Drill cores were placed in drinking straws and in ziplock bags (90 MY, 180 x 250 mm, VWR HKPK102036).</p>	
	
<p>Figure B4. 2. Tree core drill and collected tree drill core.</p> <p>At the Laboratory for Wood Anatomy and Dendrochronology at Lund University [3], the drill cores (except those kept for SSM's sample bank) were divided into separate years (2012, 2013, 214, 2015 and 2016) using a razor blade. The samples, in form of shavings, were placed in labelled containers (55 ml plastic jars: Kartell, VWR 216-2260). A certificate describing the result of the dendrochronological analysis and separation into annual rings was provided by the laboratory.</p> <p>At the Radiocarbon Dating Laboratory at Lund University [4], cellulose was extracted from the shavings representing different years. Approximately 15 mg of wood per annual sample, corresponding to a length of about 1.5 mm of one or several annual rings from the 5 mm drill cores, was used for the cellulose extraction (the yield of the cellulose extraction was about 45%). About 3 mg of cellulose per sample was taken further to ¹⁴C-analysis.</p>	
Output	Isolation of cellulose containing ¹⁴ C in atmospheric CO ₂ during the growing season of separate years in the past, to be taken further to ¹⁴ C analysis.

Sampling and sample preparation of vegetation

Vegetation (grass, moss, crops and berries) and fodder were sampled in labelled containers (55 ml jars with screw cap: Kartell, VWR 216-2260). Large vegetation samples (e.g. fruit and silage) were sampled into plastic bags (ziplock bags (90 MY, 180 x 250 mm, VWR HKPK102036)), and a representative fraction was subsequently transferred to smaller containers (55 ml jars with screw cap: Kartell, VWR 216-2260). The amount of sampled material was typically a few strands of grass, a few cm² of moss, a few berries and single larger fruits. Fruits were cut into smaller pieces. All samples were dried in an oven at 30-50 °C for several hours (until complete removal of water).



For moss samples, the length of the strands was measured.

A few strands of one of the moss samples collected at the rural background site C1 were divided into two fractions: an upper part and a lower part (3 cm). Another sample from the C1 site was divided into 3 parts (upper, lower and middle 3 cm).

A fraction of each vegetation or fodder sample (>10 mg) was put into labelled and separate 5 ml glass vials with plastic caps (5 ml, VWR 216-1759), was cut into smaller parts using a pair of scissors and was taken further to ¹⁴C-analysis.

Output	Dried vegetation samples to be taken further to ¹⁴ C analysis.
---------------	---

Sampling and sample preparation of milk

Milk was poured from the milk storage tank at the farm into a bucket provided by the farmer. A 0.25 litre stainless steel container was used to fill three 5 ml vials (VWR 216-1759) with milk. One of the samples was freeze-dried at the Radiocarbon dating laboratory. The two other samples were stored in a freezer at the Department of Geology, Lund. A fraction of the freeze-dried milk (>10 mg) was taken further to ¹⁴C-analysis.



Output	Dried milk powder to be taken further to ¹⁴ C analysis.
---------------	--

Soot monitors

Fullerene soot of fossil origin (ALFA40971.03, Alfa Aesar) was pressed into 19 Al capsules fitting the ion source of the ¹⁴C-measurement instrument. The capsules were stored in airtight glass tubes sealed with a Swagelok cap. The capsules were exposed in four 4-week periods to ambient air at the four sampling sites C1, C2, C3 and C4 (fullerene absorbs gases from the air [5]). At each sampling site, a fullerene capsule was placed in a 5 ml vial (VWR 216-1759) with a small hole in the plastic lid. The vial was turned upside down (protection from exposure to rain) and was fastened to a tree using a stainless-steel wire, see Figure B4. 3. After exposure, the soot capsules were stored in the airtight glass tubes sealed with a Swagelok cap until analysis by the ¹⁴C-instrument.

Sampling

Exposure of soot monitors to ambient air

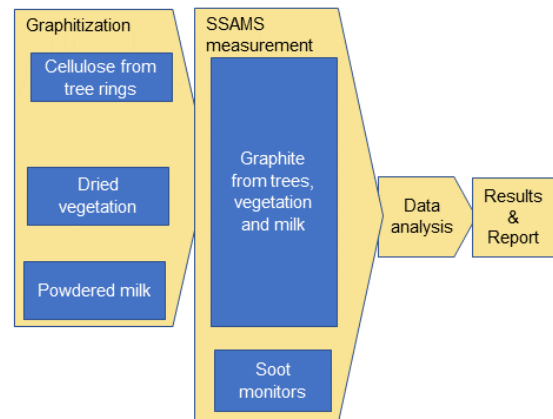


Figure B4. 3. The fullerene soot monitor.

Output	Soot monitors exposed to environmental air, to be taken further to ¹⁴ C-analysis.
---------------	--

Graphitization and ^{14}C measurement

Prior to ^{14}C -measurement, 1-2 mg carbon was extracted from all organic samples (> 2 mg dry weight) using the graphitization system AGE at the Radiocarbon Dating Laboratory at Lund University [6, 7]. After extraction, the carbon from each sample (unknown samples, standards, blanks) was pressed into separate Al sample holders, which are taken further to ^{14}C analysis in the SSAMS facility [1, 2]. The ^{14}C content was measured at the Single Stage Accelerator Mass Spectrometry (SSAMS) facility at Lund University [1, 2]. The precision of the measurements was <1% [2], certified by measurement of several standard samples of known ^{14}C content (IAEA C7, SRM 4990B and SRM 4990C). The background of the sample preparation and accelerator system was assessed by the measurement of graphitized fossil samples. The raw data was analysed by the Radiocarbon Dating Laboratory, giving results expressed as the quantity $F^{14}\text{C}$ (see below). A certificate of the results was provided by the Radiocarbon Dating Laboratory at Lund University.



The results of a quality assessment of the measurements is given in Section 4.4.1, and the results of all organic samples analysed are presented Section 4.4.2. Furthermore, the obtained ^{14}C data is compared to other European ^{14}C data.

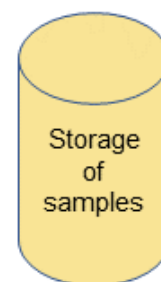
In the ion source of the SSAMS system, gaseous ^{14}C that has been adsorbed to the surface of the fullerene soot in the capsule is expected to be sputtered off a few minutes [5]. The observed $^{14}\text{C}/^{12}\text{C}$ ratio, decreasing with time of measurement, was used to provide a qualitative measure of the presence of airborne ^{14}C contamination. The ^{14}C to ^{12}C ratios in the fullerene capsules were monitored in the SSAMS system, as well as a number of standard samples of known activity and graphitized background samples (referred to as Abs and W6). Each soot sample was measured 12 times: each time for 120 seconds after a warm-up of 20 seconds. The ^{14}C to ^{12}C ratios of the Lund samples were compared with the ratios for the background samples (to indicate possible presence of airborne anthropogenic ^{14}C contamination in the ESS area). Levels were also compared to ^{14}C absorbed into fullerene soot monitors in 2009, when a contamination of ^{14}C was observed in Lund (Skog, 2010). These results are presented in Section 4.4.3.

Output	^{14}C data from of organic samples in the quantity $F^{14}\text{C}$, $^{14}\text{C}/^{12}\text{C}$ ratios of fullerene soot monitors.
---------------	--

Storage of samples

Of all samples collected, dried samples were stored for future possible analysis.

One tree ring from each site was saved for the SSM records (dried in an oven at 30 °C for several hours prior to storage). For the rest of the samples, >50 mg was saved and stored for SSM in labelled 5 ml glass vials with plastic caps (VWR 216-1759). The SSM samples (> 50 mg per sample) were stored in a labelled plastic box in a locked laboratory at the Dep of Geology, Lund University. For all samples, Lund University stored excess sample material (dried samples, not graphitized).



Output	Guarantee that sample material collected prior to the start of ESS are available for future possible measurements.
---------------	--

Note on units and further calculations

F¹⁴C in relation to activity concentration

The results of the ¹⁴C analysis were expressed as F¹⁴C [8, 9]. When comparing high-precision measurements of ¹⁴C in various environmental samples types, the dimensionless quality F¹⁴C is more suitable than reporting sample specific activity $\frac{A}{m_c}$ (in units of Bq (kg carbon)⁻¹). Firstly,

Data
analysis

specific activity $\frac{A}{m_c}$ depends on the time of measurement (due to the radioactive decay of ¹⁴C). Secondly, due to a process known as isotope fractionation, the specific activities of various species in the same environmental reservoir are not identical (isotope fractionation can occur during any chemical or physical process in nature: all isotopes are not transferred and equal rates or to equal extent, e.g. due to their difference in mass). F¹⁴C, however, remains constant over time and eliminates the effects of isotope fractionation, making F¹⁴C values of various sample types directly comparable.

The relation between F¹⁴C and specific activity $\frac{A}{m_c}$ at the time of measurement is given by

$$F^{14}C = \frac{\frac{A}{m_c}}{226 \frac{\text{Bq}}{\text{kg C}}} \cdot \left(\frac{0.975}{\left(1 + \frac{\delta^{13}C}{1000}\right)} \right)^2 \cdot e^{\frac{(y-1950)}{8267}} \quad (\text{Eq. B4.1})$$

where $\delta^{13}C$ is the isotope fractionation of the sample, and y is the year of measurement (the number 8267 in the exponent is $T_{1/2}/\ln 2$, where $T_{1/2}=5730$ years). The squared part of the equation normalizes the sample activity to $\delta^{13}C = -25\text{‰}$. The exponential part eliminates the effect of decreasing specific activity with time.

$\delta^{13}C$, which is the relative deviation of the ¹³C/¹²C ratio of the sample, $\left(\frac{^{13}C}{^{12}C}\right)_s$, compared to that of a standard material, VPDB (Vienna Pee Dee), expressed in per mil:

$$\delta^{13}C = \left(\frac{\left(\frac{^{13}C}{^{12}C}\right)_s - \left(\frac{^{13}C}{^{12}C}\right)_{\text{VPDB}}}{\left(\frac{^{13}C}{^{12}C}\right)_{\text{VPDB}}} \right) \cdot 1000\text{‰} \quad (\text{Eq. B4.2})$$

$\delta^{13}C$ of various terrestrial organic materials is commonly around -30‰ to -20‰ [10, 11]. Typical values are shown in Table B4. 1 below. If requested, $\delta^{13}C$ can be very accurately measured by means of Isotope Ratio Mass Spectrometry (IRMS).

Table B4. 1. Typical $\delta^{13}\text{C}$ values in nature [10].

Material	$\delta^{13}\text{C}$ (‰)
Marine carbonates	0 (-4 to +4)
Atmospheric CO_2	-9 (-11 to -6)
Grains, seeds, maize, millet	-10 (-13 to -7)
Marine organisms	-15 (-19 to -11)
Bone collagen, wood cellulose	-20 (-24 to -18)
Grains (wheat, oats, rice, etc)	-23 (-27 to -19)
Recent wood, charcoal	-25 (-30 to -20)
Tree leaves, wheat, straw	-27 (-32 to -22)

Conversion of $F^{14}\text{C}$ to specific activity of carbon

The specific activity of carbon in any sample, $\frac{A}{m_C}$, at the year of growth, x , is given by [9]:

$$\frac{A}{m_C} = F^{14}\text{C} \cdot \left(\frac{1 + \frac{\delta^{13}\text{C}}{1000}}{0.975} \right)^2 \cdot e^{\frac{(1950-x)}{8267}} \cdot 226 \frac{\text{Bq}}{\text{kg C}} \quad (\text{Eq. B4.3})$$

where $F^{14}\text{C}$ is the $F^{14}\text{C}$ data from the SSAMS measurement and $\delta^{13}\text{C}$ is the isotope fractionation of the sample according to Eq. B4.2.

Activity concentration in atmospheric CO_2 using tree ring data

The mass of carbon in atmospheric CO_2 per unit volume, $\frac{m_C}{V_{\text{air}}}$, is given by:

$$\frac{m_C}{V_{\text{air}}} = M[\text{C}] \cdot \frac{p}{R \cdot T} \cdot \frac{n_{\text{CO}_2}}{n_{\text{air}}} \quad (\text{Eq. B4.4})$$

where $M[\text{C}]$ is the molar mass of carbon (12.011 kg/mole), p is the pressure (in Pa), R is the gas constant (8.314 J/(mole·K), T is the temperature (in Kelvin) and $\frac{n_{\text{CO}_2}}{n_{\text{air}}}$ is the molar fraction of CO_2 in air (can be obtained from <https://www.esrl.noaa.gov/gmd/ccgg/trends/>).

The activity concentration of ^{14}C in CO_2 per unit volume of air is given by:

$$\frac{A}{V_{\text{air}}} = \frac{A}{m_C} \cdot \frac{m_C}{V_{\text{air}}} \quad (\text{Eq. B4.5})$$

Activity concentrations of organic materials

The activity concentration of organic materials is calculated by:

$$\frac{A}{m_{\text{sample}}} = \frac{A}{m_C} \cdot \frac{m_C}{m_{\text{sample}}} \quad (\text{Eq. B4.6})$$

where $\frac{m_C}{m_{\text{sample}}}$ is the mass of carbon per wet weight of the sample. This value can be obtained from elemental analysis. Generic values can e.g. be found in Ref [12] and in Table B4. 2 below.

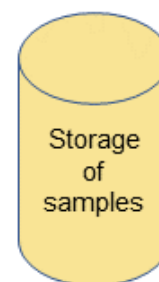
Table B4. 2. Typical proportions of stable carbon in various materials [12].

Material	$\frac{m_C}{m_{\text{sample}}} \left(\frac{\text{g carbon}}{\text{kg wet weight}} \right)$
Cow milk	65 (62 to 69)
Grass or greenfeed	100 (40 to 160)
Silage	130 (65 to 180)
Grains	390 (360 to 430)
Fruits	62 (31 to 100)

The varying proportion of stable carbon mainly depends on the amount of water in the material in question.

Output	Activity concentration of air expressed as Bq m ⁻³ , in milk and terrestrial plants as Bq kg ⁻¹ wet weight.
---------------	---

Storage of samples	
<p>Of all samples collected, dried samples were stored for future possible analysis.</p> <p>One tree ring from each site was saved for the SSM records (dried in an oven at 30 °C for several hours prior to storage). For the rest of the samples, >50 mg was saved and stored for SSM in labelled 5 ml glass vials with plastic caps (VWR 216-1759). The SSM samples (> 50 mg per sample) were stored in a labelled plastic box in a locked laboratory at the Dep of Geology, Lund University. For all samples, Lund University stored excess sample material (dried samples, not graphitized).</p>	
Output	Guarantee that sample material collected prior to the start of ESS are available for future possible measurements.



Output

The output of the procedure is quality-assured $F^{14}C$ values in tree rings, vegetation and milk, and $^{14}C/^{12}C$ ratios of fullerene soot monitors to indicate potential presence of air-borne ^{14}C contamination.

The $F^{14}C$ data offers the opportunity to directly compare different sample matrices. The activity concentration of ^{14}C in air expressed as $Bq\ m^{-3}$, and in milk and terrestrial plants as $Bq\ kg^{-1}$ wet weight, can be estimated using the information in section "Notes on units and further information".

References

- [1] Skog, G. *The single stage AMS machine at Lund University: Status report*. Nuclear Instruments and Methods in Physics Research Section B: Beam Interactions with Materials and Atoms, 259(1): 1-6, 2007.
- [2] Skog, G., Rundgren, M., Sköld, P. *Status of the Single Stage AMS machine at Lund University after 4 years of operation*. Nuclear Instruments and Methods in Physics Research Section B: Beam Interactions with Materials and Atoms, 268(7-8): 895-897, 2010.
- [3] Linderson, H. Accessed: 2018-02-01. Available from: <http://www.geology.lu.se/research/laboratories-equipment/the-laboratory-for-wood-anatomy-and-dendrochronology>.
- [4] Rundgren, M. Accessed: 2018-02-01. Available from: <http://www.geology.lu.se/research/laboratories-equipment/radiocarbon-dating-laboratory>.
- [5] Buchholz, B.A., Freeman, S.P., Haack, K.W., Vogel, J.S. *Tips and traps in the ^{14}C bio-AMS preparation laboratory*. Nuclear instruments and methods in physics research section B: Beam Interactions with Materials and Atoms, 172(1): 404-408, 2000.
- [6] Wacker, L., Němec, M., Bourquin, J. *A revolutionary graphitisation system: Fully automated, compact and simple*. Nuclear Instruments and Methods in Physics Research Section B: Beam Interactions with Materials and Atoms, 268(7): 931-934, 2010.

- [7] Adolphi, F., Muscheler, R., Friedrich, M., Güttler, D., Wacker, L., Talamo, S., Kromer, B. *Radiocarbon calibration uncertainties during the last deglaciation: Insights from new floating tree-ring chronologies*. Quaternary Science Reviews, 170: 98-108, 2017.
- [8] Reimer, P.J., Brown, T.A., Reimer, R.W. *Discussion: Reporting and calibration of post-bomb ^{14}C data*. Radiocarbon, 46(3): 1299-1304, 2004.
- [9] Eriksson Stenström, K., Skog, G., Georgiadou, E., Genberg, J., Johansson, A. *A guide to radiocarbon units and calculations*. Internal Report LUNFD6(NFFR-3111)/1-17/(2011). Lund University. D.o.N.P. Dep of Physics.
<http://lup.lub.lu.se/search/ws/files/5555659/2173661.pdf>. 2011.
- [10] Stuiver, M., Polach, H.A. *Discussion reporting of ^{14}C data*. Radiocarbon, 19(3): 355-363, 1977.
- [11] Martinsson, J., Andersson, A., Sporre, M.K., Friberg, J., Kristensson, A., Swietlicki, E., Olsson, P.-A., et al. *Evaluation of $d^{13}\text{C}$ in Carbonaceous Aerosol Source Apportionment at a Rural Measurement Site*. Aerosol and Air Quality Research, 17(8): 2081-2094, 2017.
- [12] IRSN. *Carbon-14 and the environment*. Available at
<http://www.irsn.fr/EN/Research/publications-documentation/radionuclides-sheets/environment/Pages/carbon14-environment.aspx>. 2012. Accessed: 2018-02-01.

ANNEX C **RESULTS**

Available upon request. Please contact the authors.